Molecular Quantum Mechanics and Molecular Spectra, Molecular Symmetry, and Interaction of Matter with Radiation

F. Merkt, M. Quack

ETH Zürich, Laboratory of Physical Chemistry, Wolfgang-Pauli-Str. 10, CH-8093 Zürich, Switzerland, Email: Martin@Quack.ch

reprinted from

"Handbook of High-Resolution Spectroscopy",

Vol. 1, chapter 1, pages 1–55
M. Quack, and F. Merkt, Eds. Wiley Chichester, 2011,
ISBN-13: 978-0-470-06653-9.
Online ISBN: 9780470749593,
DOI: 10.1002/9780470749593

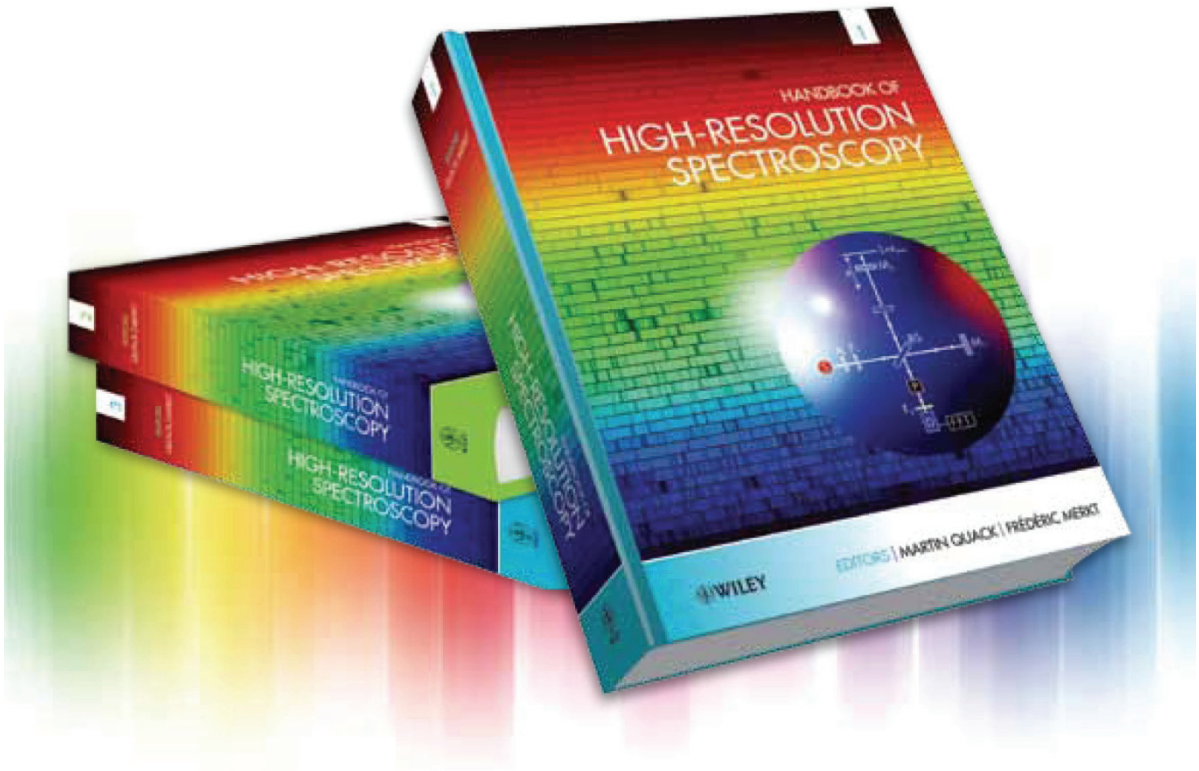

with compliments from Professor Martin Quack, ETH Zürich

Abstract

The basic experimental and theoretical concepts underlying molecular spectroscopy are presented. The equations and relations needed in practical applications of high-resolution spectroscopy are provided. Group theoretical tools and their use in high-resolution spectroscopy are introduced and illustrated by simple examples. Time-dependent processes and quantum dynamics are presented and discussed in relation to spectroscopic observations. Coherent and incoherent radiative excitation and radiationless transitions are treated in relation to applications in molecular spectroscopy.

Keywords: Quantum mechanics; time-dependent and time-independent Schrödinger equation; selection rules; stationary states; time-dependent perturbation theory; Heisenberg uncertainty principle; Fourier transformations; quantum dynamics; time-resolved spectroscopy; light scattering; Raman spectroscopy; absorption; spontaneous emission; stimulated emission; Born–Oppenheimer approximation; group theory; character tables; reducible and irreducible representations; normal modes; electronic configurations and states; lineshapes; line broadening; radiationless transitions; molecular symmetry; coherent excitation; classical mechanics

Molecular Quantum Mechanics and Molecular Spectra, Molecular Symmetry, and Interaction of Matter with Radiation

Frédéric Merkt and Martin Quack

Laboratorium für Physikalische Chemie, ETH Zürich, Zürich, Switzerland

"*The language of spectra, a true atomic music of the spheres*"
Sommerfeld (1919), as translated and cited by Pais (1991)

1 INTRODUCTION

The aim of this article is to introduce the basic experimental and theoretical concepts underlying molecular spectroscopy. At a purely empirical level, human color vision can be considered to be a form of spectroscopy, although the relation between the observed "color" of light and the electromagnetic spectrum is not simple. In that sense, auditory perception can be considered to be a better frequency analyzer, although this would be considered a spectroscopy of sound rather than of electromagnetic radiation. The relation between spectroscopy and music has been addressed in the words of Sommerfeld, which themselves refer implicitly to the earliest days of human science, as cited at the beginning of this article.

Early spectroscopic experiments, leading later to applications in chemistry, can be followed in history from Newton's spectrum, the observation of the "Fraunhofer lines" in the solar spectrum as appearing on the cover of this handbook, infrared spectra observed by the Herschels (father and son), ultraviolet (UV) photochemistry observed by Ritter, and, finally, the start of chemical, analytical, and astronomical spectroscopy with the work of Bunsen and Kirchhoff in the nineteenth century. The "mathematical harmony" of the spectral lines of the hydrogen atom was found by Balmer (1885a,b). The key to modern spectroscopy arises, however, from quantum theory, starting with an understanding of the intensity distribution of blackbody radiation on the basis of quantization by Planck (1900a,b), the understanding of the photoelectric effect with the photon concept due to Einstein (1905), and most directly the understanding of the spectrum of the hydrogen atom on the basis of the "old" quantum theory as introduced by Bohr, (1913a,b,c,d) including also Bohr's condition for spectroscopic transitions between energy levels E_i and E_f connected by the absorption or emission of photons with frequency ν_{fi} and Planck's constant h:

$$\left|\Delta E_{fi}\right| = \left|E_f - E_i\right| = h\nu_{fi} \tag{1}$$

This equation, together with Bohr's theory of the hydrogen atom as a dynamical system having a quantized energy-level structure, forms the basis of the use of line-resolved high-resolution spectroscopy in understanding the dynamics of atomic and molecular—later, also nuclear—systems. The underlying quantum dynamical theory of such microscopic systems was then completed by introducing "modern" quantum theory in the work of Heisenberg (1925), Schrödinger, (1926a,b,c,d,e), and Dirac (1927, 1929). In essence, current high-resolution molecular spectroscopy relies on the use of this theoretical framework in its application to furthering our knowledge on the fundamental aspects of molecular quantum dynamics as well as in its numerous practical applications in science and technology.

The outline of this introductory article to this handbook is thus briefly as follows. In Section 2, we introduce

Handbook of High-resolution Spectroscopy. Edited by Martin Quack and Frédéric Merkt.
ISBN: 978-0-470-74959-3.

some basic equations of quantum mechanics as needed for spectroscopy. Section 3 treats the quantum dynamics of coherent radiative transitions. Section 4 discusses the basic concepts underlying spectroscopic experiments. Section 5 gives a brief introduction to the characteristics of molecular energy levels. Section 6 discusses molecular symmetry (MS) and basic group theory as relevant to spectroscopy. Section 7 deals with radiationless transitions and lineshapes for high-resolution spectroscopy.

2 QUANTUM MECHANICS AND SPECTROSCOPY

Quantum mechanics provides the underlying theory for molecular spectroscopy. It is dealt with in much detail in relevant text books by Messiah (1961), Cohen-Tannoudji *et al*. (1973), Sakurai (1985), and Landau and Lifshitz (1985). For the historical background, one can also consult Dirac (1958) and Heisenberg (1930), which remain of interest for the fundamental concepts. The aim of the present section is to introduce some of the basic concepts and definitions. This can obviously not replace a more detailed introduction to quantum mechanics, which can be found in the textbooks cited as well as in numerous other books on this topic.

2.1 Classical Mechanics and Quantum Mechanics

Many systems in both classical and quantum mechanics can be described by the motion of interacting point particles, where the physical "particles" are replaced by points of mass m_k with position at the center of mass of the particle. For planetary systems, the "particles" would be the sun and planets with their moons (plus planetoids and artificial satellites, etc.). For atomic and molecular systems the "point particles" can be taken to be the nuclei and electrons to within a good approximation.

In classical dynamics, one describes such an N-particle system by a point in the mathematical phase space, which has dimension $6N$ with $3N$ coordinates (for instance Cartesian coordinates x_k, y_k, z_k for each particle "k") and $3N$ momenta p_{x_k}, p_{y_k}, p_{z_k}. Such a point in phase space moving in time contains all mechanically relevant information of the dynamical system. In the nineteenth-century Hamiltonian formulation of classical mechanics, one writes the Hamiltonian function H as the sum of the kinetic (T) and potential V energies:

$$H = T + V \tag{2}$$

in terms of generalized coordinates q_k and their conjugate momenta p_k (Landau and Lifshitz 1966, Goldstein 1980, Iro 2002). Following Hamilton, one obtains the canonical Hamiltonian differential equations of motion accordingly:

$$\frac{\mathrm{d}q_k}{\mathrm{d}t} = \dot{q}_k = \left(\frac{\partial H}{\partial p_k}\right) \tag{3}$$

$$\frac{\mathrm{d}p_k}{\mathrm{d}t} = \dot{p}_k = -\left(\frac{\partial H}{\partial q_k}\right) \tag{4}$$

The dynamics of the classical system is thus obtained from the solution of $6N$ coupled differential equations. Provided that one knows some exact initial condition for one point in phase space, all future and past states of the system in terms of the set $\{q_k(t), p_k(t)\}$ can be calculated exactly. Further considerations arise if the initial state is not known exactly, but we do not pursue this further.

One approach to quantum dynamics replaces the functions H, p_k, q_k by the corresponding quantum mechanical operators ($\hat{H}$, $\hat{p}_k$, $\hat{q}_k$) or their matrix representations ($\boldsymbol{H}$, $\boldsymbol{p}_k$, $\boldsymbol{q}_k$) resulting in the Heisenberg equations of motion:

$$\frac{\mathrm{d}\hat{q}_k}{\mathrm{d}t} = \frac{2\pi}{\mathrm{i}h}\left[\hat{q}_k, \hat{H}\right] \tag{5}$$

$$\frac{\mathrm{d}\hat{p}_k}{\mathrm{d}t} = \frac{2\pi}{\mathrm{i}h}\left[\hat{p}_k, \hat{H}\right] \tag{6}$$

which involve now Planck's quantum of action (or constant) h, and $\mathrm{i} = \sqrt{-1}$. Following Dirac (1958), these equations are the quantum mechanical equivalent of the Poisson-bracket formulation of classical mechanics and one can, in fact, derive the corresponding classical equations of motion from the Heisenberg equations of motion if one uses quantum mechanics as the more fundamental starting point (see Sakurai (1985), for instance). The classical limit of quantum mechanics has also found interest in molecular reaction dynamics in a different framework (Miller 1974, 1975). Equations (5) and (6) contain the commutator of two operators $\hat{A}$ and $\hat{B}$ in general notation:

$$\left[\hat{A}, \hat{B}\right] = \hat{A}\hat{B} - \hat{B}\hat{A} \tag{7}$$

As quantum mechanical operators and their matrix representations do not, in general, commute, this introduces a new element into quantum mechanics as compared to classical mechanics. For instance, in Cartesian coordinates the coordinate operator $\hat{x}_k$ is simply multiplicative, while the momentum operator $\hat{p}_{x_k}$ is given by the differential operator

$$\hat{p}_{x_k} = \frac{h}{2\pi\mathrm{i}}\frac{\partial}{\partial x_k} \tag{8}$$

leading to the commutator

$$\left[\hat{x}_k,\ \hat{p}_{x_k}\right] = \mathrm{i}\frac{h}{(2\pi)} \tag{9}$$

and the corresponding Heisenberg uncertainty relation (Messiah 1961)

$$\Delta x_k \Delta p_{x_k} \geq \frac{h}{(4\pi)} \tag{10}$$

where Δx_k and Δp_{x_k} are defined as the root mean square deviations of the corresponding ideal measurement results for the coordinates x_k and momenta p_{x_k}. Similar equations apply to y_k, z_k with p_{y_k}, p_{z_k}, etc. for all particles labeled by their index k. It is thus impossible in quantum mechanical systems to know experimentally the position of the "point in phase space" to a better accuracy than allowed by the Heisenberg uncertainty relation in a quantum mechanical state. In classical mechanics, on the other hand, the x_k and p_{x_k}, etc., commute and the point in phase space can, in principle, be defined and measured with arbitrary accuracy.

A somewhat more complex reasoning leads to a similar "fourth" uncertainty relation for energy E and time t:

$$\Delta E \Delta t \geq \frac{h}{(4\pi)} \tag{11}$$

We note that equations (10) and (11) are strictly *inequalities*, not equations in the proper sense. Depending on the system considered, the uncertainty can be *larger* than what would be given by the strict equation. If the equal sign in equations (10) and (11) applies, one speaks of a "minimum-uncertainty state or wave packet" (see below). The commutators in equations (5) and (6) are readily obtained from the form of the kinetic energy operator in Cartesian coordinates:

$$\hat{T} = \frac{1}{2} \sum_{k=1}^{N} \left(\frac{\hat{p}_{x_k}^2}{m_k} + \frac{\hat{p}_{y_k}^2}{m_k} + \frac{\hat{p}_{z_k}^2}{m_k} \right) \tag{12}$$

and

$$\hat{H} = \hat{T} + \hat{V} \tag{13}$$

if the potential energy $\hat{V}$ is a multiplicative function of the coordinates of the particles (for instance, with the Coulomb potential for charged particles).

While this so-called Heisenberg representation of quantum mechanics is of use for some formal aspects and also certain calculations, frequently, the "Schrödinger representation" turns out to be useful in spectroscopy.

2.2 Time-dependent and Time-independent Schrödinger Equation

2.2.1 Time-dependent Schrödinger Equation

In the Schrödinger formulation of quantum mechanics ("wave mechanics"), one introduces the "wavefunction" $\Psi(x_1, y_1, z_1, \ldots, x_N, y_N, z_N, t)$ depending on the particle coordinates and time and satisfying the differential equation (time-dependent Schrödinger equation)

$$\mathrm{i}\frac{h}{2\pi} \frac{\partial \Psi(x_1, y_1, z_1, \ldots, x_N, y_N, z_N, t)}{\partial t} = \hat{H}\, \Psi(x_1, y_1, z_1, \ldots, x_N, y_N, z_N, t) \tag{14}$$

The physical significance of the wavefunction Ψ (also called *state function*) can be visualized by the probability density

$$\begin{aligned} &P(x_1, y_1, z_1, \ldots, x_N, y_N, z_N, t) \\ &\quad = \Psi(x_1 \ldots z_N, t) \Psi^*(x_1 \ldots z_N, t) \\ &\quad = |\Psi(x_1 \ldots z_N, t)|^2 \end{aligned} \tag{15}$$

P is real, positive, or zero, whereas Ψ is, in general, a complex-valued function.

$P(x_1, y_1, z_1, \ldots, z_N, t)\, \mathrm{d}x_1 \mathrm{d}y_1 \mathrm{d}z_1 \ldots \mathrm{d}z_N$ gives the probability of finding the quantum mechanical system of point particles in the volume element $(\mathrm{d}x_1 \ldots \mathrm{d}z_N)$ at position $(x_1, \ldots, z_N)$ at time t.

The differential operator in equation (14) is sometimes called the *energy operator* $\hat{E}$

$$\hat{E} = \mathrm{i}\frac{h}{2\pi} \frac{\partial}{\partial t} \tag{16}$$

Thus one can write

$$\hat{E}\, \Psi(r, t) = \hat{H}\, \Psi(r, t) \tag{17}$$

where we introduce the convention that r represents, in general, a complete set of space (and spin) coordinates and includes the special case of systems depending only on one coordinate, which then can be called r.

The solution of equation (14) has the form

$$\Psi(r, t) = \hat{U}\,(t, t_0) \Psi(r, t_0) \tag{18}$$

The time-evolution operator $\hat{U}\,(t, t_0)$ operating on $\Psi(r, t_0)$ produces the function $\Psi(r, t)$. $\hat{U}$ satisfies the differential equation

$$\mathrm{i}\frac{h}{2\pi} \frac{\partial \hat{U}\,(t, t_0)}{\partial t} = \hat{H}\hat{U}\,(t, t_0) \tag{19}$$

Thus, in general, one has to solve this differential equation in order to obtain $\hat{U}\,(t, t_0)$. If, however, $\hat{H}$ does not depend upon time, $\hat{U}\,(t, t_0)$ is given by the equation

$$\hat{U}\,(t, t_0) = \exp\left[-\frac{2\pi\mathrm{i}}{h} \hat{H} \cdot (t - t_0) \right] \tag{20}$$

The exponential function of an operator $\hat{Q}$ as a matrix representation of this operator is given by equation (21):

$$\exp(\hat{Q}) = \sum_{n=0}^{\infty} \frac{\hat{Q}^n}{n!} \tag{21}$$

One of the most important properties of Ψ is that it satisfies the principle of linear superposition. If $\Psi_1(r, t)$ and $\Psi_2(r, t)$ satisfy equation (14) as possible representations of the dynamical state of the system, then the linear superposition

$$\Psi(r, t) = c_1\Psi_1(r, t) + c_2\Psi_2(r, t) \tag{22}$$

is also a possible dynamical state satisfying equation (14), as is readily shown, given that $\hat{H}$ is a linear operator and c_1, c_2 are complex coefficients. However, $\Psi(r, t)$, in general, is not an eigenstate of $\hat{H}$.

2.2.2 *Special Case of Stationary States and Time-independent Schrödinger Equation*

We assume that $\hat{H}$ does not depend on time. We consider the special case where $\Psi_k(r, t)$ is an eigenfunction of $\hat{H}$ with eigenvalue E_k. Thus

$$\hat{H}\,\Psi_k(r, t) = \hat{E}\Psi_k(r, t) = E_k\Psi_k(r, t) \tag{23}$$

The solution for this special case is given by equation (24):

$$\begin{aligned} \mathrm{i}\frac{h}{2\pi}\frac{\partial\Psi_k(r, t)}{\partial t} &= E_k\Psi_k(r, t) \\ &= E_k\psi_k(r)\exp\left(-2\pi\mathrm{i}\frac{E_k t}{h}\right) \end{aligned} \tag{24}$$

$\hat{H}$ being independent of time, one can divide equation (23) by $\exp(-2\pi\mathrm{i}E_k t / h)$ and obtain

$$\hat{H}\,\psi_k(r) = E_k\psi_k(r) \tag{25}$$

The eigenfunctions of $\hat{H}$ are called *stationary states*

$$\Psi_k(r, t) = \psi_k(r)\exp\left(-2\pi\mathrm{i}\frac{E_k t}{h}\right) \tag{26}$$

The name for stationary states is related to the time independence of the probability density

$$P(r, t) = \Psi_k(r, t)\,\Psi_k^*(r, t) = |\Psi_k(r, t)|^2 = \left|\psi_k(r)\right|^2 \tag{27}$$

The time-independent Schrödinger equation (25) is thus derived as a special case from the time-dependent Schrödinger equation.

2.2.3 *General Time-dependent States*

Making use of the superposition principle (equation 22), the general solution of the Schrödinger equation results as follows:

$$\Psi(r, t) = \sum_k c_k\psi_k(r)\exp\left(-2\pi\mathrm{i}\frac{E_k t}{h}\right) = \sum_k c_k\Psi_k(r, t) \tag{28}$$

If $\hat{H}$ does not depend on time, such as in the case of isolated atomic and molecular systems, the coefficients c_k are time independent, generally complex coefficients. According to the principle of spectral decomposition, the probability of measuring an energy E_k in the time-dependent state given by equation (28) is

$$p_k(E_k) = |c_k|^2 = c_k c_k^* \tag{29}$$

Thus, with time-independent $\hat{H}$, the p_k are independent of time as is also the expectation value of the energy

$$\langle E(t)\rangle = \sum |c_k|^2\,E_k \tag{30}$$

Figure 1 illustrates the spectral decomposition for two types of spectra. With high-resolution spectroscopy providing the E_k and ψ_k, equation (28) provides the basis for

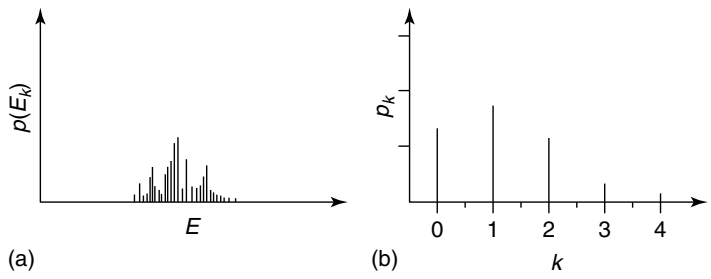

Figure 1 Spectral decomposition schemes: illustration of spectral decomposition of a time-dependent state. $p_k(E_k) = |c_k|^2$ is the probability of measuring the eigenvalue E_k in the time-dependent state given by $\Psi(r, t)$. (a) Irregular spectrum and distribution. (b) Harmonic oscillator with a Poisson distribution.

constructing a general time-dependent state from high-resolution spectroscopic results. The energy in a time-dependent state is therefore not a well-defined quantity, but it is only defined by means of a statistical distribution given by p_k. The distribution satisfies the uncertainty relation given by equation (11).

2.3 Time-evolution Operator Formulation of Quantum Mechanics

Equation (19) can be made the starting point for a general formulation of quantum mechanics. $\hat{U}$ provides not only the solution of the Schrödinger equation according to equation (18) but also of the time dependence of the density operator (see, for instance, Messiah (1961) and Sakurai (1985))

$$\hat{\rho}(t) = \sum_n p_n \left|\Psi_n\right\rangle \left\langle\Psi_n\right| \tag{31}$$

satisfying the Liouville–von Neumann equation

$$\mathrm{i}\frac{h}{2\pi}\frac{\mathrm{d}\hat{\rho}(t)}{\mathrm{d}t} = \left[\hat{H}, \hat{\rho}(t)\right] \tag{32}$$

by means of the solution

$$\hat{\rho}(t) = \hat{U}(t, t_0)\hat{\rho}(t_0)\hat{U}^{\dagger}(t, t_0) \tag{33}$$

This equation is of particular importance for statistical mechanics.

Furthermore, the Heisenberg equations of motion (equations 5 and 6) for the operators $\hat{p}_k$ and $\hat{q}_k$, as for any generalized operator $\hat{Q}$ corresponding to the dynamical observable Q, are solved by means of the equation

$$\hat{Q}(t) = \hat{U}^{\dagger}(t, t_0)\hat{Q}(t_0)\hat{U}(t, t_0) \tag{34}$$

This equation is of importance for time-resolved spectroscopy, where one might, for instance, observe the time-dependent electric dipole moment $\boldsymbol{M}(t)$ described by the dipole operator $\hat{\boldsymbol{\mu}}$. We note the difference in sign of equation (32) and the Heisenberg equations of motion, with resulting differences for the solutions given by equations (33) and (34). This is no contradiction, as the density operator $\hat{\rho}$ does not correspond to a dynamical variable (observable) of the quantum system.

Given a complete orthonormal basis φ_k, which can also be the eigenstate basis ψ_k, one can define matrix representations of the various operators

$$Q_{jk} = \left\langle \varphi_j \middle| \hat{Q} \middle| \varphi_k \right\rangle = \int_{-\infty}^{+\infty} \varphi_j^* \hat{Q} \varphi_k \mathrm{d}r \tag{35}$$

where, consistent with our definitions above, the notation r stands either for the relevant coordinate in a one-dimensional system and the integration is carried out over the range of definition of r, or else r represents the set of all coordinates and the integration corresponds to a multiple integral over the space of all coordinates. The equations given above for operators remain valid for the corresponding matrix representations replacing the operators $\hat{Q}$ by the corresponding matrices $\boldsymbol{Q}$.

2.4 Time-dependent Perturbation Theory and Matrix Representation of the Schrödinger Equation

We consider a decomposition of the Hamiltonian $\hat{H}$ according to a zero-order Hamiltonian $\hat{H}_0$ (which might be useful, if the Schrödinger equation with $\hat{H}_0$ has a simple analytical solution such as a collection of harmonic oscillators) and a "perturbation" operator $\hat{V}$ needed to complement $\hat{H}_0$ in order to describe the complete Hamiltonian

$$\hat{H} = \hat{H}_0 + \hat{V} \tag{36}$$

We assume $\hat{H}_0$ and $\hat{V}$ to be time independent, although many of the following steps can be carried out similarly with time-dependent Hamiltonians and "perturbations" $\hat{V}$. The perturbation might sometimes be small, but this is not necessary. We assume the solution of the Schrödinger equation to be known with $\hat{H}_0$

$$\hat{H}_0\varphi_k(r) = E_k\varphi_k(r) \tag{37}$$

The φ_k form a complete basis and the general wavefunction is given by

$$\Psi(r, t) = \sum c_k(t)\varphi_k(r)\exp\left(-2\pi\mathrm{i}\frac{E_k t}{h}\right) \tag{38}$$

Here the coefficients $c_k(t)$ depend explicitly upon time because the φ_k are *not* eigenfunctions of $\hat{H}$. If the $\varphi_k(r)$ and E_k are known, the time dependence of the $c_k(t)$ provides, in essence, the solution of the Schrödinger equation with the complete Hamiltonian including the perturbation $\hat{V}$. Inserting $\Psi(r, t)$ into the time-dependent Schrödinger equation (14) with $\hat{H} = \hat{H}_0 + \hat{V}$ and simplifying the equations by means of the matrix representation of the operator $\hat{V}$ (equation 35)

$$V_{jk} = \left\langle \varphi_j \middle| \hat{V} \middle| \varphi_k \right\rangle \tag{39}$$

one obtains a set of coupled differential equations

$$\mathrm{i}\frac{h}{2\pi}\frac{\mathrm{d}c_j(t)}{\mathrm{d}t} = \sum_k \exp(\mathrm{i}\omega_{jk}t)V_{jk}c_k(t) \tag{40}$$

where we use the abbreviations

$$\omega_{jk} = \omega_j - \omega_k = \frac{2\pi E_j}{h} - \frac{2\pi E_k}{h} \tag{41}$$

Defining a matrix element of some kind of Hamiltonian matrix,

$$\tilde{H}_{jk} = \exp(\mathrm{i}\omega_{jk}t)V_{jk} \tag{42}$$

the set of equations defined by equation (40) can be written in matrix notation:

$$\mathrm{i}\frac{h}{2\pi}\frac{\mathrm{d}\boldsymbol{c}(t)}{\mathrm{d}t} = \tilde{\boldsymbol{H}}(t)\boldsymbol{c}(t) \tag{43}$$

In this matrix representation, $\tilde{\boldsymbol{H}}(t)$ depends on time. However, one can make the substitution

$$a_k = \exp(-\mathrm{i}\omega_k t)c_k \tag{44}$$

and obtain

$$\mathrm{i}\frac{h}{2\pi}\frac{\mathrm{d}a_j}{\mathrm{d}t} = \left(\sum_k V_{jk}a_k\right) + \frac{h}{2\pi}\omega_j a_j \tag{45}$$

Defining the diagonal matrix

$$\boldsymbol{E}_{\mathrm{Diag}} = \left\{E_j = \frac{h\omega_j}{(2\pi)}\right\} \tag{46}$$

one obtains

$$\mathrm{i}\frac{h}{2\pi}\frac{\mathrm{d}\boldsymbol{a}(t)}{\mathrm{d}t} = \left\{\boldsymbol{E}_{\mathrm{Diag}} + \boldsymbol{V}\right\}\boldsymbol{a} = \boldsymbol{H}^{(a)}\boldsymbol{a}(t) \tag{47}$$

where $\boldsymbol{a}$ is the column matrix of coefficients $\boldsymbol{a} = (a_1, a_2, \ldots a_k, \ldots a_n)^{\mathrm{T}}$ and $\boldsymbol{H}^{(a)}$ is a time-independent matrix representation of the Hamiltonian as defined above.

Equation (47) is thus a matrix representation of the original Schrödinger equation, which makes the influence of the perturbation $\hat{V}$ explicit. The corresponding time-independent Schrödinger equation is obtained following Section 2.2.2 and we do not repeat the corresponding equations. The solution of equation (47) is given by the matrix representations of equations (18)–(20). Thus

$$\boldsymbol{a}(t) = \boldsymbol{U}^{(a)}(t, t_0)\boldsymbol{a}(t_0) \tag{48}$$

with

$$\boldsymbol{U}^{(a)}(t, t_0) = \exp(-2\pi\mathrm{i}\boldsymbol{H}^{(a)}(t - t_0)/h) \tag{49}$$

These equations are generally useful for numerical computation, provided that the basis functions φ_k and the E_k are known and the matrix elements V_{jk} needed in equation (47) can be computed accordingly. Equations (48) and (49) are equivalent to the original Schrödinger equation. Approximations arise from the truncation of the generally infinite matrices at finite size, from errors introduced by the numerical algorithms used for the calculations of matrix elements, and in the calculations of the various matrix operations.

3 QUANTUM DYNAMICS OF SPECTROSCOPIC TRANSITIONS UNDER EXCITATION WITH COHERENT MONOCHROMATIC RADIATION

3.1 General Aspects

While traditional spectroscopy in the optical domain has used weak, incoherent (quasi-thermal) light sources (see also Section 4), present-day spectroscopy frequently uses high-power coherent laser light sources allowing for a variety of phenomena ranging from coherent single-photon transitions to multiphoton transitions of different types. Figure 2 provides a summary of mechanisms for such transitions.

While excitation with incoherent light can be based on a statistical treatment (Section 4), excitation with coherent light can be handled by means of quantum dynamics as outlined in Section 2. Intense, coherent laser radiation as also electromagnetic radiation in the radiofrequency domain used in nuclear magnetic resonance (NMR) spectroscopy (Ernst *et al*. 1987) can be treated as a classical electromagnetic wave satisfying the general wave equations (50) and (51) resulting from Maxwell's theory:

$$\nabla^2\boldsymbol{E} = \mu\mu_0\varepsilon\varepsilon_0\frac{\partial^2\boldsymbol{E}}{\partial t^2} \tag{50}$$

$$\nabla^2\boldsymbol{B} = \mu\mu_0\varepsilon\varepsilon_0\frac{\partial^2\boldsymbol{B}}{\partial t^2} \tag{51}$$

$\boldsymbol{E}$ is the electric field vector and $\boldsymbol{B}$ the magnetic field vector (magnetic induction), μ, μ_0, ε, ε_0 are the normal field constants (*see* Stohner and Quack 2011: **Conventions, Symbols, Quantities, Units and Constants for High-resolution Molecular Spectroscopy**, this handbook), with $\varepsilon = \mu = 1$ in vacuo. The nabla operator ∇ is defined by equation (52):

$$\nabla = \boldsymbol{e}_x\frac{\partial}{\partial x} + \boldsymbol{e}_y\frac{\partial}{\partial y} + \boldsymbol{e}_z\frac{\partial}{\partial z} \tag{52}$$

where $\boldsymbol{e}_x$, $\boldsymbol{e}_y$, $\boldsymbol{e}_z$ are the unit vectors in a right-handed Cartesian coordinate system. The classical electromagnetic

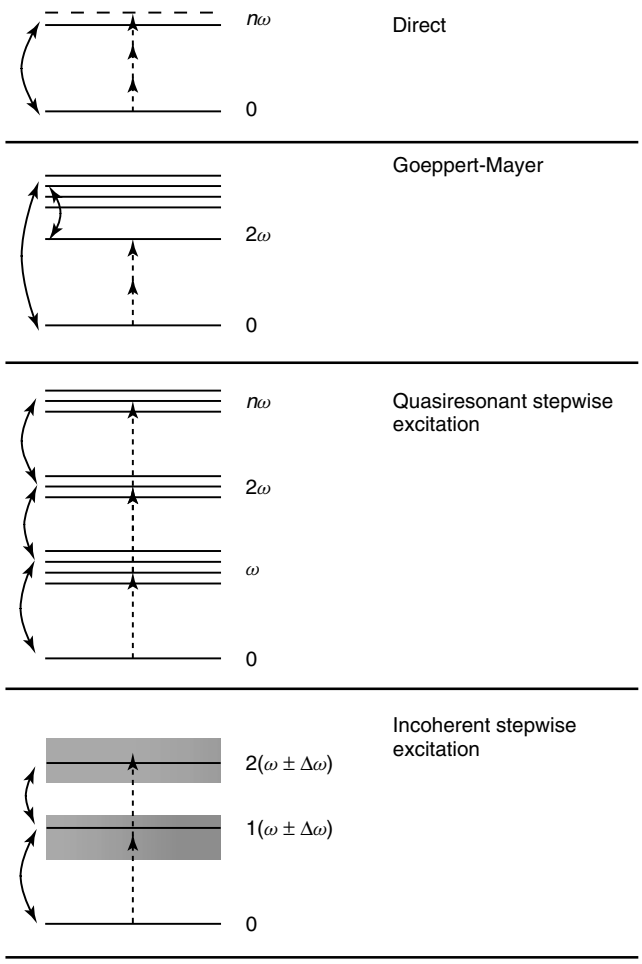

Figure 2 Mechanisms for radiative excitation. [After Quack (1998).] Dotted lines give the transitions, curved full lines, the dipole coupling.

wave can be understood as the coherent state description of the quantum field in the limit of very large average number $\langle n \rangle$ of quanta per field mode (Glauber 1963a,b, Perelomov 1986). Coherent laser radiation and also radiofrequency radiation are frequently characterized by $\langle n \rangle > 10^{10}$. Thus the classical approximation to the electromagnetic field is excellent. The situation of weak thermal light sources in the optical domain is very different ($\langle n \rangle < 1$), requiring a quantum statistical treatment (Section 4).

We consider here, for simplicity, the special case of a classical z-polarized electromagnetic wave propagating in vacuo in the y-direction with slowly varying (or constant) field amplitudes $\boldsymbol{E}_0(t)$ and $\boldsymbol{B}_0(t)$ (see Figure 3):

$$E_z(y,t) = |E_0(t)| \cos(\omega t + \eta' - k_\omega y) \tag{53}$$

$$B_x(y,t) = |B_0(t)| \cos(\omega t + \eta' - k_\omega y) \tag{54}$$

$\omega = 2\pi\nu$ is the angular frequency, $k_\omega = 2\pi/\lambda$ the angular wavenumber, $\nu = c/\lambda$ the ordinary frequency and λ the wavelength. At a given position y the phase η' can be combined with the phase $-k_\omega y$ to an overall phase ($\eta = k_\omega y - \eta'$).

The extension to more general cases is straightforward (see also Quack (1998)). The intensity of the radiation is, in general,

$$I(y,t) = |E_z(y,t)|^2 \sqrt{\frac{\varepsilon\varepsilon_0}{\mu\mu_0}} \tag{55}$$

and averaging over time with $\langle \cos^2 x \rangle = 1/2$, one has from equations (53) and (55)

$$I(t) = \frac{1}{2} |E_0(t)|^2 \sqrt{\frac{\varepsilon\varepsilon_0}{\mu\mu_0}} \tag{56}$$

For the speed of light, one has in some medium with refractive index n_m

$$c_m = (\mu\mu_0\varepsilon\varepsilon_0)^{-1/2} = \frac{c}{n_m} \tag{57}$$

and in vacuo ($\mu = \varepsilon = 1$)

$$c = (\mu_0\varepsilon_0)^{-1/2} \tag{58}$$

We can mention here some practical equations for calculating electric and magnetic field strengths when irradiating with monochromatic radiation of given intensity I:

$$\left| \frac{E_0}{V\ \mathrm{cm}^{-1}} \right| \simeq 27.44924 \sqrt{\frac{I}{W\ \mathrm{cm}^{-2}}} \tag{59}$$

$$\left| \frac{B_0}{T} \right| \simeq 9.156 \times 10^{-6} \sqrt{\frac{I}{W\ \mathrm{cm}^{-2}}} \tag{60}$$

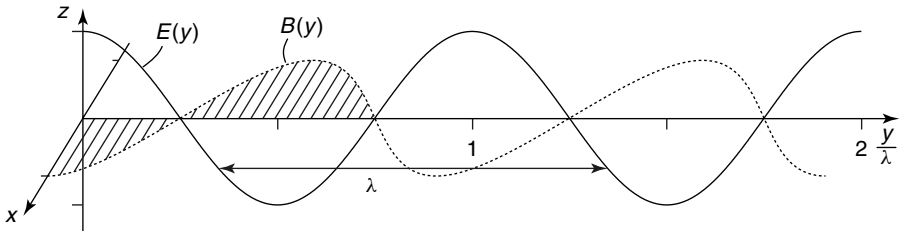

Figure 3 Schematic representation of a z-polarized monochromatic wave.

A further quantity characterizing the irradiation over some period of time t is the fluence $F(t)$ defined by equation (61):

$$F(t) = \int_0^t I(t')\mathrm{d}t' \tag{61}$$

For wavelengths $\lambda > 100\,\mathrm{nm}$, one can assume E and B to be constant over the extension of the atomic or molecular system at any given time ($\Delta y > 1\,\mathrm{nm}$), which leads to the dipole approximation for the interaction energy between molecule and field:

$$\hat{V}_{\text{el. dipole}} = -\boldsymbol{\mu}_{\text{el}} \cdot \boldsymbol{E} \tag{62}$$

where $\boldsymbol{\mu}_{\text{el}}$ is the electric dipole vector given by equation (63), with charges q_i for the particles with position vector $\boldsymbol{r}_i$:

$$\boldsymbol{\mu}_{\text{el}} = \sum_i q_i \boldsymbol{r}_i \tag{63}$$

Similarly, one has the interaction energy with a magnetic dipole $\boldsymbol{\mu}_{\text{magn}}$

$$\hat{V}_{\text{magn. dipole}} = -\boldsymbol{\mu}_{\text{magn}} \cdot \boldsymbol{B} \tag{64}$$

For the present quantum dynamical treatment of coherent excitation, we restrict our attention to electric dipole transitions in a field given by equation (53), and therefore we can write, with the z-component μ_z of the electric dipole operator (and abbreviating $\eta = k_\omega y - \eta'$), as follows:

$$\hat{V}_{\text{el. dipole}} = -\hat{\mu}_z E_z(y,t) = -\hat{\mu}_z \,|E_0(t)|\cos(\omega t - \eta) \tag{65}$$

The extension to magnetic dipole transitions is straightforward. We give here only a brief summary and refer to Quack (1978, 1982, 1998) for more detail.

3.2 Time-dependent Quantum Dynamics in an Oscillatory Electromagnetic Field

We consider now the time-dependent Schrödinger equation (14) with a time-dependent Hamiltonian

$$\hat{H}(t) = \hat{H}_{\text{Mol}} - \mu_z \,|E_0(t)|\cos(\omega t - \eta) \tag{66}$$

which is of the form of equation (36), with $\hat{H}_{\text{Mol}}$ being the time-independent Hamiltonian for the isolated molecule in the absence of fields and the interaction Hamiltonian $\hat{V}$ is now a time-dependent, oscillatory function. We assume the solution of the time-independent Schrödinger equation for the isolated molecule to be given by equation (67) ($\hbar = h/2\pi$):

$$\hat{H}_{\text{Mol}}\varphi_k = E_k\varphi_k = \hbar\omega_k\varphi_k \tag{67}$$

and write the solution of the time-dependent Schrödinger equation in the basis φ_k of molecular eigenstates with time-dependent coefficients:

$$\Psi(r,t) = \sum_k b_k(t)\varphi_k(r) \tag{68}$$

Inserting this into equation (14), we obtain a set of coupled differential equations:

$$i\hbar\frac{\mathrm{d}b_j}{\mathrm{d}t} = \sum_k H_{jk}b_k(t) \tag{69}$$

or in matrix notation,

$$i\hbar\frac{\mathrm{d}\mathbf{b}(t)}{\mathrm{d}t} = \boldsymbol{H}(t)\mathbf{b}(t) \tag{70}$$

This is again, in essence, a matrix representation of the original Schrödinger equation (see Section 2). Assuming molecular states of well-defined parity, the diagonal electric dipole matrix elements vanish and we have the diagonal elements of $\boldsymbol{H}(t)$:

$$H_{ii} = E_i = \left\langle \varphi_i \left| \hat{H}_{\text{Mol}} \right| \varphi_i \right\rangle \equiv \hbar\omega_i \tag{71}$$

For other situations such as for chiral molecules or if parity violation were important (*see* Quack 2011: **Fundamental Symmetries and Symmetry Violations from High-resolution Spectroscopy**, this handbook), one would have also a diagonal contribution from the electric dipole interaction energy. Disregarding such cases here, the electric dipole interaction energy leads to off-diagonal matrix elements:

$$H_{kj} = \left\langle \varphi_k \left| \hat{V}_{\text{el. dipole}}(t) \right| \varphi_j \right\rangle \tag{72}$$

Dividing H_{kj} by $\hbar\cos(\omega t - \eta)$ we obtain a matrix element V_{kj}, which is independent of time, if we can assume $|E_0(t)|$ to be sufficiently slowly varying in time that it can be taken constant for the time period under consideration, as we shall do, replacing $E_0(t)$ by E_0,

$$V_{kj} = \frac{H_{kj}}{[\hbar\cos(\omega t - \eta)]} = -\left\langle \varphi_k \left| \hat{\mu}_z \right| \varphi_j \right\rangle \frac{|E_0|}{\hbar} = V_{jk}^* \tag{73}$$

We then obtain a set of coupled differential equations in matrix notation:

$$\mathrm{i}\frac{\mathrm{d}}{\mathrm{d}t}\mathbf{b}(t) = \{\mathbf{W} + \mathbf{V}\cos(\omega t - \eta)\}\,\mathbf{b}(t) \tag{74}$$

where we have defined the diagonal matrix $\boldsymbol{W}$ by the matrix elements $W_{kk} \equiv \omega_k$.

This is still a practically exact representation of the original time-dependent Schrödinger equation for the physical situation considered here. Because of the essential time dependence in $\mathbf{V}\cos(\omega t - \eta)$, there is no simple closed expression in the form of the exponential function analogous to equations (18), (20) or (48), (49). Apart from numerical, stepwise solutions discussed in Quack (1998), one can make use of series expansions such as the Magnus expansion. This solves equation (70) by means of the following series for $\boldsymbol{U}(t, t_0)$:

$$\mathbf{b}(t) = \boldsymbol{U}(t, t_0)\mathbf{b}(t_0) \tag{75}$$

$$\boldsymbol{U}(t_0, t_0) = 1 \tag{76}$$

$$\boldsymbol{U}(t, t_0) = \exp\left(\sum_{n=0}^{\infty} \mathbf{C}_n\right) \tag{77}$$

The first two terms are given by the following expressions:

$$\mathrm{i}\hbar\mathbf{C}_0 = \int_{t_0}^{t} \boldsymbol{H}(t')\mathrm{d}t' \tag{78}$$

$$\mathrm{i}\hbar\mathbf{C}_1 = -\frac{1}{2}\int_{t_0}^{t}\left\{\int_{t_0}^{t''}\left[\boldsymbol{H}(t'), \boldsymbol{H}(t'')\right]\mathrm{d}t'\right\}\mathrm{d}t'' \tag{79}$$

Higher terms contain more complex combinations of commutators of the type $\left[\boldsymbol{H}(t'), \boldsymbol{H}(t'')\right]$. From this one recognizes that the series terminates after the first term given by equation (78), if $\boldsymbol{H}(t')$ and $\boldsymbol{H}(t'')$ commute at all t', t'', which is true if $\boldsymbol{H}$ does not depend on time, resulting in the exponential solutions already discussed. There are other (rare) cases of time-dependent $\boldsymbol{H}(t)$, but with $\left[\boldsymbol{H}(t'), \boldsymbol{H}(t'')\right] = 0$. One can, however, also make use of the periodicity of the field using Floquet's theorem (Quack 1978, 1998).

3.3 Floquet Solution for Hamiltonians with Strict Periodicity

With $\boldsymbol{H} = \hbar\{\boldsymbol{W} + \boldsymbol{V}\cos(\omega t - \eta)\}$ from equation (74), one has obviously

$$\boldsymbol{H}(t + \tau) = \boldsymbol{H}(t) \tag{80}$$

with period $\tau = 2\pi/\omega$.

Making use of the Floquet theorem (or Floquet–Liapounoff theorem, see Quack, (1978, 1998) for the historical references), one has the following form for the time-evolution matrix (with some integer n):

$$\boldsymbol{U}(t, t_0) = \mathbf{F}(t, t_0)\exp\left(\boldsymbol{A}(t - t_0)\right) \tag{81}$$

$$\mathbf{F}(t_0, t_0) = 1 \tag{82}$$

$$\mathbf{F}(t + n\tau) = \mathbf{F}(t) \tag{83}$$

$$\boldsymbol{A}(t') = \boldsymbol{A}(t'') \quad (\text{all } t', t'') \tag{84}$$

It is then sufficient to integrate numerically over one period τ and then obtain the evolution for all times by matrix multiplications according to equations (81)–(84). In particular, at multiples of the period τ one finds (with $t_0 = 0$),

$$\boldsymbol{U}(\tau) = \exp(\boldsymbol{A}\tau) \tag{85}$$

$$\boldsymbol{U}(n\tau) = [\boldsymbol{U}(\tau)]^n \tag{86}$$

There has been considerable literature making use of Floquet's theorem for the treatment of coherent excitation and there also exist computer program packages (see Quack (1998)). We discuss here a further useful approximation.

3.4 Weak-field Quasi-resonant Approximation (WF-QRA) for Coherent Monochromatic Excitation

We consider a level scheme for coherent excitation with levels near the resonance as shown in Figure 4. One can then associate with each molecular level of energy $E_k = \hbar\omega_k$ an integer photon number n_k for near-resonant excitation such that

$$\omega_k = n_k\omega + x_k \tag{87}$$

where x_k is a frequency mismatch for exact resonance at the best choice of n_k.

Under the conditions that (i) there is a sequential near-resonant excitation path, (ii) only levels with a general resonance mismatch satisfying $\left|D_{kj}\right| \ll \omega$ contribute effectively to excitation (quasi-resonant condition), and (iii) the coupling matrix elements satisfy $\left|V_{kj}\right| \ll \omega$ (weak-field condition), one can approximately derive a set of coupled equations with an effective Hamiltonian that does not depend upon time. For this purpose, one makes the simple substitution (Quack 1978, 1998)

$$a_k = \exp(\mathrm{i}n_k\omega t)b_k \tag{88}$$

resulting in the set of differential equations

$$\mathrm{i}\frac{\mathrm{d}a_k}{\mathrm{d}t} = x_k a_k + \frac{1}{2}\sum_{j\neq k} V_{kj}a_j \tag{89}$$

or in matrix form (with the diagonal matrix $\boldsymbol{X}$ and $X_{kk} = x_k$)

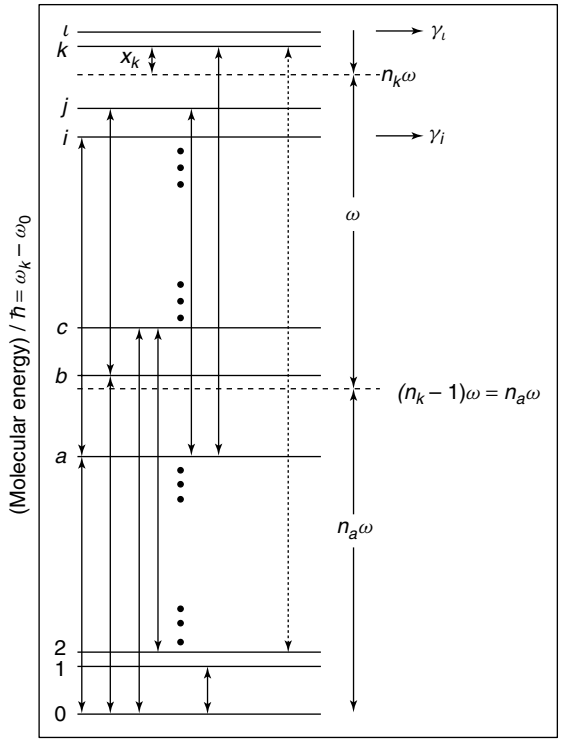

Figure 4 Energy-level scheme [(After Quack 1982).] The molecular energy levels are marked as horizontal full lines. The horizontal dashed lines correspond to the energies $E_0 + n_k\hbar\omega$ of the ground state (E_0) with n_k photons. It is sometimes useful to describe decay phenomena by adding an imaginary energy contribution, for instance $E_l = Re(E_l) - \mathrm{i}\gamma_\ell/2$ as indicated.

$$\mathrm{i}\frac{\mathrm{d}\boldsymbol{a}}{\mathrm{d}t} = \left\{\boldsymbol{X} + \frac{1}{2}\boldsymbol{V}'\right\}\boldsymbol{a} \tag{90}$$

One can interpret this equation by means of an "effective Hamiltonian"

$$\boldsymbol{H}^{(a)}_{\mathrm{eff}} = \hbar\left\{\boldsymbol{X} + \frac{1}{2}\boldsymbol{V}'\right\} \tag{91}$$

and the corresponding effective time-evolution matrix

$$\boldsymbol{U}^{(a)}_{\mathrm{eff}}(t, t_0) = \exp\left[-2\pi\mathrm{i}\frac{\boldsymbol{H}^{(a)}_{\mathrm{eff}}(t - t_0)}{h}\right] \tag{92}$$

$$= \exp\left[-\mathrm{i}\left(\boldsymbol{X} + \frac{1}{2}\boldsymbol{V}'\right)(t - t_0)\right]$$

$$\boldsymbol{a}(t) = \boldsymbol{U}^{(a)}_{\mathrm{eff}}(t, t_0)\,\mathbf{a}\,(t_0) \tag{93}$$

This is quite a remarkable result as it corresponds to replacing the molecular energies E_k by new effective energies $\hbar X_{kk}$ and the couplings V_{kj} by new effective couplings $(V_{kj}/2)$ for near-resonant levels (and implicitly by zero for far off-resonant levels). We can therefore

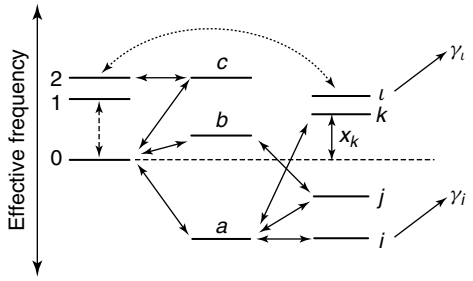

Figure 5 Effective-frequency scheme corresponding to the energy-level scheme of Figure 4.

use $\boldsymbol{V}'/2$ rather than $\boldsymbol{V}/2$ for the general matrix. This is graphically shown in Figure 5 for the same level scheme as in Figure 4, but with effective energies that are "on the same energy shell" and thus effective couplings between levels of similar effective energy. We note the close analogy to the dressed atom (dressed molecule) picture by Cohen-Tannoudji, which uses, however, a different derivation (Cohen-Tannoudji *et al*. 1992). We note that the quasi-resonant transformation as given in Quack (1978, 1998) can be written in matrix notation:

$$\boldsymbol{a} = \boldsymbol{S}\boldsymbol{b} \tag{94}$$

with the diagonal matrix

$$S_{kk} = \exp(\mathrm{i}n_k\omega t) \tag{95}$$

Similarly, a transformation for the density matrix $\boldsymbol{P}^{(a)}$ from $\boldsymbol{P}^{(b)}$ can be derived in this approximation, resulting in the solution of the Liouville–von Neumann equation for $\boldsymbol{P}(t)$ by

$$\boldsymbol{P}^{(a)}(t) = \boldsymbol{S}\boldsymbol{P}^{(b)}\mathbf{S}^{\dagger} \tag{96}$$

$$\boldsymbol{P}^{(a)}(t) = \boldsymbol{U}^{(a)}_{\mathrm{eff}}(t, t_0)\boldsymbol{P}^{(a)}(t_0)\boldsymbol{U}^{(a)\dagger}_{\mathrm{eff}}(t, t_0) \tag{97}$$

For details, we refer to Quack (1978, 1982, 1998). We turn now to a simple application to the special case of coherent radiative excitation connecting just two quantum states.

3.5 Coherent Monochromatic Excitation between Two Quantum States

If only two quantum states are considered, one obtains a scheme for the coherent monochromatic radiative excitation as shown in Figure 6.

Equation (70) simplifies to the set of just two coupled differential equations:

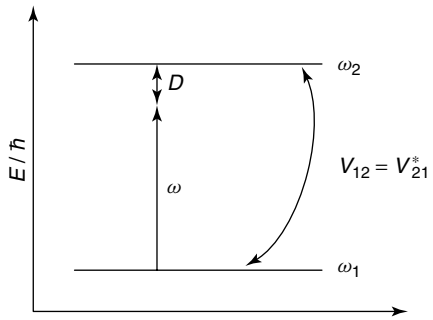

Figure 6 Two-level scheme for coherent radiative excitation with frequency ω.

$$\mathrm{i}\frac{\mathrm{d}b_1}{\mathrm{d}t} = \omega_1 b_1 + V_{12}\cos(\omega t - \eta)\; b_2 \tag{98}$$

$$\mathrm{i}\frac{\mathrm{d}b_2}{\mathrm{d}t} = V_{21}\cos(\omega t - \eta) b_1 + \omega_2 b_2 \tag{99}$$

One might think that this rather simple set of coupled differential equations has a simple solution, but, in fact, it seems that until today no simple general analytical solution in the form of a closed expression is known (see the discussion in Quack (1978, 1998), also for special cases). Of course, one can write down formal series expansions (Sections 3.2 and 3.3.) or quite easily solve the equations numerically.

However, following the discussion of Section 3.4, an analytical solution in the form of a closed expression can be derived in the weak-field quasi-resonant approximation (WF-QRA). The most general solution in terms of the time-evolution matrix $\boldsymbol{U}^{(a)}_{\mathrm{eff}}$ is given by the matrix elements, omitting the index "eff" to simplify the notation, and taking a real $V_{12} = V^*_{21} = V$ as parameter,

$$U^{(a)}_{11} = \exp(-\mathrm{i}\lambda_1 t)\left[x^2 + y^2\exp(\mathrm{i}\omega_R t)\right] \tag{100}$$

$$U^{(a)}_{22} = \exp(-\mathrm{i}\lambda_1 t)\left[y^2 + x^2\exp(\mathrm{i}\omega_R t)\right] \tag{101}$$

$$U^{(a)}_{12} = U^{(a)}_{21} = \exp(-\mathrm{i}\lambda_1 t)xy\left[1 - \exp(\mathrm{i}\omega_R t)\right] \tag{102}$$

where we have used the following parameters as abbreviations

$$\omega_R = (\lambda_1 - \lambda_2) = \sqrt{V^2 + D^2} = \frac{2\pi}{\tau_R} \tag{103}$$

$$\lambda_1 = \frac{1}{2}\left(D + \sqrt{V^2 + D^2}\right) \tag{104}$$

$$\lambda_2 = \frac{1}{2}\left(D - \sqrt{V^2 + D^2}\right) \tag{105}$$

$$x = \left[\frac{1}{2} - \frac{D}{2\omega_R}\right]^{1/2} \tag{106}$$

$$y = \left[\frac{1}{2} + \frac{D}{2\omega_R}\right]^{1/2} \tag{107}$$

We note that in Quack (1998) some of the expressions were misprinted, and these are corrected here. We also give the explicit form of the effective Hamiltonian corresponding to equation (91):

$$\frac{\boldsymbol{H}^{(a)}_{\mathrm{eff}}}{\hbar} = \begin{pmatrix} 0 & 0 \\ 0 & D \end{pmatrix} + \frac{1}{2}\begin{pmatrix} 0 & V \\ V & 0 \end{pmatrix} \tag{108}$$

$$= \boldsymbol{X} + \frac{1}{2}\boldsymbol{V} \tag{109}$$

In the two-level case, the distinction between $\boldsymbol{V}$ and $\boldsymbol{V}'$ is not necessary.

$\boldsymbol{U}^{(a)}_{\mathrm{eff}}$ is explicitly derived by means of the eigenvalues and eigenstates of $\boldsymbol{H}^{(a)}_{\mathrm{eff}}$ (Quack 1998)

$$\mathbf{Z}^{-1}\left(\boldsymbol{X} + \frac{1}{2}\boldsymbol{V}\right)\mathbf{Z} = \boldsymbol{\Lambda} = \mathbf{Diag}(\lambda_1, \lambda_2) \tag{110}$$

$$\boldsymbol{U}^{(a)}_{\mathrm{eff}}(t - t_0) = \mathbf{Z}\exp\left[-\mathrm{i}\boldsymbol{\Lambda}(t - t_0)\right]\mathbf{Z}^{-1} \tag{111}$$

While these general equations can be used to derive numerous properties of the coherent monochromatic excitation in the two-level problem, we conclude here with the result for the time-dependent population of the excited level $p_2(t)$, if, initially, at time zero, only the ground state is populated ($p_1(t = 0) = 1$).

One obtains equation (112) for the population of the upper level:

$$p_2(t) = |b_2(t)|^2 = \frac{V^2}{V^2 + D^2}\left[\sin\left(\frac{t}{2}\sqrt{V^2 + D^2}\right)\right]^2$$
$$= 1 - p_1(t) \tag{112}$$

This is a periodic exchange of population between ground and excited states with a period

$$\tau_R = \frac{2\pi}{\sqrt{V^2 + D^2}} \tag{113}$$

This period is called the *Rabi period*, with ω_R being the *Rabi frequency*, as these equations were derived on the basis of the so-called rotating wave approximation by Rabi (1937) (see also Rabi *et al*. (1938)) in the context of early NMR experiments (in beams, with a magnetic dipole transition matrix element V, of course).

The rotating wave approximation becomes identical with the quasi-resonant approximation for the special case of a two-level problem. Equation (112) is frequently called the *Rabi formula*.

Figure 7 shows the time-dependent level populations for a fairly typical case. With increasing resonance mismatch D, the amplitude of the oscillation decreases, but the frequency of oscillation increases. The initial time evolution

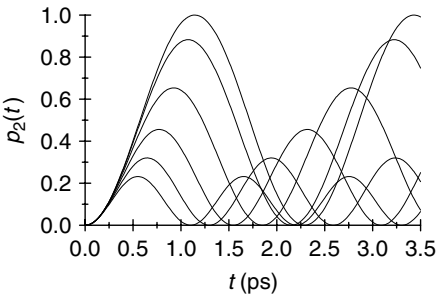

Figure 7 Time dependent level populations from Eq. (112). The population p_2 of the upper level in the scheme of Figure 6 is shown with different resonant defects $D = (0, 1, 2, 3, 4, 5) \times 10^{12}$ s^{-1} for an electric dipole transition with the laser wave number $\tilde{\nu} = 1000\,cm^{-1}$, intensity $I = 1\,GW\,cm^{-2}$ and transition moment $|\mu_{21}| = \langle\varphi_2|\hat{\mu}_z|\varphi_1\rangle = 1$ Debye.

is independent of the resonance mismatch as is readily seen from the series expansion of the $\sin x$ function for small arguments x ($\sin x = x + \ldots$) giving at sufficiently small times,

$$p_2(t) \simeq V^2 t^2/4 \quad (\text{small } t) \tag{114}$$

One can also consider the time-averaged population $\langle p_2(\omega)\rangle_t$ as a function of the exciting laser frequency ω at fixed resonance frequency $\omega_{12} = \omega_2 - \omega_1$. Because $\langle \sin^2 x \rangle = 1/2$, one has

$$\langle p_2(\omega)\rangle_t = \frac{1}{2}\frac{V^2}{V^2 + (\omega - \omega_{12})^2} \tag{115}$$

$\langle p_2(\omega)\rangle$ is proportional to the average absorbed energy as a function of frequency ω, so that one can interpret this expression as the effective absorption lineshape under intense coherent excitation. Indeed, equation (115) corresponds to a Lorentzian lineshape with full width at half maximum $\Gamma_{FWHM} = 2V$. This effect is called *power broadening* because $V \propto \sqrt{I}$ (cf. equations 59 and 73, sometimes the term *intensity broadening* is used as well). We have neglected here effects from spontaneous emission or collisions, as is obviously appropriate for the timescales applicable to Figure 7, but not necessarily always so.

We may finally conclude with an estimate of errors arising when the conditions of the WF-QRA are not fulfilled. The special case of the degenerate two-level problem has been solved exactly (Quack 1978). In this case, one has $\omega_1 = \omega_2$ and therefore $D^2 = \omega^2$. The Rabi formula (equation 112) thus would give

$$p_2^{\text{Rabi}}(t) = \frac{V^2}{V^2 + \omega^2}\left[\sin\left(\frac{t}{2}\sqrt{V^2 + \omega^2}\right)\right]^2 \tag{116}$$

The exact solution (Quack 1978) is

$$p_2^{\text{ex}}(t) = \left\{\sin\left[\left(\frac{V}{\omega}\right)\sin(\omega t)\right]\right\}^2 \tag{117}$$

One can consider the limit $|V| \ll \omega$ because this must be assumed for the validity of the Rabi formula, and considering this limit, one obtains

$$p_2^{\text{Rabi}}(t) = \frac{V^2}{\omega^2}\left[\sin\left(\frac{\omega t}{2}\right)\right]^2 \tag{118}$$

$$p_2^{\text{ex}}(t) = \frac{V^2}{\omega^2}\left[\sin(\omega t)\right]^2 \tag{119}$$

Thus the exact solution gives the same amplitude as the Rabi formula, but the period differs by a factor of 2. Of course the second condition for the validity of the WF-QRA is not satisfied, as one cannot have $|D| \ll \omega$ (rather by definition of the special case, one has $|D| = \omega$). If $|D| \ll \omega$, the Rabi formula gives a very good approximation, as one can show numerically. We may note here that closed analytical expressions for the solutions are available for the excitation of the harmonic oscillator both with the exact treatment (equation 70) and within the WF-QRA (equation 90), taking an infinite number of levels into account, which may, perhaps, seem surprising. The derivation has been given by Marquardt and Quack (1989) and leads to a further estimate of the ranges of validity and uncertainties introduced by the WF-QRA, in this case for a many-level system.

4 BASIC CONCEPTS OF EXPERIMENTAL SPECTROSCOPY

4.1 General Remarks

Spectroscopy is the main experimental method to obtain quantitative information on, and study fundamental properties of, molecular systems. Molecular systems obey the laws of quantum mechanics, as summarized in Section 2. Quantitative information must be acquired through reproducible experiments carried out under specified experimental conditions. In the case of molecular systems and other quantum systems, the outcome of experiments can be described statistically. Repeating the same measurement of an observable twice does not always give the same result, but the outcomes of a sufficiently large set of identical measurements are characterized by a probability distribution.

Molecules are mechanical systems that can be influenced by external forces applied by an experimentalist. Because they are long-range forces and easily applied, electromagnetic forces are of particular importance in the study of

molecular systems. Classically, the behavior of a particle of charge q in an electromagnetic field $(\boldsymbol{E}(\boldsymbol{r},t),\boldsymbol{B}(\boldsymbol{r},t))$ is described by the Lorentz force:

$$\boldsymbol{F} = q(\boldsymbol{E} + \boldsymbol{v} \times \boldsymbol{B}) \tag{120}$$

By varying $\boldsymbol{E}$ and $\boldsymbol{B}$, the experimentalist varies $\boldsymbol{F}$ and thus acts on the particle according to Newton's second axiom:

$$\boldsymbol{F}(t) = \frac{\mathrm{d}(m\boldsymbol{v}(t))}{\mathrm{d}t} \tag{121}$$

In quantum mechanics, one describes the Hamiltonian of the system in terms of the vector potential $\boldsymbol{A}(\boldsymbol{r},t)$ and the scalar potential $\phi(\boldsymbol{r},t)$:

$$\boldsymbol{B}(\boldsymbol{r},t) = \mathrm{rot}(\boldsymbol{A}(\boldsymbol{r},t)) \tag{122}$$

$$\boldsymbol{E}(\boldsymbol{r},t) = -\mathrm{grad}(\phi(\boldsymbol{r},t)) - \frac{\partial \boldsymbol{A}(\boldsymbol{r},t)}{\partial t} \tag{123}$$

For a single, free particle of mass m and charge q, the Hamiltonian takes the form

$$H(t) = \frac{1}{2m}\left(p - q\boldsymbol{A}(\boldsymbol{Q},t)\right)^2 + q\phi(\boldsymbol{Q},t) \tag{124}$$

However, in most spectroscopic studies described in the literature, $\boldsymbol{E}$ and $\boldsymbol{B}$ are used as primary parameters.

A quantum system under the influence of external time-dependent electromagnetic fields (which we call *external perturbations*) is described by a time-dependent Hamilton operator $\hat{H}(t)$ (see Equation 36)

$$\hat{H}(t) = \hat{H}_0 + \hat{V}(t) \tag{125}$$

where $\hat{H}_0$ is the time-independent Hamilton operator of the system without external perturbation and

$$\hat{V}(t) = -\sum_n b_n(t)\hat{B}_n \tag{126}$$

is an operator representing the effects of the external forces applied by the experimentalist. In all practical cases, $\hat{V}(t)$ is a sum of contributions $-b_n(t)\hat{B}_n$, where $\hat{B}_n$ is a time-independent Hermitian operator and $b_n(t)$ is a real function of time.

Example 1 **Interaction of light with molecular systems in the dipole approximation (see also previous sections)**

A monochromatic electromagnetic wave of wavelength λ propagating along the y-axis of a suitably chosen laboratory coordinate system is schematically represented in Figure 3. The interaction of a molecular system with an electromagnetic wave can be described by the interaction of the electric and magnetic dipole moments with the electric and magnetic fields, respectively, of the electric and magnetic quadrupole moments with the electric and magnetic field gradients, etc. The dipole approximation to describe the interaction of electromagnetic radiation with a molecular system consists of neglecting all interactions other than those between the dipoles and the fields. The approximation is valid as long as the electric or magnetic field strength does not change over the size d of the molecular system, i.e., as long as $\lambda \gg d$ because then the interactions involving the quadrupole and higher moments, which require a variation of the field strength in the immediate vicinity of the molecule, are negligible. In the dipole approximation, the interaction operator with a monochromatic field of angular frequency ω can be written as follows:

$$\hat{V}(t) = \hat{V}_{\mathrm{el}}(t) + \hat{V}_{\mathrm{magn}}(t) \tag{127}$$

with

$$\hat{V}_{\mathrm{el}}(t) = -\hat{\boldsymbol{\mu}}_{\mathrm{el}} \cdot \boldsymbol{E} = -\left(\sum_i q_i \boldsymbol{r}_i\right) \cdot \boldsymbol{E}_0 \cos(\omega t - \eta) \tag{128}$$

and

$$\hat{V}_{\mathrm{magn}}(t) = -\hat{\boldsymbol{\mu}}_{\mathrm{magn}} \cdot \boldsymbol{B} = -\hat{\boldsymbol{\mu}}_{\mathrm{magn}} \cdot \boldsymbol{B}_0 \cos(\omega t - \eta) \tag{129}$$

where $\hat{\boldsymbol{\mu}}_{\mathrm{el}} = (\sum_i q_i \boldsymbol{r}_i)$ and $\hat{\boldsymbol{\mu}}_{\mathrm{magn}}$ are the electric and magnetic dipole-moment operators of the molecular system, respectively. One sees immediately that equations (128) and (129) have the general form of equation (126). If $d \approx \lambda$, the electric and magnetic field strengths vary over the size of the molecular system, and one must also consider the interaction of the electromagnetic fields with the quadrupoles, octupoles, etc. of the molecules. The electric dipole interaction is the dominant interaction in the microwave, infrared, visible, and ultraviolet ranges of the electromagnetic spectrum (λ large). The magnetic dipole interaction is used in spectroscopies probing the magnetic moments resulting from the electron or nuclear spins such as electron paramagnetic resonance (EPR) and NMR, and it is also important in optical spectroscopy if the electric dipole transition is forbidden. At short wavelength, i.e., for X- and γ-rays, the dipole approximation breaks down because $\lambda \leq d$.

The art of experimenting consists of (i) choosing a suitable interaction operator $\hat{B}_n$, (ii) designing functions $b_n(t)$ (called experimental *stimuli*) so as to act on the system under investigation, and, finally, (iii) detecting and analyzing the response of the system to the stimulus. Many tools are at the disposal of the experimentalist to generate

the external perturbations, such as microwave synthesizers, lamps, electromagnets, masers, and lasers. In many spectroscopic experiments, the sample consists of molecules in thermal equilibrium, and the external perturbation induces transitions between the energy levels of the molecules in the system, causing a departure from thermal equilibrium. In analyzing the response of the system to the stimulus, it is necessary to also consider possible interactions of the system under investigation with its environment. These interactions, e.g., the collisions with foreign gas particles or with the walls of an apparatus, or the interaction with the vacuum radiation field, lead to the relaxation of the system to thermal equilibrium. The distinction between the system under investigation and its environment is sometimes difficult to make and a given choice has implications on the way the results of an experiment are analyzed.

We now turn to an introductory description of the relationship between an experimental stimulus and the response of a system induced by this stimulus in the realm of response theory.

4.2 An Introduction to Response Theory

A spectroscopic experiment can be viewed as an information transfer in which the system—here, a molecular quantum system—gives a response to a stimulus—here, a classical electromagnetic field. In general, it is advisable, in an experiment that aims at looking at the properties of a system, to disturb the system as little as possible during the measurement, so that the intrinsic properties of the system are highlighted. In the extreme case where the perturbation $\hat{V}(t)$ is very much larger than $\hat{H}_0$, one risks to primarily obtain information on the experimental perturbation, the properties of the system becoming negligible. This consideration justifies a restriction of the discussion to the linear response of the system.

The response $x(t)$ of a system to a stimulus $y(t)$ can be described mathematically by the transformation

$$x(t) = \boldsymbol{R}y(t) \tag{130}$$

where $\boldsymbol{R}$ represents the response operator. In a spectroscopic measurement, the system may be viewed as the sample probed in the experiment, the stimulus as the radiation field(s) used to perturb the system, and the response as a signal emitted by the sample and collected by the measurement device. The response operator is thus the characteristic property of the system and represents the quantity to be derived from an analysis of the response to the stimulus.

$\boldsymbol{R}$ can be determined by discrete sampling of $y(t)$ and $x(t)$, e.g., using a digital oscilloscope, at the times $t_n = t_0 + n\Delta t$, with $n = 0, 1, 2, \ldots, N$, as illustrated by Figure 8. The response $x_n = x(t_n)$ at time t_n can be viewed as being caused by the stimulus $y_m = y(t_m)$ at all times between t_0 and t_N:

$$x_n = \boldsymbol{R}_n(y_0, y_1, \ldots, y_N) \tag{131}$$

where $n = 0, 1, \ldots N$, and $\boldsymbol{R}_n$ has the form $R^N \rightarrow R$. A Taylor expansion around the point $y_0, y_1, \ldots, y_N = 0$ gives for well-behaved systems:

$$x_n = \boldsymbol{R}_n^{(0)} + \sum_{i=0}^{N} \boldsymbol{R}_{n,i}^{(1)} y_i + \frac{1}{2!} \sum_{i=0}^{N} \sum_{j=0}^{N} \boldsymbol{R}_{n,i,j}^{(2)} y_i y_j + \ldots \tag{132}$$

where $\boldsymbol{R}_{n,i}^{(1)} = \left(\dfrac{\partial \boldsymbol{R}_n(y_0, y_1, \ldots y_N)}{\partial y_i} \right)_{y_k \neq y_i}$, $\boldsymbol{R}_{n,i,j}^{(2)} = \left(\dfrac{\partial^2 \boldsymbol{R}_n(y_0, y_1, \ldots y_N)}{\partial y_i \partial y_j} \right)_{y_k \neq y_i, y_j}$, etc. For $\Delta t \rightarrow 0$, one can replace the sum by an integral and obtain a *Volterra expansion*:

$$x(t) = \boldsymbol{R}^{(0)}(t) + \int_{-\infty}^{\infty} \boldsymbol{R}^{(1)}(t, s) y(s) \mathrm{d}s + \frac{1}{2!} \int_{-\infty}^{\infty} \int_{-\infty}^{\infty} \boldsymbol{R}^{(2)}(t, s, s') y(s) y(s') \mathrm{d}s \mathrm{d}s' + \ldots \tag{133}$$

$\boldsymbol{R}^{(0)}(t)$ can be viewed as the response of the system without stimulus, i.e., it represents a background signal fluctuating with t. $\boldsymbol{R}^{(1)}(t, s)$ is the linear response at time t of the stimulus at time s; $\boldsymbol{R}^{(2)}(t, s, s')$ is the quadratic response at

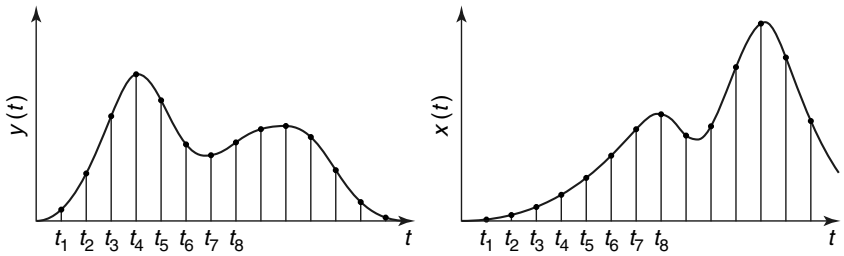

Figure 8 Discrete sampling of stimulus and response in a spectroscopic measurement.

time t of the stimulus at times s and s', etc. If the stimuli are small, as is often required by a good spectroscopic experiment (see above), the quadratic and higher terms in equation (133) can be neglected and one deals with a linear system.

Spectroscopic measurements are causal, i.e., the response at time t can only be a function of the stimulus at time s such that $s \leq t$. The response of a causal system can thus be expressed as follows:

$$x(t) = \boldsymbol{R}^{(0)}(t) + \int_{-\infty}^{t} \boldsymbol{R}^{(1)}(t,s)y(s)\mathrm{d}s + \frac{1}{2!}\int_{-\infty}^{t}\int_{-\infty}^{t} \boldsymbol{R}^{(2)}(t,s,s')y(s)y(s')\mathrm{d}s\mathrm{d}s' + \ldots \tag{134}$$

When the parameters describing the system under study remain constant with time, the system is said to be *time invariant*. The systems studied spectroscopically are often time-invariant (counterexamples would be a system undergoing a chemical reaction, or a system exposed to varying stray fields), and in these systems, the response functions show the behavior described by Figure 9. The response $x_\mathrm{T}(t) = x(t+T)$ to a time-shifted stimulus $y_\mathrm{T}(t) = y(t+T)$ stands in the same relationship to $y_\mathrm{T}(t)$ as the response $x(t)$ to the stimulus $y(t)$. By replacing t by $t+T$ in the Volterra expansion (133) one obtains

$$\begin{aligned} x_\mathrm{T}(t) &= x(t+T) \\ &= \boldsymbol{R}^{(0)}(t+T) + \int_{-\infty}^{\infty} \boldsymbol{R}^{(1)}(t+T,s)y(s)\mathrm{d}s \qquad (135) \\ &\quad + \frac{1}{2!}\int_{-\infty}^{\infty}\int_{-\infty}^{\infty} \boldsymbol{R}^{(2)}(t+T,s,s') \\ &\quad \times y(s)y(s')\mathrm{d}s\mathrm{d}s' + \ldots \qquad (136) \end{aligned}$$

$x_\mathrm{T}(t)$ can also be expressed by making the Volterra expansion using y_T (see Figure 9):

$$x_\mathrm{T}(t) = \boldsymbol{R}^{(0)}(t) + \int_{-\infty}^{\infty} \boldsymbol{R}^{(1)}(t,s)y_\mathrm{T}(s)\mathrm{d}s + \frac{1}{2!}\int_{-\infty}^{\infty}\int_{-\infty}^{\infty} \boldsymbol{R}^{(2)}(t,s,s')y_\mathrm{T}(s)y_\mathrm{T}(s')\mathrm{d}s\mathrm{d}s' + \ldots$$

$$\begin{aligned} &= \boldsymbol{R}^{(0)}(t) + \int_{-\infty}^{\infty} \boldsymbol{R}^{(1)}(t,s)y(s+T)\mathrm{d}s \\ &\quad + \frac{1}{2!}\int_{-\infty}^{\infty}\int_{-\infty}^{\infty} \boldsymbol{R}^{(2)}(t,s,s')y(s+T) \\ &\quad \times y(s'+T)\mathrm{d}s\mathrm{d}s' + \ldots \\ &= \boldsymbol{R}^{(0)}(t) + \int_{-\infty}^{\infty} \boldsymbol{R}^{(1)}(t,s-T)y(s)\mathrm{d}s \\ &\quad + \frac{1}{2!}\int_{-\infty}^{\infty}\int_{-\infty}^{\infty} \boldsymbol{R}^{(2)}(t,s-T,s'-T) \\ &\quad \times y(s)y(s')\mathrm{d}s\mathrm{d}s' + \ldots \qquad (137) \end{aligned}$$

Comparing equations (135) and (137) term by term, one gets

$$\boldsymbol{R}^{(0)}(t+T) = \boldsymbol{R}^{(0)}(t) = \phi^{(0)} \tag{138}$$

and

$$\boldsymbol{R}^{(1)}(t+T,s) = \boldsymbol{R}^{(1)}(t,s-T) \tag{139}$$

One sees from equation (139) that $R^{(1)}$ only depends on the time difference between stimulus and response, and therefore

$$\boldsymbol{R}^{(1)}(t,s) = \phi^{(1)}(t-s) \tag{140}$$

Inserting equations (138) and (140) into equation (133) leads to the following expression describing the response of a time-invariant system:

$$\begin{aligned} x(t) &= \phi^{(0)} + \int_{-\infty}^{\infty} \phi^{(1)}(t-s)y(s)\mathrm{d}s + \ldots \\ &= \phi^{(0)} + \int_{-\infty}^{\infty} \phi^{(1)}(s)y(t-s)\mathrm{d}s + \ldots \qquad (141) \end{aligned}$$

where the second line was obtained by making the substitution $s' = t - s$. The response of time-invariant causal systems, for which $s \leq t$, i.e., for which $s' \geq 0$ (see above), can therefore be obtained from equation (141) by changing the integration range:

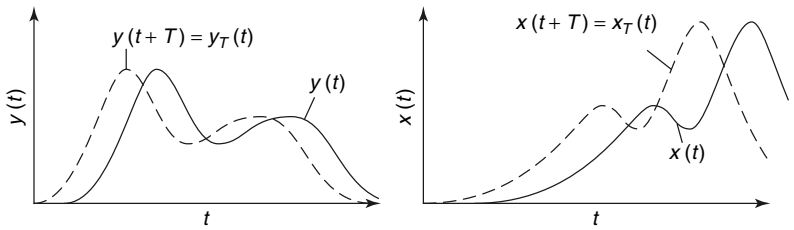

Figure 9 Stimulus and response in a time-invariant system.

$$x(t) = \phi^{(0)} + \int_0^\infty \phi^{(1)}(s')y(t-s')\mathrm{d}s' + \ldots \qquad (142)$$

As expected, the background is constant in a time-invariant system (see equation 138). If one only considers the linear response in such a system, one can write $\phi^{(1)}(s) = \phi(s)$. After background subtraction, the response of a time-invariant linear system can finally be written as

$$x(t) = \int_{-\infty}^{\infty} \phi(s)y(t-s)\mathrm{d}s \qquad (143)$$

The linearity of the system implies the following superposition principle: the response $x(t)$ to a sum of stimuli $y(t) = \sum_i y_i(t)$ is the sum $x(t) = \sum_i x_i(t)$ of the responses $x_i(t)$ to the stimuli $y_i(t)$. In spectroscopy, one often uses oscillatory stimuli (for instance, $E_0\cos(\omega t)$). The superposition principle enables one to avoid using trigonometric functions. Indeed, the response $x(t)$ to the stimulus $y_0\mathrm{e}^{-\mathrm{i}\omega t}$ can be expressed as $\Re(x(t)) - \mathrm{i}\Im(x(t))$ where the real part $\Re(x(t))$ is the response to the stimulus $y_0\cos(\omega t)$ and the imaginary part $\Im(x(t))$ is the response to the stimulus $y_0\sin(\omega t)$.

4.3 Time-resolved Versus Frequency-resolved Spectroscopy

In this section, we briefly discuss the responses to two special stimuli that are of particular importance in spectroscopy, Dirac's delta function $y(t) = \delta(t)$ and an oscillatory function $y(t) = \mathrm{e}^{-\mathrm{i}\omega t}$. The former stimulus plays a special role in *time-resolved* spectroscopy, in which the response of a system is monitored following exposure to a very short impulsion, for instance an ultrashort laser pulse. The latter stimulus plays a special role in *frequency-resolved* spectroscopy, in which the response of the system to a monochromatic electromagnetic wave is monitored as a function of the frequency.

(a) Response to an impulsion $\delta(t)$
In the limit of an infinitely short experimental perturbation $y(t) = \delta(t)$, where $\delta(t)$ represents Dirac's delta function,

$$\begin{aligned} \delta(t) &= 0 \quad \text{for } t \neq 0 \\ &\infty \quad \text{for } t = 0 \end{aligned} \qquad (144)$$

which is the derivative of the Heaviside function $H(t)$

$$\begin{aligned} H(t) &= 0 \quad \text{for } t \leq 0 \\ &1 \quad \text{for } t > 0 \end{aligned} \qquad (145)$$

Two important properties of the delta function $\delta(t)$ are given by Equations (146) and (147):

$$\delta(t) = \frac{1}{2\pi}\int_{-\infty}^{\infty} \mathrm{e}^{\pm\mathrm{i}\omega t}\mathrm{d}\omega \qquad (146)$$

$$\int_{-\infty}^{\infty} f(t)\delta(t-t_0)\mathrm{d}t = f(t_0) \qquad (147)$$

Using equation (143), the linear response to the delta function can be determined to be

$$x(t) = \int_{-\infty}^{\infty} \phi(s)\delta(t-s)\mathrm{d}s = \phi(t) \qquad (148)$$

which implies that the response function $\phi(t)$, which characterizes the linear response to any stimulus, is simply the response to $\delta(t)$. Experimentally, delta functions can only be realized approximately by a short impulsion, e.g., an ultrashort laser pulse (today femtosecond (fs) pulses are easily generated and the first laser systems producing attosecond pulses are becoming available (Brabec and Krausz 2000, *see also* Gallmann and Keller 2011: **Femtosecond and Attosecond Light Sources and Techniques for Spectroscopy** and Wörner and Corkum 2011: **Attosecond Spectroscopy**, this handbook)). In a spectroscopic experiment using one such short impulsion as stimulus, one monitors, in real time, the response of the system to the impulsion and one uses the term *time-resolved* spectroscopy. The response, called a *free induction decay* in NMR spectroscopy (Ernst *et al.* 1987), EPR (Schweiger and Jeschke 2001), and Fourier-transform microwave spectroscopy (*see* Bauder 2011: **Fundamentals of Rotational Spectroscopy**, Jäger and Xu 2011: **Fourier Transform Microwave Spectroscopy of Doped Helium Clusters** and Grabow 2011: **Fourier Transform Microwave Spectroscopy Measurement and Instrumentation**, this handbook), is the response function which, by means of a Fourier transformation, can be converted in the power spectrum of the system (see (b) below). Several important spectroscopic techniques rely on this principle, such as, for instance, Fourier-transform microwave spectroscopy, Fourier-transform NMR, EPR, and fs laser spectroscopy.

(b) Response to an oscillatory function $\mathrm{e}^{-\mathrm{i}\omega t}$
Three types of oscillatory stimulus can be used:

$$y_1(t) = \mathrm{e}^{-\mathrm{i}\omega t} = \cos(\omega t) - \mathrm{i}\sin(\omega t) \qquad (149)$$

$$y_2(t) = \cos(\omega t) = \Re\left\{\mathrm{e}^{-\mathrm{i}\omega t}\right\} \qquad (150)$$

$$y_3(t) = \sin(\omega t) = -\Im\left\{\mathrm{e}^{-\mathrm{i}\omega t}\right\} \qquad (151)$$

Because of the superposition principle discussed above, it is advantageous to determine the response to $y_1(t)$ from which the response to either $y_2(t)$ or $y_3(t)$ may be derived. One gets from equation (143):

$$\begin{aligned} x(t) &= \int_{-\infty}^{\infty} \phi(s) \mathrm{e}^{-\mathrm{i}\omega(t-s)} \mathrm{d}s \\ &= \int_{-\infty}^{\infty} \phi(s) \mathrm{e}^{\mathrm{i}\omega s} \mathrm{d}s \mathrm{e}^{-\mathrm{i}\omega t} \\ &= \chi(\omega) \mathrm{e}^{-\mathrm{i}\omega t} \end{aligned} \tag{152}$$

where

$$\chi(\omega) = \int_{-\infty}^{\infty} \phi(s) \mathrm{e}^{\mathrm{i}\omega s} \mathrm{d}s \tag{153}$$

Formulating this result starting from equation (130),

$$x(t) = \boldsymbol{R} y(t) = \boldsymbol{R} \mathrm{e}^{-\mathrm{i}\omega t} = \chi(\omega) \mathrm{e}^{-\mathrm{i}\omega t} \tag{154}$$

one sees that the functions $\mathrm{e}^{-\mathrm{i}\omega t}$ are the eigenfunctions of the response operator $\boldsymbol{R}$ for any linear system with complex eigenvalues $\chi(\omega)$. Depending on the magnitude of the eigenvalue $\chi(\omega)$, the system responds more or less strongly to the stimulus , i.e., it is more or less susceptible to it. The eigenvalue $\chi(\omega)$ is therefore called the *susceptibility* of the system. It is a function of the angular frequency of the stimulus and it represents the power spectrum of the system. Equation (153) shows that $\chi(\omega)$ is the Fourier transform of the response function.

Fourier transformations

Combining equations (146) and (147), one gets the so-called Fourier identity:

$$\begin{aligned} f(t) &= \frac{1}{2\pi} \int_{-\infty}^{\infty} \mathrm{d}\omega \int_{-\infty}^{\infty} \mathrm{d}s \ \mathrm{e}^{-\mathrm{i}\omega(t-s)} f(s) \\ &= \frac{1}{2\pi} \int_{-\infty}^{\infty} \mathrm{e}^{-\mathrm{i}\omega t} \mathrm{d}\omega \int_{-\infty}^{\infty} \mathrm{e}^{\mathrm{i}\omega s} f(s) \mathrm{d}s \end{aligned} \tag{155}$$

With the Fourier transform

$$\hat{f}(\omega) = \int_{-\infty}^{\infty} \mathrm{e}^{\mathrm{i}\omega s} f(s) \mathrm{d}s \tag{156}$$

one can define the inverse Fourier transform from equation (155)

$$f(t) = \frac{1}{2\pi} \int_{-\infty}^{\infty} \mathrm{e}^{-\mathrm{i}\omega t} \hat{f}(\omega) \mathrm{d}\omega \tag{157}$$

By analogy, and with equation (153), we can write the response function $\phi(t)$ as the inverse Fourier transform of the susceptibility

$$\phi(t) = \frac{1}{2\pi} \int_{-\infty}^{\infty} \mathrm{e}^{-\mathrm{i}\omega t} \chi(\omega) \mathrm{d}\omega \tag{158}$$

Consequently, if one knows the susceptibility $\chi(\omega)$ at all frequencies, ω, one can determine the response function $\phi(t)$ by inverse Fourier transformation. To obtain the complete response behavior of a linear system using oscillatory stimuli, one must measure $\chi(\omega)$ at each angular frequency, ω. Such a determination can be made either by sweeping the frequency of a tunable monochromatic radiation source (lasers, microwaves, etc.) or, equivalently, by dispersing a white light source into its spectral components using a grating or a prism. Spectroscopic experiments carried out in the frequency domain are called *frequency-resolved* experiments.

Whether one measures $\chi(\omega)$ as a function of ω in a frequency-resolved experiment or $\phi(t)$ as a function of t in a time-resolved experiment, the same information is obtained. $\chi(\omega)$ can be converted into $\phi(t)$ by means of an inverse Fourier transformation, and vice versa. Time- and frequency-resolved spectroscopies are thus two sides of the same medal. Whether time-resolved or frequency-resolved spectroscopy is used to extract the spectrum of a sample depends on experimental convenience and on the availability of suitable sources of short pulses or monochromatic radiation. Another spectroscopic technique that relies on Fourier transformations is interferometric Fourier-transform spectroscopy, which is related, but not identical, to time-resolved spectroscopy. The principles and applications of interferometric Fourier-transform spectroscopy are described in Albert *et al.* 2011: **High-resolution Fourier Transform Infrared Spectroscopy**, this handbook.

4.4 The Radiation Field

This section describes the properties of the radiation field in a perfectly evacuated container, the walls of which are held at a temperature T, and contains a derivation of Planck's radiation law. It is a prerequisite to introduce Einstein's treatment of transitions induced by radiation in the Section 4.5.

The radiation field in an empty volume (for instance, the empty volume $V = L^3$ of a cubic container of side length L, see Figure 10) in thermal equilibrium with a container at temperature T can be viewed as a superposition of standing harmonic waves (also called *oscillators* or *modes*, in this context).

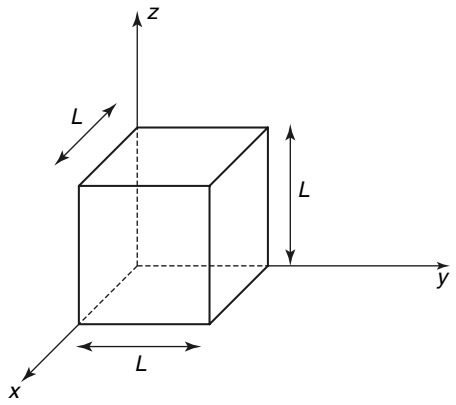

Figure 10 Empty volume, taken here as the interior of a cubic container with side length L.

(a) The mode density
The waves are solutions of the wave equation

$$\Delta\Psi(\boldsymbol{r},t) - \frac{1}{c^2}\frac{\partial^2}{\partial t^2}\Psi(\boldsymbol{r},t) = 0 \qquad (159)$$

Taking into account the boundary conditions

$$\Psi(x=0,y,z,t) = \Psi(x=L,y,z,t) = 0 \qquad (160)$$

and analogous conditions for the y and z dimensions, the solutions of equation (159) have the form

$$\begin{aligned}\Psi(\boldsymbol{r},t) &= A(t)\sin(k_1x)\sin(k_2y)\sin(k_3z)\\ &= A(t)B(x,y,z)\end{aligned} \qquad (161)$$

with $\sin(k_iL) = 0$ from which follows $k_iL = n_i\pi$ for $i = 1, 2, 3$ and $n_i = 1, 2, \ldots$. Inserting equation (161) in equation (159), one obtains

$$\begin{aligned}&-\left(n_1^2+n_2^2+n_3^2\right)\frac{\pi^2}{L^2}A(t)B(x,y,z)\\ &-\frac{1}{c^2}B(x,y,z)\frac{\partial^2}{\partial t^2}A(t) = 0\end{aligned} \qquad (162)$$

from which follows

$$A(t) = A_0\cos(\omega t+\phi) \qquad \text{with}$$

$$\omega^2 = \frac{c^2\pi^2}{L^2}\left(n_1^2+n_2^2+n_3^2\right) \qquad (163)$$

The number of modes with angular frequency between 0 and ω is

$$N(\omega) = \int_0^{\omega} g(\omega)\mathrm{d}\omega \qquad (164)$$

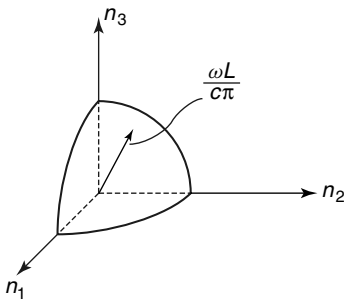

Figure 11 Schematic diagram representing the possible combinations (n_1, n_2, n_3) describing the modes of the radiation field with angular frequency $\leq \omega$.

where $g(\omega) = \frac{\mathrm{d}N(\omega)}{\mathrm{d}\omega}$ represents the number density of oscillators, which corresponds to all combinations of n_1, n_2, and n_3 that satisfy the equation

$$n_1^2+n_2^2+n_3^2 \leq \frac{\omega^2L^2}{c^2\pi^2} \qquad (165)$$

Equation (165) is the equation of a sphere (see Figure 11) with radius

$$r = \sqrt{n_1^2+n_2^2+n_3^2} = \frac{\omega L}{c\pi} \qquad (166)$$

n_1,n_2,n_3 are positive and therefore

$$N(\omega) = \frac{1}{8}\left(\frac{4}{3}\pi\frac{\omega^3L^3}{c^3\pi^3}\right) = \frac{\omega^3V}{6c^3\pi^2} \qquad (167)$$

Since $\omega = 2\pi\nu$, one obtains from equation (167)

$$N(\nu) = \frac{8\pi^3\nu^3V}{6c^3\pi^2} \qquad (168)$$

The mode density for a given polarization is therefore

$$g(\nu) = \frac{\mathrm{d}N(\nu)}{\mathrm{d}\nu} = \frac{4\pi\nu^2V}{c^3}; \quad g(\omega) = \frac{\mathrm{d}N(\omega)}{\mathrm{d}\omega} = \frac{1}{2}\frac{\omega^2V}{c^3\pi^2} \qquad (169)$$

Since two polarization directions have to be considered for each mode, the mode density is twice as large as that given by equation (169) and amounts to

$$g(\nu) = \frac{8\pi\nu^2}{c^3}V \qquad (170)$$

(b) The energy density
In classical electrodynamics, each mode has an energy kT and the energy of the radiation field in a volume V

at temperature T and between frequency ν and $\nu + d\nu$ is

$$U(\nu)\mathrm{d}\nu = g(\nu)kT\mathrm{d}\nu = \frac{8\pi}{c^3}\nu^2 VkT\mathrm{d}\nu \qquad (171)$$

The energy density (i.e., the energy per unit volume) is therefore given by

$$\rho(\nu) = \frac{U(\nu)}{V} = \frac{8\pi}{c^3}\nu^2 kT \qquad (172)$$

a relation known as *Rayleigh–Jeans law*. The expression (172) is valid for $kT \gg h\nu$ but incorrect for $\nu \to \infty$, as it predicts that in this case the energy density should become infinite. This physically incorrect property of equation (172) would lead to what has been termed *UV catastrophe*.

Planck's radiation law is derived by assuming that each radiation mode can be described by a quantized harmonic oscillator with energy

$$E'_v = h\nu\left(v + \frac{1}{2}\right) \qquad v = 0, 1, 2, \ldots \qquad (173)$$

Referencing the energy of each oscillator to the ground state ($v = 0$) of the oscillators

$$E_v = E'_v - E'_{v=0} = vh\nu \qquad (174)$$

one can determine the average energy of an oscillator using statistical mechanics:

$$\langle E(\nu)\rangle = \sum_{v=0}^{\infty} vh\nu \frac{\mathrm{e}^{-vh\nu/kT}}{\sum_{v=0}^{\infty}\mathrm{e}^{-vh\nu/kT}} \qquad (175)$$

with $vh\nu$ the energy of the oscillator and $\frac{\mathrm{e}^{-vh\nu/kT}}{\sum_{v=0}^{\infty}\mathrm{e}^{-vh\nu/kT}}$ the probability (≤ 1) that the oscillator has the energy $vh\nu$ (Boltzmann factor).

Making the substitution $x = \mathrm{e}^{-h\nu/kT}$ in equation (175) leads to

$$\langle E(\nu)\rangle = h\nu\sum_{v=0}^{\infty} v\frac{x^v}{\sum_{v=0}^{\infty}x^v} = h\nu\frac{x}{1-x}$$

$$= h\nu\frac{\mathrm{e}^{-h\nu/kT}}{1-\mathrm{e}^{-h\nu/kT}} = h\nu\frac{1}{\mathrm{e}^{h\nu/kT}-1} \qquad (176)$$

The energy density is the product of the mode density per unit volume and the average energy of the modes and is therefore given by (Planck 1900a)

$$\rho(\nu) = \frac{g(\nu)}{V}\langle E(\nu)\rangle = \frac{U(\nu)}{V} = \frac{8\pi h\nu^3}{c^3}\frac{1}{\mathrm{e}^{h\nu/kT}-1} \qquad (177)$$

a relation known as *Planck's law for the energy density of the radiation field*. The total energy U_V^{T} per unit volume is

$$U_V^{\mathrm{T}} = \int_0^{\infty}\rho(\nu)\mathrm{d}\nu = \frac{4}{c}\sigma_s T^4 \qquad (178)$$

where $\sigma_s = \frac{2\pi^5 k^4}{15c^2h^3} = 5.67\times10^{-5}\,\mathrm{g\ s^{-3}\,K^{-4}}$ represents the Stefan–Boltzmann constant. The heat capacity of a volume V of free space can be derived from the total internal energy $U^{\mathrm{T}} = V\cdot U_V^{\mathrm{T}}$

$$\left(\frac{\partial U^{\mathrm{T}}}{\partial T}\right)_V = V\cdot\frac{16}{c}\sigma_s T^3 \qquad (179)$$

At high T, U_V^{T} becomes very large and eventually sufficiently large that electron–positron pairs can be formed, at which point, vacuum fills with matter and antimatter, first by spontaneous generation of electrons and positrons.

4.5 Kinetics of Absorption and Emission of Incoherent, Quasi-thermal Radiation

This section presents Einstein's theory of absorption and emission kinetics in a thermal radiation field and introduces the main processes detected in a spectroscopic experiment: the absorption and emission of photons (Einstein1916a,b, Einstein 1917). By absorbing or emitting radiation, a quantum system makes a transition from an initial state $|1\rangle$ to a final state $|2\rangle$. Three processes must be considered: (i) absorption, (ii) spontaneous emission, and (iii) stimulated emission (Figure 12).

The resonance condition (energy conservation) requires that

$$E_2 - E_1 = h\nu_{12} \qquad (180)$$

We consider a system in thermal equilibrium with the radiation field at temperature T, where N_1, N_2 are the populations per unit volume in states $|1\rangle$ and $|2\rangle$, respectively. The

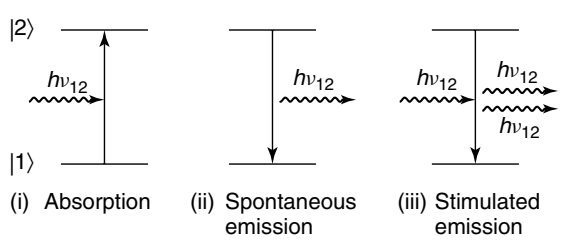

Figure 12 Processes arising from the interaction of a two-level system with a radiation field.

rate equations for processes 1–3 in Figure 12, respectively, are

$$-\frac{\mathrm{d}N_1^{(\mathrm{i})}}{\mathrm{d}t} = B_{21}\rho(\nu_{12})N_1 \quad \text{second-order kinetics} \tag{181}$$

$$\frac{\mathrm{d}N_1^{(\mathrm{ii})}}{\mathrm{d}t} = A_{12}N_2 \quad \text{first-order kinetics} \tag{182}$$

$$\frac{\mathrm{d}N_1^{(\mathrm{iii})}}{\mathrm{d}t} = B_{12}\rho(\nu_{12})N_2 \quad \text{second-order kinetics} \tag{183}$$

where $\rho(\nu_{12})$ represents the radiation energy density (equation 172). The conditions for thermal equilibrium are as follows:

- N_1 and N_2 remain constant, which leads to the following equations:

$$\frac{\mathrm{d}N_1}{\mathrm{d}t} = A_{12}N_2 + \rho(\nu_{12})(B_{12}N_2 - B_{21}N_1) = 0$$

$$\text{or} \quad A_{12}N_2 + B_{12}\rho(\nu_{12})N_2 = B_{21}\rho(\nu_{12})N_1 \tag{184}$$

- the populations in the levels are described by Boltzmann's distribution:

$$\frac{N_2}{N_1} = \mathrm{e}^{-(E_2-E_1)/kT} = \mathrm{e}^{-h\nu_{12}/kT} \tag{185}$$

Equations (184) and (185) are valid for all T. For $T \to \infty$, $N_2 = N_1$ and $\rho(\nu_{12}) = \infty$ (see equation 177). Because A_{12} and B_{12} are constants (i.e., are independent of T) and, in this case, $B_{12}\rho(\nu_{12}) \gg A_{12}$, one can write

$$B_{12}\rho(\nu_{12}) + A_{12} \cong B_{12}\rho(\nu_{12}) \tag{186}$$

From equations (184) and (186) and the condition $N_2 = N_1$ for $T \to \infty$, one can derive the following results:

$$B_{12} = B_{21} \Rightarrow A_{12}N_2 = B_{12}\rho(\nu_{12})(N_1 - N_2) \tag{187}$$

and

$$\rho(\nu_{12}) = \frac{A_{12}}{B_{12}}\left(\frac{N_1 - N_2}{N_2}\right)^{-1} = \frac{A_{12}}{B_{12}}\frac{1}{\mathrm{e}^{h\nu_{12}/kT} - 1} \tag{188}$$

with

$$\frac{N_1 - N_2}{N_2} = \mathrm{e}^{h\nu_{12}/kT} - 1$$

where the last equality was obtained from equation (185). Equation (188) can serve as a starting point to derive Planck's radiation law without involving quantized oscillators, as follows:

In the limit $T \to \infty$, $\nu \to 0$, Rayleigh–Jeans' law (equation 172) is valid, so that

$$\rho(\nu) = \frac{8\pi}{c^3}\nu^2 kT \tag{189}$$

Since, in this limit, $kT \gg h\nu$, $\frac{h\nu}{kT} \ll 1$, one can approximate $\mathrm{e}^{h\nu/kT}$ by the first two terms of a power series expansion

$$\mathrm{e}^{h\nu/kT} = 1 + \frac{h\nu}{kT} + \ldots \tag{190}$$

Inserting equation (190) into equation (188) and comparing with equation (189), one obtains

$$\rho(\nu_{12}) = \frac{A_{12}}{B_{12}}\left(\frac{1}{1 + \frac{h\nu_{12}}{kT} - 1}\right) = \frac{A_{12}}{B_{12}}\frac{kT}{h\nu_{12}} = \frac{8\pi}{c^3}\nu_{12}^2 kT \Rightarrow \frac{A_{12}}{B_{12}} = \frac{8\pi}{c^3}h\nu_{12}^3 \tag{191}$$

Since A_{12} and B_{12} are constants, equation (191) is valid for all temperatures and for any frequency ν_{12}. Inserting equation (191) into equation (188), one obtains Planck's radiation law (equation (177)):

$$\rho(\nu_{12}) = \frac{8\pi}{c^3}h\nu_{12}^3\left(\frac{1}{\mathrm{e}^{h\nu_{12}/kT} - 1}\right) \tag{192}$$

A_{12} is thus related to B_{12}, so that a single parameter suffices to describe radiative transitions between the quantum states 1 and 2, or more generally between states i and f (i for initial, f for final). In the electric dipole approximation, the Einstein coefficients can be expressed as

$$A_{\mathrm{fi}} = \frac{64\pi^4\nu_{\mathrm{fi}}^3}{3hc^3(4\pi\epsilon_0)}\langle \mathrm{f}|\boldsymbol{\mu}_{\mathrm{el}}|\mathrm{i}\rangle^2 \tag{193}$$

$$B_{\mathrm{fi}} = \frac{8\pi^3}{3h^2(4\pi\epsilon_0)}\langle \mathrm{f}|\boldsymbol{\mu}_{\mathrm{el}}|\mathrm{i}\rangle^2 \tag{194}$$

One can combine all rate processes (equations 181–183 and 193, 194) in the presence of a thermal (blackbody) radiation field at T into one rate coefficient for generalized first-order kinetics (see Quack (1998)).

$$K_{\mathrm{fi}} = A_{\mathrm{fi}}\frac{\mathrm{sign}(E_{\mathrm{f}} - E_{\mathrm{i}})}{\exp[(E_{\mathrm{f}} - E_{\mathrm{i}})/kT] - 1} \tag{195}$$

Einstein's derivation does not rely on Planck's description of the radiation field in terms of quantized oscillators, but

it makes use of the mode density from the Rayleigh–Jeans law. The energy density corresponds to the product of the mode density and the energy per mode and can be used to derive the average number of photons per mode $n(\nu)$:

$$U(\nu)\mathrm{d}\nu = V\rho(\nu)\mathrm{d}\nu = g(\nu)h\nu n(\nu)\mathrm{d}\nu \qquad (196)$$

with $g(\nu)$ the mode density, $h\nu$ the photon energy, and $n(\nu)$ the average number of photons or quanta per mode.

From equation (176) one obtains

$$n(\nu) = \frac{\langle E(\nu)\rangle}{h\nu} = \frac{1}{\mathrm{e}^{h\nu/kT} - 1} \qquad (197)$$

Of course, the number of photons in a mode must be an integer $(0, 1, 2, \ldots)$ and $n(\nu) < 1$ refers to an *average* number of photons. In the high-temperature limit, $\mathrm{e}^{h\nu/kT} \rightarrow 1$ and the number of photons per mode becomes very large. Depending on the value of $\mathrm{e}^{h\nu/kT}$ the average number of photons per mode can be larger or smaller than 1:

$$\begin{aligned} &\mathrm{e}^{h\nu/kT} = 2 \Rightarrow n(\nu) = 1 \quad \text{and} \quad \frac{h\nu}{kT} = \ln 2, \\ &\mathrm{e}^{h\nu/kT} < 2 \Rightarrow n(\nu) > 1, \\ &\mathrm{e}^{h\nu/kT} > 2 \Rightarrow n(\nu) < 1 \end{aligned} \qquad (198)$$

4.6 The Quantities in Quantitative Absorption Spectroscopy

This section provides a short summary of the physical quantities used in the literature to quantify the interaction of light with matter. The measurement of the strength of this interaction can be used to determine the concentration of particles in a given sample, with applications in analytical chemistry, or to model the radiative processes taking place in a certain system with applications, e.g., in atmospheric chemistry and physics.

The generic spectroscopic experiment is depicted in Figure 13, which illustrates the attenuation of a radiation beam as it traverses a sample.

I_0 and I represent the energy flow per unit surface and time, i.e., the intensity (with SI unit $\mathrm{W/m^2}$) of the radiation beam before and after traversing the sample. Instead of the intensity, one can also use the flow of photons per unit surface and time $I_{\mathrm{ph},0}$ and I_{ph} because of the relation

$$I = I_{\mathrm{ph}} h\nu \qquad (199)$$

The flow of photons per unit surface and time can be expressed as

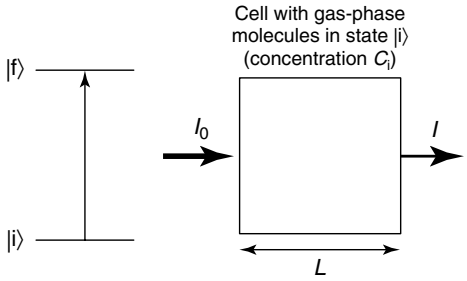

Figure 13 Generic spectroscopic experiment.

$$I_{\mathrm{ph}} = c \cdot C_{\mathrm{ph}} \qquad (200)$$

where c represents the speed of light and C_{ph} the photon concentration in the light beam as a particle density.

The number of absorbed photons per unit length $\mathrm{d}x$ is proportional to the concentration C_{i} of absorbing particles (as particle density) and to the intensity, so that

$$-\mathrm{d}I = \sigma_{\mathrm{fi}} I C_{\mathrm{i}} \mathrm{d}x \qquad (201)$$

where σ_{fi} is the molecular absorption cross section associated with the transition from state i to state f. σ_{fi} depends on the frequency, and one sees from equation (201) that σ_{fi} must have the unit $\mathrm{m^2}$ or, as often used, $\mathrm{cm^2}$. σ_{fi} can be interpreted as the surface of a completely absorbing disc that has the same absorption effect as the atom or molecule under investigation. Integrating equation (201) over the sample length one obtains

$$-\int_{I_0}^{I} \frac{\mathrm{d}I}{I} = \int_0^L \sigma_{\mathrm{fi}} C_{\mathrm{i}} \mathrm{d}x \qquad (202)$$

The result of the integration

$$\ln\left(\frac{I_0}{I}\right) = \sigma_{\mathrm{fi}} C_{\mathrm{i}} L \qquad (203)$$

is the well-known Lambert–Beer law. The quantity $\ln(\frac{I_0}{I})$ is known as the *Napierian absorbance*. Another form of the Lambert–Beer law is

$$\lg\left(\frac{I_0}{I}\right) = \epsilon_{\mathrm{fi}} c_{\mathrm{i,m}} L \qquad (204)$$

where $\lg\left(\frac{I_0}{I}\right)$ is the *decadic absorbance*, ϵ_{fi} the molar extinction coefficient usually expressed in $\mathrm{dm^3/(cm \cdot mol)}$, and $c_{\mathrm{i,m}}$ the concentration in $\mathrm{mol/dm^3}$.

Absorption can be viewed as a bimolecular process between a photon and an atom or a molecule:

$$-\frac{\mathrm{d}C_{ph}}{\mathrm{d}t} = k_{\mathrm{fi}}^{\mathrm{bim}} C_{\mathrm{ph}} C_{\mathrm{i}} \qquad (205)$$

With $c = \frac{dx}{dt}$ and using equation (200), equation (205) can be rewritten as

$$-\frac{dI_{ph}}{dx} = -\frac{d(c \cdot C_{ph})}{dx} = -\frac{dC_{ph}}{dt}$$
$$\overset{\text{equation (205)}}{=} k_{fi}^{bim} C_{ph} C_i \overset{\text{equation (201)}}{=} \sigma_{fi} \cdot I_{ph} \cdot C_i$$
$$\overset{\text{equation (200)}}{=} \sigma_{fi} c \cdot C_{ph} C_i = k_{fi}^{abs} C_i = -\frac{dC_i}{dt} \quad (206)$$

with $k_{fi}^{abs} = \sigma_{fi} c \cdot C_{ph}$ the effective first-order kinetics rate constant. Comparing this expression with equation (181), one obtains ($C_i = N_i$)

$$-\frac{dN_i}{dt} = B_{fi}\rho(\nu_{fi})N_i = k_{fi}^{abs} N_i \quad (207)$$

$$\text{with} \quad k_{fi}^{abs} = B_{fi}\rho(\nu_{fi}) = \sigma_{fi} c \cdot C_{ph}(\nu_{fi}) \quad (208)$$

In general, $C_{ph}(\nu)$ depends on the light source, and $C_{ph}(\nu)d\nu$ represents the concentration of photons with frequency lying in the interval between ν and $\nu + d\nu$ (see Figure 14). σ_{fi} also depends on ν, and often has maxima at the positions where the frequency ν corresponds to the frequency ν_{fi} of a transition between two quantum states of the system under investigation (see Figure 15). Section 7 presents the factors determining the lineshapes of the transitions in more detail.

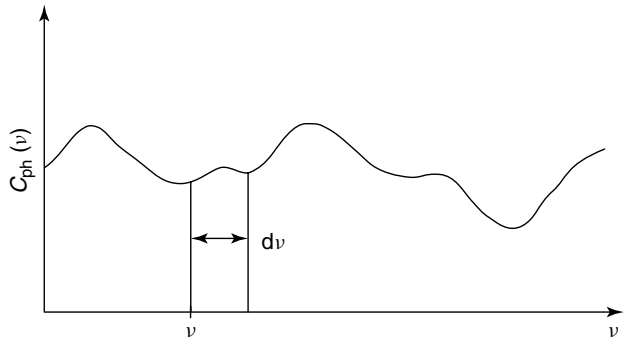

Figure 14 Concentration of photons as a function of the frequency.

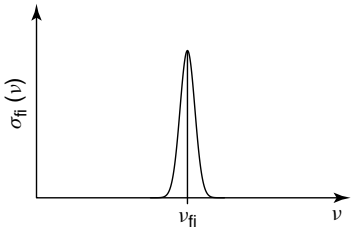

Figure 15 Schematic illustration of the frequency dependence of the molecular absorption cross section σ in the vicinity of a transition.

To take the frequency dependence of σ_{fi} and C_{ph} into account, equation (208) can be rewritten as

$$k_{fi}^{abs} = c \int_0^\infty \sigma_{fi}(\nu) C_{ph}(\nu) d\nu \quad (209)$$

Because the energy density $\rho(\nu) = h\nu \frac{n_{ph}(\nu)}{V}$, the concentration of photons can be expressed as

$$C_{ph}(\nu) = \frac{\rho(\nu)}{h\nu} \quad (210)$$

and the bimolecular rate constant introduced in equation (205) becomes

$$k_{fi}^{abs} = \frac{c}{h} \int_0^\infty \frac{\rho(\nu_{fi})\sigma_{fi}(\nu)}{\nu} d\nu \quad (211)$$

If $\rho(\nu)$ does not vary over the absorption line, which is the case if the radiation source does not have too narrow a bandwidth or if the line associated with the transition i $\rightarrow$ f is narrow, then

$$k_{fi}^{abs} = \frac{c}{h}\rho(\nu_{fi}) \int_0^\infty \frac{\sigma_{fi}(\nu)}{\nu} d\nu$$
$$= \frac{c}{h}\rho(\nu_{fi}) G_{fi} \quad (212)$$

with G_{fi} the *integrated absorption cross section*. With equation (208), G_{fi} can be related to the Einstein coefficient B_{fi},

$$B_{fi} = \frac{c}{h} G_{fi} \quad (213)$$

and thus represents an intrinsic property of the transition between the states i and f. One sees that B_{fi} is T-independent, as assumed by Einstein (see Section 4.5). Experimentally, one can also determine the *line strength* S_{fi} as the integral of the spectral intensity over the line profile (Figure 16):

$$S_{fi} = \int_0^\infty \sigma_{fi}(\nu) d\nu \quad (214)$$

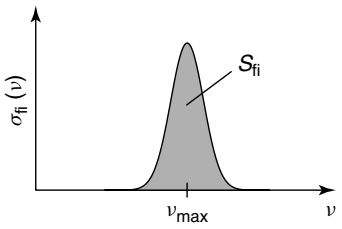

Figure 16 Line strength S_{fi} as integral of the spectral intensity over the line profile.

If the line is narrow, the function $\frac{1}{\nu}$ does not vary significantly over the line profile and can be approximated by $\frac{1}{\nu_{\mathrm{fi,max}}}$, so that the integrated absorption cross section G_{fi} is proportional to the line strength S_{fi}:

$$G_{\mathrm{fi}} = \int_0^\infty \frac{\sigma_{\mathrm{fi}}(\nu)}{\nu} \mathrm{d}\nu \cong \frac{1}{\nu_{\mathrm{fi,max}}} \int_0^\infty \sigma_{\mathrm{fi}}(\nu) \mathrm{d}\nu = \frac{S_{\mathrm{fi}}}{\nu_{\mathrm{fi,max}}} \quad (215)$$

The treatment outlined above suggests the following experimental procedure to characterize the transition between i and f:

1. For given values of L and c_{i}, measure the spectrum of the transition f $\leftarrow$ i.
2. Determine S_{fi} using equation (214).
3. Determine G_{fi} using equation (212) or (215).
4. Determine B_{fi} using equation (213).
5. Determine A_{fi} using equation (191):

$$A_{\mathrm{fi}} = \frac{8\pi}{c^3} h\nu_{\mathrm{fi}}^3 B_{\mathrm{fi}} = \frac{8\pi}{c^2} \nu_{\mathrm{fi}}^3 G_{\mathrm{fi}} \quad (216)$$

One can also use the *transition moment* $M_{\mathrm{fi}} = \langle \mathrm{f}|\boldsymbol{M}|\mathrm{i}\rangle$ instead of B_{fi} (see equation 194):

$$B_{\mathrm{fi}} = \frac{8\pi^3}{3h^2(4\pi\epsilon_0)} |M_{\mathrm{fi}}|^2 \quad \Rightarrow \quad (217)$$

$$|M_{\mathrm{fi}}|^2 = \frac{3h^2(4\pi\epsilon_0)}{8\pi^3} B_{\mathrm{fi}} = \frac{3h^2(4\pi\epsilon_0)c}{8\pi^3 h} G_{\mathrm{fi}} \quad (218)$$

where the transition dipole moment M_{fi} is expressed in the SI unit system. M_{fi} is often given in Debye (cgs unit; 1 Debye $= 1\,\mathrm{D} = 3.33564 \times 10^{-30}\,\mathrm{Cm}$) or in atomic units making use of the Bohr radius a_0 and the elementary charge e (1 a.u. (dipole moment) $= ea_0 = 2.54175$ D). A useful approximate relation between G_{fi} in pm^2 and M_{fi} in Debye is

$$G_{\mathrm{fi}}/\mathrm{pm}^2 \simeq 41.624 \left| \frac{M_{\mathrm{fi}}}{\mathrm{D}} \right|^2 \quad (219)$$

In electronic spectroscopy, one often uses the *oscillator strength*, a number without dimension (unitless):

$$f_{\mathrm{fi}} = \frac{(4\pi\epsilon_0) m_e c}{8\pi^2 \mathrm{e}^2} \lambda_{\mathrm{fi}}^2 A_{\mathrm{fi}}$$
$$= 1.4992 \times 10^{-14} \left(\frac{A_{\mathrm{fi}}}{\mathrm{s}^{-1}}\right) \left(\frac{\lambda}{\mathrm{nm}}\right)^2 \quad (220)$$

The use of oscillator strengths in electronic spectroscopy is justified by a sum rule, which states that the sum of all oscillator strengths equals the number of electrons.

Another method to determine the transition probability is to measure the time-dependent decay of excited states with concentration C_2 (using labels of Figure 12), satisfying equation (221) in the absence of external fields

$$C_2(t) = C_2(t_0) \exp(-A_{12} t) \quad (221)$$

This determines also B_{12}, and G_{21} by means of equations (216) and thus provides a route quite independent of absorption spectroscopy to determine these quantities.

More information on unit systems and recommended conventions to label physical quantities are provided in Stohner and Quack 2011: **Conventions, Symbols, Quantities, Units and Constants for High-resolution Molecular Spectroscopy**, this handbook. Some further useful equations for numerical calculations of the relevant quantities in radiative transitions can be found in Quack (1998).

4.7 Light Scattering, Raman Effect and Raman Spectroscopy

If the electric dipole transition moments M_{fi} for direct transitions are zero, for instance by symmetry for rotational and vibrational transitions in homonuclear diatomic molecules, one still can observe the relevant spectra by Raman scattering spectroscopy, which is illustrated in Figure 17. Generally, light is scattered by molecules as by other particles. If the scattered light has the same frequency ν as the incoming light, one speaks of *elastic* or *Rayleigh scattering*. However, the frequency of the scattered light may also change according to the equation for the scattered frequency ν'

$$h\nu' = h\nu \pm \Delta E \quad (222)$$

where ΔE is a quantum energy interval of the scattering molecule (or atom, etc.). Here one speaks of *inelastic* or *Raman scattering*. The effect was predicted theoretically by Smekal, Kramers, and Heisenberg in the early 1920s and observed experimentally by C. V. Raman (1928) (the history is briefly discussed by Weber (2011): **High-resolution Raman Spectroscopy of Gases**, this handbook). The frequency is shifted according to equation (222) by a quantized amount leading to sharp lines in the spectrum of scattered light. If $h\nu' < h\nu$, then one speaks of "Stokes" lines and if $h\nu' > h\nu$, one speaks of "Anti-Stokes" lines.

The energy difference ΔE is either deposited in the molecule (Stokes) or provided by the molecule (Anti-Stokes), as illustrated in Figure 17 for a rotational Raman transition in a homonuclear diatomic molecule (see Section 5). While weak population transfer is, in principle, possible with off-resonant monochromatic radiation by direct dipole coupling, as discussed in Section 3 (the near-degenerate Rabi problem would be an extreme example),

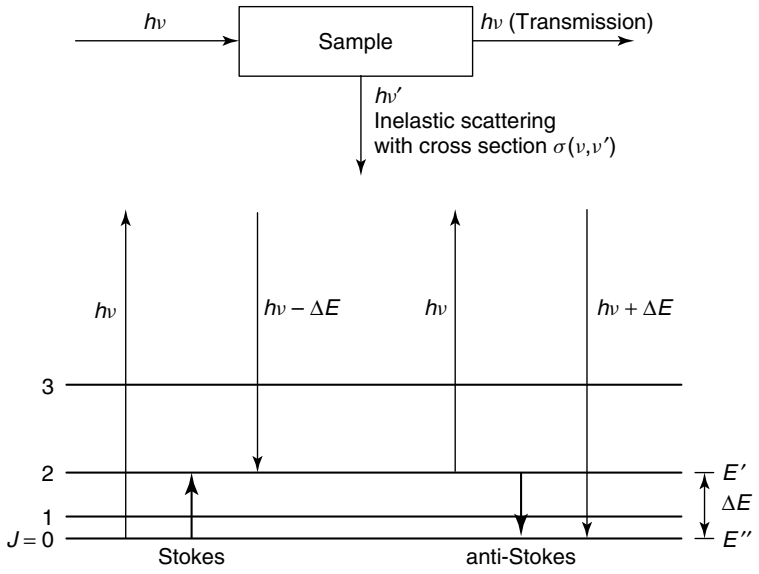

Figure 17 Top: Generic Raman spectroscopic experiment. Bottom: Schematic representation of the processes involved in Raman scattering. The thin arrows correspond to the incident ($h\nu$) and scattered ($h\nu' = h\nu \pm \Delta E$) radiations. The thick arrows represent rotational Raman transitions involving the $J = 0$ ground state.

the mechanism of Raman scattering is really very different, being more closely related to the Goeppert–Mayer two-photon absorption scheme of Figure 2 involving coupling matrix elements to intermediate levels, which may, however, be very far off resonance, as is illustrated in Figure 18. This scheme allows us to understand the selection rule

$$\Delta J = 0, \pm 2 \tag{223}$$

The Raman scattering cross section can be calculated approximately from equation (224):

$$\sigma_{fi}(\nu, \nu') \simeq \alpha(\nu')^4 \left| \sum_r \left(\frac{\langle f | \hat{\mu}_{\mathrm{el}} | r \rangle \langle r | \hat{\mu}_{\mathrm{el}} | \mathrm{i} \rangle}{E_r - E_i - h\nu + \mathrm{i}\Gamma_r} + \frac{\langle r | \hat{\mu}_{\mathrm{el}} | \mathrm{i} \rangle \langle f | \hat{\mu}_{\mathrm{el}} | r \rangle}{E_r - E_f + h\nu + \mathrm{i}\Gamma_r} \right) \right|^2 \tag{224}$$

α is a constant of proportionality. The matrix elements $\langle f | \hat{\mu}_{\mathrm{el}} | r \rangle$ and $\langle r | \hat{\mu}_{\mathrm{el}} | \mathrm{i} \rangle$ have an angular momentum selection rule $\Delta J = \pm 1$ each (see below); thus for the products in equation (224) one obtains a combined selection rule $\Delta J = 0, \pm 2$. The parity of the molecular levels must also be the same, when connected by a Raman transition, if parity is well defined (*see* Quack 2011: **Fundamental Symmetries and Symmetry Violations from High-resolution Spectroscopy**, this handbook).

In the normal Raman effect, none of the intermediate levels r in the scheme of Figure 18 satisfies the Bohr resonance condition. The states $|r\rangle$ are never populated appreciably

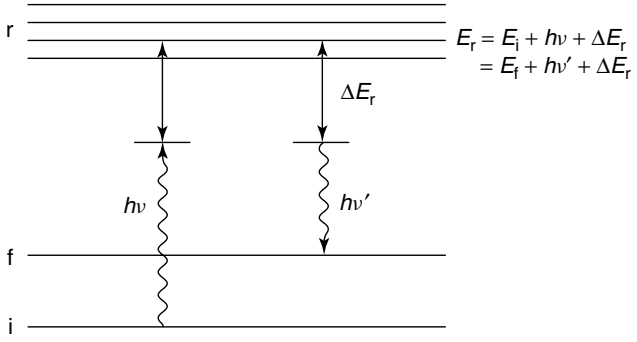

Figure 18 Stokes Raman transition between an initial state i and a final state f. The frequency of the incident and scattered radiations is detuned from resonance with excited states r by the detuning ΔE_{r}.

during the scattering process, which is instantaneous. If one of the states $|r\rangle$ matches the Bohr resonance condition for an intermediate level, then $E_r - E_i = h\nu$, and one denominator in the sum becomes small (and imaginary, $\mathrm{i}\Gamma_r$ with Γ_r being the full width at half maximum from the lifetime for that level; see Section 7).

In this case, the intermediate level gains an appreciable population, and one speaks of "resonance Raman scattering" and also of resonance fluorescence, if the process can be considered as absorption followed by spontaneous emission (fluorescence). These resonance processes have much larger cross sections leading to very high sensitivity in this type of spectroscopy. Otherwise, very similar selection rules apply to the spectroscopic transitions viewed as scattering to obtain accurate molecular energy intervals

ΔE, including intervals relevant to a variety of molecular processes such as tunneling splittings (Quack and Stockburger 1972, Stockburger 1973). Using laser radiation for excitation of the fluorescence, this process of laser-induced fluorescence (LIF) has been introduced and exploited as the basis for one of the most sensitive spectroscopic techniques (Sinha *et al*. 1973).

More generally, the Raman scattering cross section can be further related to molecular polarizibility. Details of high-resolution Raman spectroscopy are discussed in the article by Weber 2011: **High-resolution Raman Spectroscopy of Gases**, this handbook, including many examples and also further scattering processes such as CARS (coherent anti-Stokes Raman scattering) and DFWM (degenerate four-wave mixing).

5 MOLECULAR ENERGY LEVELS

Spectroscopic measurements provide information on the sample under study encoded in the form of line positions, line intensities, and lineshapes. The line positions can be used to extract information on the energy-level structure of molecules. One must realize, however, that a line position (i.e., its frequency ν_{if}) is only a measure of an energy difference $\Delta E_{\mathrm{fi}} = E_{\mathrm{f}} - E_{\mathrm{i}} = h\nu_{\mathrm{if}}$ between two quantum states i and f. To obtain the absolute positions of the energy levels, one can rely on existing knowledge on the energy positions E_{i} or E_{f} of one of the two states involved in the transition. One can also derive additional information on the energy-level structure by determining *combination differences*, i.e., by taking the differences between the positions of two lines originating from, or terminating on, a common energy level, as illustrated in Figure 19, which presents the essence of the Ritz (1908) combination principle (see also Sommerfeld 1919).

The purpose of this section is to briefly review the most general aspects of the energy-level structure of atoms and molecules that are essential for the interpretation and the analysis of spectral positions in the rotational, vibrational, and electronic spectra of molecules. Much more detailed information and many more examples can be found in subsequent articles of this handbook. In particular, the articles by Bauder 2011: **Fundamentals of Rotational Spectroscopy**, Albert *et al*. 2011: **Fundamentals of Rotation–Vibration Spectra** and Wörner and Merkt 2011: **Fundamentals of Electronic Spectroscopy**, this handbook, provide treatments of the rotational, vibrational, and electronic energy-level structures of molecules, respectively, and of the corresponding spectroscopies.

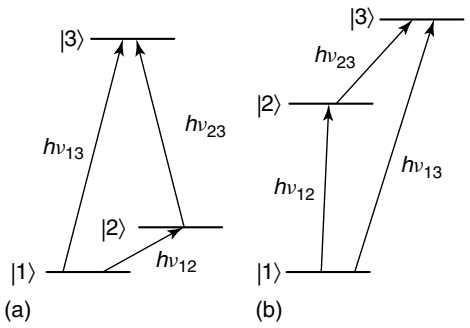

Figure 19 Combination differences method. (a) The energy difference between states $|1\rangle$ and $|2\rangle$ can be determined from the measured position $h\nu_{13}$ and $h\nu_{23}$ of transitions from levels $|1\rangle$ and $|2\rangle$ to a common level $|3\rangle$ by building the initial-state combination difference $h\nu_{12} = h\nu_{13} - h\nu_{23}$. (b) The energy difference between states $|2\rangle$ and $|3\rangle$ can be determined from the measured positions $h\nu_{12}$ and $h\nu_{13}$ of transitions from level $|1\rangle$ to levels $|2\rangle$ and $|3\rangle$ by building the final-state combination difference $h\nu_{23} = h\nu_{13} - h\nu_{12}$.

5.1 Time-independent Schrödinger Equation and Stationary States

For a system of N particles with coordinates $\boldsymbol{q}_i = (x_i, y_i, z_i)$ with $i = 1, \ldots, N$, the time-independent Schrödinger equation is

$$\hat{H}\Psi_n(x_1, y_1, z_1, \ldots, x_N, y_N, z_N) = E_n\Psi_n(x_1, y_1, z_1, \ldots, x_N, y_N, z_N) \qquad (225)$$

with

$$\hat{H} = \hat{T} + \hat{V} = \sum_{i=1}^{N} \frac{\hat{\boldsymbol{p}}_i^2}{2m_i} + \hat{V}(x_1, y_1, z_1, \ldots, x_N, y_N, z_N) = \hat{H}(\hat{\boldsymbol{p}}_i, \hat{\boldsymbol{q}}_i) \qquad (226)$$

where $\hat{\boldsymbol{p}}_i = (\hat{p}_{x_i}, \hat{p}_{y_i}, \hat{p}_{z_i})$; $\hat{p}_{x_i} = -\mathrm{i}\hbar\frac{\partial}{\partial x_i}$, $\hat{p}_{y_i} = -\mathrm{i}\hbar\frac{\partial}{\partial y_i}$, $\hat{p}_{z_i} = -\mathrm{i}\hbar\frac{\partial}{\partial z_i}$; $\hat{p}_{x_i}^2 = -\hbar^2\frac{\partial^2}{\partial x_i^2}$, $\hat{p}_{y_i}^2 = -\hbar^2\frac{\partial^2}{\partial y_i^2}$, $\hat{p}_{z_i}^2 = -\hbar^2\frac{\partial^2}{\partial z_i^2}$; $\hat{\boldsymbol{q}}_i = (\hat{x}_i, \hat{y}_i, \hat{z}_i)$; $\hat{x}_i = x_i$, $\hat{y}_i = y_i$, $\hat{z}_i = z_i$.

$\Psi_n(x_1, y_1, z_1, \ldots, x_N, y_N, z_N)$ are the eigenfunctions of $\hat{H}$ and E_n the corresponding energies. $|\Psi_n(x_1, \ldots, z_N)|^2\, \mathrm{d}x_1\mathrm{d}y_1\mathrm{d}z_1 \cdots \mathrm{d}z_N$ is the probability that, in state n, particle 1 is located between x_1, y_1, z_1 and $x_1 + \mathrm{d}x_1, y_1 + \mathrm{d}y_1, z_1 + \mathrm{d}z_1$, particle 2 between x_2, y_2, z_2 and $x_2 + \mathrm{d}x_2, y_2 + \mathrm{d}y_2, z_2 + \mathrm{d}z_2$, etc., and n represents a label (a quantum number or a set of quantum numbers) for the state. The eigenstates (Ψ_n, E_n) are stationary states. Usually, but not always, one uses the convention $E_1 = 0$, where $\Psi_1 = |1\rangle$ represents the lowest energy eigenstate of the system.

5.2 Exact Separability of the Schrödinger Equation

The solution of the eigenvalue equation (225) is simplified if the Hamiltonian $\hat{H}(\hat{\boldsymbol{p}}_i, \hat{\boldsymbol{q}}_i)$ can be written as a sum of two or more operators that act on distinct sets of variables,

$$\hat{H}(\hat{\boldsymbol{p}}_i, \hat{\boldsymbol{q}}_i) = \hat{H}_a(\hat{\boldsymbol{p}}_j, \hat{\boldsymbol{q}}_j) + \hat{H}_b(\hat{\boldsymbol{p}}_k, \hat{\boldsymbol{q}}_k) \tag{227}$$

where i runs from 1 to z, j from 1 to m, and k from $m+1$ to z, in steps of 1. The eigenfunctions $\Psi_n(\boldsymbol{q}_i)$ can, in this case, be written as products

$$\Psi_n(\boldsymbol{q}_i) = \varphi_{a,n_a}(\boldsymbol{q}_j)\varphi_{b,n_b}(\boldsymbol{q}_k), \tag{228}$$

and their energies as sums

$$E_n = E_{n_a} + E_{n_b} \tag{229}$$

whereby

$$\begin{aligned} &\hat{H}_a\varphi_{a,n_a}(\boldsymbol{q}_j) = E_{n_a}\varphi_{a,n_a}(\boldsymbol{q}_j) \qquad \text{and} \\ &\hat{H}_b\varphi_{b,n_b}(\boldsymbol{q}_k) = E_{n_b}\varphi_{b,n_b}(\boldsymbol{q}_k) \end{aligned} \tag{230}$$

Example 2 **The particle in a two-dimensional box**

The potential energy of a particle in a two-dimensional box is

$$V(x, y) = \begin{cases} 0 & \text{for } 0 < x < L_a \text{ and } 0 < y < L_b, \\ \infty & \text{otherwise} \end{cases} \tag{231}$$

In the box, $V(x, y) = 0$ and thus

$$\hat{H} = \underbrace{-\frac{\hbar^2}{2m}\frac{\partial^2}{\partial x^2}}_{\hat{H}_a(\hat{p}_x,\hat{q}_x)} \underbrace{-\frac{\hbar^2}{2m}\frac{\partial^2}{\partial y^2}}_{\hat{H}_b(\hat{p}_y,\hat{q}_y)} \tag{232}$$

Inserting the ansatz,

$$\Psi(x, y) = \varphi_{a,n_a}(x)\varphi_{b,n_b}(y) \tag{233}$$

into equation (232) gives

$$\begin{aligned} \hat{H}\varphi_{a,n_a}(x)\varphi_{b,n_b}(y) &= -\varphi_{b,n_b}(y)\frac{\hbar^2}{2m}\frac{\partial^2}{\partial x^2}\varphi_{a,n_a}(x) \\ &\quad - \varphi_{a,n_a}(x)\frac{\hbar^2}{2m}\frac{\partial^2}{\partial y^2}\varphi_{b,n_b}(y) \\ &= \varphi_{b,n_b}(y)E_{n_a}\varphi_{a,n_a}(x) \\ &\quad + \varphi_{a,n_a}(x)E_{n_b}\varphi_{b,n_b}(y) \\ &= (E_{n_a} + E_{n_b})\varphi_{a,n_a}(x)\varphi_{b,n_b}(y) \\ &= E_n\varphi_{a,n_a}(x)\varphi_{b,n_b}(y) \end{aligned} \tag{234}$$

Dividing equation (234) by $\varphi_{a,n_a}(x)\varphi_{b,n_b}(y)$ gives

$$E_n = \underbrace{-\frac{1}{\varphi_{a,n_a}(x)}\frac{\hbar^2}{2m}\frac{\partial^2}{\partial x^2}\varphi_{a,n_a}(x)}_{E_{n_a}} \underbrace{-\frac{1}{\varphi_{b,n_b}(y)}\frac{\hbar^2}{2m}\frac{\partial^2}{\partial y^2}\varphi_{b,n_b}(y)}_{E_{n_b}} \tag{235}$$

We have therefore the following solution:

$$\begin{aligned} &-\frac{\hbar^2}{2m}\frac{\partial^2}{\partial x^2}\varphi_{a,n_a}(x) = E_{n_a}\varphi_{a,n_a}(x); \\ &-\frac{\hbar^2}{2m}\frac{\partial^2}{\partial y^2}\varphi_{b,n_b}(y) = E_{n_b}\varphi_{b,n_b}(y); \end{aligned} \tag{236}$$

$$\begin{aligned} &\varphi_{a,n_a}(x) = \sqrt{\frac{2}{L_a}}\sin\left(\frac{n_a\pi x}{L_a}\right); \\ &\varphi_{b,n_b}(y) = \sqrt{\frac{2}{L_b}}\sin\left(\frac{n_b\pi y}{L_b}\right); \end{aligned} \tag{237}$$

$$\begin{aligned} &E_n = E_{n_a} + E_{n_b} = \frac{\hbar^2\pi^2}{2m}\left(\frac{n_a^2}{L_a^2} + \frac{n_b^2}{L_b^2}\right); \\ &\Psi_{n_a,n_b}(x, y) = \varphi_{a,n_a}(x)\varphi_{b,n_b}(y) \end{aligned} \tag{238}$$

5.3 Separation of the Center-of-mass Motion

In atoms and molecules in free space, the motion of the center of mass is exactly separable from the internal motion, because the potential $V(q_i)$ in equation (226) only depends on the distances r_{ij} between the nuclei and electrons:

$$\hat{H} = \hat{H}_{\text{cm}}(\hat{P}_{\text{cm}}, \hat{Q}_{\text{cm}}) + \hat{H}_{\text{int}}(\hat{p}^{\text{int}}, \hat{q}^{\text{int}}) \tag{239}$$

where $\hat{p}^{\text{int}}$ and $\hat{q}^{\text{int}}$ describe the internal motion and $\hat{P}_{\text{cm}}$, $\hat{Q}_{\text{cm}}$ the center-of-mass motion.

Equation (239) fulfills the condition for exact separability:

$$E_n = E_{\text{cm}} + E_{\text{int}} \tag{240}$$

$$\begin{aligned} \hat{H}_{\text{cm}} = &-\frac{\hbar^2}{2M}\left[\frac{\partial^2}{\partial X_{\text{cm}}^2} + \frac{\partial^2}{\partial Y_{\text{cm}}^2} + \frac{\partial^2}{\partial Z_{\text{cm}}^2}\right] \\ &+ V(X_{\text{cm}}, Y_{\text{cm}}, Z_{\text{cm}}) \end{aligned} \tag{241}$$

with $M = \sum_{i=1}^{N} m_i$. The overall translational motion of the atom/molecule can be treated as that of a free particle of mass M in a three-dimensional box. For a particle in a

3D box,

$$\Psi_{\mathrm{cm},n_{\mathrm{cm}}}(X_{\mathrm{cm}}, Y_{\mathrm{cm}}, Z_{\mathrm{cm}}) = \frac{2^{3/2}}{\sqrt{L_a L_b L_c}} \sin\left(\frac{n_a \pi X_{\mathrm{cm}}}{L_a}\right) \times \sin\left(\frac{n_b \pi Y_{\mathrm{cm}}}{L_b}\right) \sin\left(\frac{n_c \pi Z_{\mathrm{cm}}}{L_c}\right) \quad (242)$$

with $n_a, n_b, n_c = 1, 2, \ldots$ and $E_{\mathrm{cm},n} = \frac{\hbar^2\pi^2}{2M}\left(\frac{n_a^2}{L_a^2} + \frac{n_b^2}{L_b^2} + \frac{n_c^2}{L_c^2}\right)$. In spectroscopy, one studies the transitions between the energy levels associated with the *internal* motion of atoms and molecules and concentrates on a problem of reduced dimensionality $3N - 3$:

$$\hat{H}_{\mathrm{int}}(\hat{p}^{\mathrm{int}}, \hat{q}^{\mathrm{int}})\varphi_n^{\mathrm{int}}(q_i^{\mathrm{int}}) = E_n \varphi_n^{\mathrm{int}}(q_i^{\mathrm{int}}) \quad (243)$$

5.4 Near separability

In many instances, the Schrödinger equation is almost perfectly separable:

$$\hat{H}(\hat{\boldsymbol{p}}_i, \hat{\boldsymbol{q}}_i) = \hat{H}_a(\hat{\boldsymbol{p}}_j, \hat{\boldsymbol{q}}_j) + \hat{H}_b(\hat{\boldsymbol{p}}_k, \hat{\boldsymbol{q}}_k) + \hat{H}'(\hat{\boldsymbol{p}}_i, \hat{\boldsymbol{q}}_i) \quad (244)$$

with $i = 1, 2, \ldots, z$, $j = 1, 2, \ldots, m$ and $k = (m+1)$, $(m+2), \ldots, z$, and the expectation value of $\hat{H}'$ is much smaller than those of $\hat{H}_a$ and $\hat{H}_b$. The functions $\varphi_{a,n_a}(\boldsymbol{q}_j)\varphi_{b,n_b}(\boldsymbol{q}_k)$, where $\varphi_{a,n_a}(\boldsymbol{q}_j)$ and $\varphi_{b,n_b}(\boldsymbol{q}_k)$ are the eigenfunctions of $\hat{H}_a$ and $\hat{H}_b$, respectively, are very similar to the eigenfunctions of $\hat{H}$ and can serve as zero-order approximations of the eigenfunctions of $\hat{H}$ in a perturbation-theory treatment.

5.5 Hierarchy of Motions and Energies in Molecules

The different types of motion in a molecule (e.g., electronic, vibrational, and rotational) take place on different timescales and are associated with different contributions to the total energy, as shown in Table 1. This hierarchy of timescales implies the approximate separability of the corresponding motions that lies behind the *Born–Oppenheimer (BO) approximation*: The nuclei appear immobile to the fast-moving electrons, and hardly any rotation takes place during a vibrational period. The vibrational motion can thus be viewed as taking place in an "average" electronic cloud, and the rotational motion at a nuclear configuration corresponding to an average over the vibrational motion. The approximate separability can be expressed as

Table 1 Different types of motion in a molecule and corresponding timescale and energy intervals.

Motion	Typical period	Typical energy interval/(hc)
Electronic	~ 1 fs	$> 5000\,\mathrm{cm}^{-1}$ $(30\,000\,\mathrm{cm}^{-1})$
Vibrational	10–100 fs	$300–3000\,\mathrm{cm}^{-1}$
Rotational	0.1 ps 10 ps	$3–300\,\mathrm{cm}^{-1}$

$$\hat{H}_{\mathrm{int}} = \hat{H}_{\mathrm{e}}(\boldsymbol{q}_i) + \hat{H}_{\mathrm{v}}^{(\mathrm{e})}(\boldsymbol{Q}_\alpha) + \hat{H}_{\mathrm{r}}^{(\mathrm{ev})}(\theta, \phi, \chi) + \hat{H}_{\mathrm{ns}}^{(\mathrm{evr})} \quad (245)$$

$$E = E_{\mathrm{e}} + E_{\mathrm{v}}^{(\mathrm{e})} + E_{\mathrm{r}}^{(\mathrm{ev})} + E_{\mathrm{ns}}^{(\mathrm{evr})} \quad (246)$$

$$\Psi = \varphi_{\mathrm{e}}(\boldsymbol{q}_i, \boldsymbol{R}_\alpha)\varphi_{\mathrm{v}}^{(\mathrm{e})}(\boldsymbol{Q}_\alpha)\varphi_{\mathrm{r}}^{(\mathrm{ev})}(\theta, \phi, \chi)\phi_{\mathrm{ns}}^{(\mathrm{evr})} \quad (247)$$

where e, v, r, and ns stand for electronic, vibrational, rotational, and nuclear spin, respectively, and the superscripts indicate which motion is averaged out and leads to an implicit dependence of the relevant quantity. The separability enables one to reduce a problem of high dimensionality to several problems of reduced dimensionality. It also justifies the chemist's description of molecules in terms of "rigid" geometries. $\boldsymbol{Q}_\alpha$ and $\boldsymbol{q}_i$ are the position vectors of the nuclei $(\alpha = 1, 2, \ldots, N_{\mathrm{k}})$ and the electrons $(i = 1, 2, \ldots, N_{\mathrm{e}})$, respectively, and θ, ϕ, χ are the Euler angles describing the orientation of the molecule axis system in the laboratory frame. $\boldsymbol{R}_\alpha$ is used in equation (247) instead of $\boldsymbol{Q}_\alpha$ to indicate a parametric dependence (see below).

5.6 The Born–Oppenheimer (BO) Approximation

The BO approximation enables the separation of electronic and nuclear degrees of freedom in a molecule. The Hamilton operator of a molecule with N_{k} nuclei and N_{e} electrons has the form

$$\hat{H}(\hat{\boldsymbol{Q}}_\alpha, \hat{\boldsymbol{P}}_\alpha, \hat{\boldsymbol{q}}_i, \hat{\boldsymbol{p}}_i) = \hat{T}_{\mathrm{k}} + \hat{T}_{\mathrm{e}} + V(\boldsymbol{Q}_\alpha, \boldsymbol{q}_i) \quad \alpha = 1, \ldots, N_{\mathrm{k}}, i = 1, \ldots, N_{\mathrm{e}}, \quad (248)$$

$$\hat{T}_{\mathrm{k}} = \sum_{\alpha=1}^{N_{\mathrm{k}}} -\frac{\hbar^2}{2M_\alpha}\Delta_\alpha$$

$$\hat{T}_{\mathrm{e}} = \sum_{i=1}^{N_{\mathrm{e}}} -\frac{\hbar^2}{2m_{\mathrm{e}}}\Delta_i,$$

$$V(\boldsymbol{Q}_\alpha, \boldsymbol{q}_i) = \sum_{\alpha=1}^{N_{\mathrm{k}}}\sum_{\beta>\alpha}^{N_{\mathrm{k}}} \frac{Z_\alpha Z_\beta e^2}{4\pi\epsilon_0|\boldsymbol{Q}_\alpha - \boldsymbol{Q}_\beta|} + \sum_{i=1}^{N_{\mathrm{e}}}\sum_{j>i}^{N_{\mathrm{e}}} \frac{e^2}{4\pi\epsilon_0|\boldsymbol{q}_j - \boldsymbol{q}_i|} - \sum_{\alpha=1}^{N_{\mathrm{k}}}\sum_{i=1}^{N_{\mathrm{e}}} \frac{Z_\alpha e^2}{4\pi\epsilon_0|\boldsymbol{Q}_\alpha - \boldsymbol{q}_i|} \quad (249)$$

and the Schrödinger equation

$$\hat{H}\Psi_n(\boldsymbol{Q}_\alpha, \boldsymbol{q}_i) = E_n\Psi_n(\boldsymbol{Q}_\alpha, \boldsymbol{q}_i) \qquad (n : \text{set of quantum numbers designating the eigenstates}) \quad (250)$$

involves $3(N_k + N_e)$ coordinates. By making the BO approximation, one reduces the dimensionality of the problem and solves an equation of $3N_e$ variables for the electronic motion and an equation of $3N_k$ variables for the nuclear motion. Separating the center-of-mass translational motion (see Section 5.3) and the overall rotation of the molecule enables the reduction of the number of nuclear degrees of freedom by 6 for nonlinear molecules and by 5 for linear molecules.

In the BO treatment, $\Psi_n(\boldsymbol{Q}_\alpha, \boldsymbol{q}_i)$ is represented as a product

$$\Psi_n(\boldsymbol{Q}_\alpha, \boldsymbol{q}_i) = \varphi_m^{(n)}(\boldsymbol{Q}_\alpha)\phi_n(\boldsymbol{q}_i, \boldsymbol{Q}_\alpha) \qquad (251)$$

of a nuclear wavefunction $\varphi_m^{(n)}(\boldsymbol{Q}_\alpha)$ and an electronic wavefunction $\phi_n(\boldsymbol{q}_i, \boldsymbol{Q}_\alpha)$ (separability). The treatment exploits the fact that the nuclei hardly move during a period of the electronic motion. The index m is needed to distinguish different states of the nuclear motion (e.g., vibrational, rotational) associated with a given electronic state n.

The BO treatment consists of two steps:

Step 1. The nuclei are frozen at a given geometry $\boldsymbol{R}_\alpha$: $\boldsymbol{Q}_\alpha \to \boldsymbol{R}_\alpha$. As a result $\hat{T}_k = 0$ and the first term of equation (249) becomes constant. A purely electronic Schrödinger equation is then solved (the nuclear coordinates are treated as parameters, and *not* as variables):

$$\hat{H} \to \hat{H}_e = \hat{T}_e + \hat{V}(\boldsymbol{q}_i, \boldsymbol{R}_\alpha) \qquad (252)$$

Inserting equations (251) and (252) into equation (250) we obtain

$$\left[\hat{T}_e + \hat{V}(\boldsymbol{q}_i, \boldsymbol{R}_\alpha)\right]\varphi_m^{(n)}(\boldsymbol{Q}_\alpha)\phi_n(\boldsymbol{q}_i, \boldsymbol{R}_\alpha) = V_n\varphi_m^{(n)}(\boldsymbol{Q}_\alpha)\phi_n(\boldsymbol{q}_i, \boldsymbol{R}_\alpha) \qquad (253)$$

Because neither $\hat{T}_e$ nor $\hat{V}$ acts on the nuclear coordinates $\boldsymbol{Q}_\alpha$, $\varphi_m^{(n)}(\boldsymbol{Q}_\alpha)$ cancels out in equation (253):

$$\left[\hat{T}_e + \hat{V}(\boldsymbol{q}_i, \boldsymbol{R}_\alpha)\right]\phi_n(\boldsymbol{q}_i, \boldsymbol{R}_\alpha) = V_n\phi_n(\boldsymbol{q}_i, \boldsymbol{R}_\alpha) \qquad (254)$$

The solutions of equation (254) are sets of electronic wavefunctions $\phi_n(\boldsymbol{q}_i, \boldsymbol{R}_\alpha)$ and energies $V_n(\boldsymbol{R}_\alpha)$, where $n = 1, 2, \ldots$ corresponds to a label for the electronic states.

Determining $V_n(\boldsymbol{R}_\alpha)$ for a large number of possible configurations $\boldsymbol{R}_\alpha$, one obtains the *BO potential hypersurface*, which represents the dependence of the electronic energy on the nuclear coordinates. The dimensionality of the BO potential hypersurface is $3k - 5$ for diatomic molecules and $3k - 6$ for polyatomic molecules and equals the number of internal degrees of freedom f. $V_n(\boldsymbol{R}_\alpha)$ does not depend on the mass of the nuclei and is therefore isotope independent.

Example 3 **Rough estimate of the error in the dissociation energy of H_2^+ associated with the BO approximation.**

H_2^+ has two nuclei and one internal degree of freedom, the internuclear separation R.

At $R \to \infty$, H_2^+ in its ground state dissociates into H^+ + H(1s). The dissociation energies D_e of H_2^+ and D_2^+ are identical within the BO approximation (see Figure 20) and amount to $D_e \cong 22\,500\,\text{cm}^{-1}$. Extremely precise ab initio calculations have been performed of the dissociation energies of H_2^+ and its deuterated isotopomers, including adiabatic and nonadiabatic corrections (Moss 1993a,b, 1996, Korobov 2006, 2008) and the calculations of rovibronic energy levels of these ions agree with precise spectroscopic measurements (see, for instance, Carrington *et al.* (1993), Leach and Moss (1995), Liu *et al.* (2010)).

The order of magnitude error of the BO approximation on the dissociation energy of H_2^+ can be estimated to be $\approx 30\ \text{cm}^{-1}$ (i.e., 0.13%) because the ionization energies E_I of H and

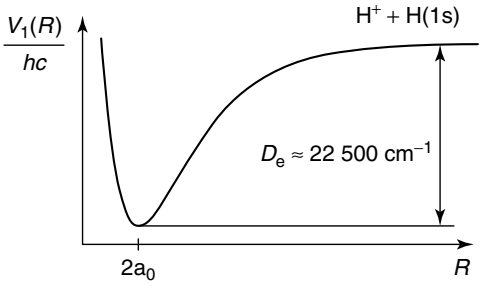

Figure 20 Schematic representation of the potential energy function of the $X\ ^2\Sigma_g^+$ ground electronic state of H_2^+ ($n = 1$).

D differ by $\approx 30\ \mathrm{cm}^{-1}$: $\frac{E_\mathrm{I}}{hc}(H) = R_\mathrm{H} = 109\,677\ \mathrm{cm}^{-1}$ and $\frac{E_\mathrm{I}}{hc}(D) = R_\mathrm{D} = 109\,706\ \mathrm{cm}^{-1}$.

Assuming that at least 10 points must be calculated per internal degree of freedom, equation (254) must be solved 10 times for a diatomic molecule ($f = 1$), 1000 times for a nonlinear triatomic molecule (H_2O, $f = 3$), and 10^{30} times for C_6H_6 ($f = 30$), if one wants to determine the complete potential energy hypersurface. The general calculation and representation of such potential hypersurfaces is discussed in Yamaguchi and Schaefer 2011: **Analytic Derivative Methods in Molecular Electronic Structure Theory: A New Dimension to Quantum Chemistry and its Applications to Spectroscopy**, Tew *et al*. 2011: **Ab Initio Theory for Accurate Spectroscopic Constants and Molecular Properties**, Breidung and Thiel 2011: **Prediction of Vibrational Spectra from Ab Initio Theory** and Marquardt and Quack 2011: **Global Analytical Potential Energy Surfaces for High-resolution Molecular Spectroscopy and Reaction Dynamics**, this handbook. Relativistic effects are treated by Mastalerz and Reiher 2011: **Relativistic Electronic Structure Theory for Molecular Spectroscopy**, this handbook.

Stable molecular configurations correspond to local minima on the BO hypersurface and adiabatic isomerization reactions can be viewed as trajectories connecting two local minima on the BO hypersurface.

Step 2. The Schrödinger equation describing the nuclear motion on the nth potential hypersurface is solved. Inserting equation (254) with the solution $\varphi_m^{(n)}(\boldsymbol{Q}_\alpha)$ and $\phi_n(\boldsymbol{q}_i, \boldsymbol{Q}_\alpha)$ in equation (248) leads to an equation describing the nuclear motion

$$\begin{aligned}
&\hat{H}_N \phi_n(\boldsymbol{q}_i, \boldsymbol{Q}_\alpha)\varphi_m^{(n)}(\boldsymbol{Q}_\alpha) \\
&\quad = \left[\hat{T}_N + \hat{T}_e + \hat{V}(\boldsymbol{q}_i, \boldsymbol{Q}_\alpha)\right]\phi_n(\boldsymbol{q}_i, \boldsymbol{Q}_\alpha)\varphi_m^{(n)}(\boldsymbol{Q}_\alpha) \\
&\quad = \left[\hat{T}_N + V_n(\boldsymbol{Q}_\alpha)\right]\phi_n(\boldsymbol{q}_i, \boldsymbol{Q}_\alpha)\varphi_m^{(n)}(\boldsymbol{Q}_\alpha) \qquad (255)
\end{aligned}$$

with

$$\hat{T}_N = -\sum_\alpha^k \frac{\hbar^2}{2M_\alpha}\Delta_\alpha \doteq -\sum_\alpha^k \frac{\hbar^2}{2M_\alpha}\frac{\partial^2}{\partial \boldsymbol{Q}_\alpha^2} \qquad (256)$$

The notation in equation (256) implies

$$\begin{aligned}
&\frac{\partial}{\partial \boldsymbol{Q}_\alpha}\phi_n(\boldsymbol{q}_i, \boldsymbol{Q}_\alpha)\varphi_m^{(n)}(\boldsymbol{Q}_\alpha) \\
&\quad = \phi_n(\boldsymbol{q}_i, \boldsymbol{Q}_\alpha)\frac{\partial}{\partial \boldsymbol{Q}_\alpha}\varphi_m^{(n)}(\boldsymbol{Q}_\alpha) \\
&\qquad + \varphi_m^{(n)}(\boldsymbol{Q}_\alpha)\frac{\partial}{\partial \boldsymbol{Q}_\alpha}\phi_n(\boldsymbol{q}_i, \boldsymbol{Q}_\alpha) \\
&\quad = \phi_n\varphi_m^{(n)\prime} + \varphi_m^{(n)}\phi_n' \qquad (257)
\end{aligned}$$

and

$$\frac{\partial^2}{\partial \boldsymbol{Q}_\alpha^2}\phi_n\varphi_m^{(n)} = \underbrace{\phi_n\varphi_m^{(n)\prime\prime}}_{T_1} + \underbrace{2\phi_n'\varphi_m^{(n)\prime}}_{T_2} + \underbrace{\varphi_m^{(n)}\phi_n''}_{T_3} \qquad (258)$$

Using equations (256) and (258), equation (255) can be rewritten as

$$\begin{aligned}
&\hat{H}_N\phi_n\varphi_m^{(n)} \\
&\quad = \left[-\sum_{\alpha=1}^k \frac{\hbar^2}{2M_\alpha}[T_1 + T_2 + T_3] + V_n(\boldsymbol{Q}_\alpha)\right]\phi_n\varphi_m^{(n)} \\
&\quad = E_m^n\phi_n\varphi_m^{(n)} \qquad (259)
\end{aligned}$$

The term T_1 is the direct contribution to the nuclear kinetic energy. The terms T_2 and T_3 are indirect contributions to the kinetic energy of the nuclei, which originate from the dependence of the electronic wavefunction on the nuclear coordinate. In low electronic states for which the BO hypersurfaces are usually well separated, this variation is smooth and these terms can be neglected to a good approximation.

We thus get, when neglecting T_2 and T_3

$$\begin{aligned}
&\hat{H}_N\phi_n(\boldsymbol{q}_i, \boldsymbol{Q}_\alpha)\varphi_m^{(n)}(\boldsymbol{Q}_\alpha) \\
&\quad = -\sum_{\alpha=1}^k \frac{\hbar^2}{2M_\alpha}\phi_n(\boldsymbol{q}_i, \boldsymbol{Q}_\alpha)\Delta_\alpha\varphi_m^{(n)}(\boldsymbol{Q}_\alpha) \\
&\qquad + V_n(\boldsymbol{Q}_\alpha)\phi_n(\boldsymbol{q}_i, \boldsymbol{Q}_\alpha)\varphi_m^{(n)}(\boldsymbol{Q}_\alpha) \\
&\quad = E_m^n\phi_n(\boldsymbol{q}_i, \boldsymbol{Q}_\alpha)\varphi_m^{(n)}(\boldsymbol{Q}_\alpha) \qquad (260)
\end{aligned}$$

Dividing both sides of equation (260) by $\phi_n(\boldsymbol{q}_i, \boldsymbol{Q}_\alpha)$ enables one to eliminate the electron coordinates $\boldsymbol{q}_i$ and to obtain the equation describing the nuclear motion:

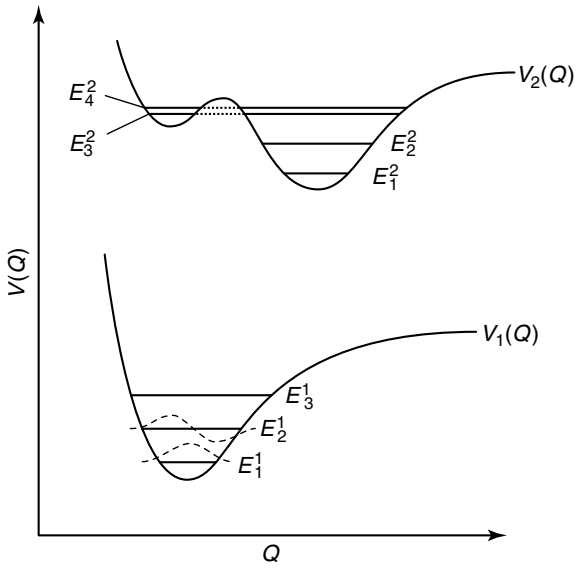

Figure 21 Born–Oppenheimer potential energy functions of two electronic states of a diatomic molecule. In diatomic molecules, the hypersurfaces reduce to one-dimensional potential energy functions ($f = 1$).

$$\hat{H}_N \varphi_m^{(n)}(\boldsymbol{Q}_\alpha) = \left[-\sum_{\alpha=1}^{k} \frac{\hbar^2}{2M_\alpha} \Delta_\alpha + V_n(\boldsymbol{Q}_\alpha) \right] \varphi_m^{(n)}(\boldsymbol{Q}_\alpha) = E_m^n \varphi_m^{(n)}(\boldsymbol{Q}_\alpha) \quad (261)$$

This equation has the usual form for a Schrödinger equation and consists of a kinetic energy term (first term in the square brackets) and a potential energy term $V_n(\boldsymbol{Q}_\alpha)$. The equation can be solved numerically; E_m^n represents the total (rovibronic) energy and $\varphi_m^{(n)}$ the nuclear wavefunction. For further discussion of the BO approximation, we refer also to Bauder 2011: **Fundamentals of Rotational Spectroscopy**, this handbook.

To make this procedure less abstract, we consider, in the next subsection, the simplest case of diatomic molecules. This illustration will enable us to visualize the nuclear motion as consisting of a vibrational motion and a rotational motion. In diatomic molecules, the potential energy hypersurfaces reduce to one-dimensional potential energy functions because $f = 1$ (see Figure 21).

5.7 Nuclear Motion of a Diatomic Molecule

In the BO approximation, the nuclear motion of a diatomic molecule in electronic state n is described by

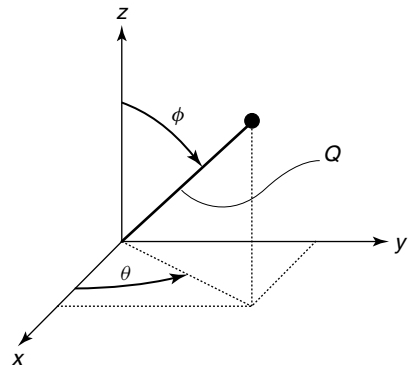

Figure 22 Representation of the nuclear motion of a diatomic molecule using polar coordinates ($Q = R, \varphi, \theta$).

$$\hat{H}_N = \frac{\hat{P}_1^2}{2M_1} + \frac{\hat{P}_2^2}{2M_2} + V_n(|\boldsymbol{Q}_2 - \boldsymbol{Q}_1|) = \frac{1}{2M} \hat{P}_{\mathrm{CM}}^2 + \frac{1}{2\mu} \hat{P}_{\mathrm{int}}^2 + V_n(|\boldsymbol{Q}_2 - \boldsymbol{Q}_1|) \quad (262)$$

with $M = M_1 + M_2$ and $\mu = \frac{M_1 M_2}{M_1 + M_2}$.

The internal motion can be described by that of a fictive particle of mass μ and position $\boldsymbol{Q} = \boldsymbol{Q}_2 - \boldsymbol{Q}_1$, where $|\boldsymbol{Q}| = Q(= R)$ represents the internuclear distance (see Figure 22)

$$\hat{H}_N \varphi_m^{(n)}(\boldsymbol{Q}) = -\frac{\hbar^2}{2\mu} \Delta_Q \varphi_m^{(n)}(\boldsymbol{Q}) + V_n(Q) \varphi_m^{(n)}(\boldsymbol{Q}) = E_m^n \varphi_m^{(n)}(\boldsymbol{Q}) \quad (263)$$

Expressing Δ_Q in polar coordinates, one gets

$$\Delta_Q = \frac{\partial^2}{\partial Q^2} + \frac{2}{Q} \frac{\partial}{\partial Q} - \frac{1}{\hbar^2 Q^2} \hat{J}^2 \quad (264)$$

with

$$\hat{J}^2 = -\hbar^2 \left(\frac{1}{\sin\theta} \frac{\partial}{\partial\theta} \sin\theta \frac{\partial}{\partial\theta} + \frac{1}{\sin^2\theta} \frac{\partial}{\partial\phi^2} \right) \quad (265)$$

where $\hat{J}$ is the rotational angular momentum operator. Inserting equations (264) and (265) in equation (263) leads to

$$\left[-\frac{\hbar^2}{2\mu} \left(\frac{\partial^2}{\partial Q^2} + \frac{2}{Q} \frac{\partial}{\partial Q} \right) + \frac{1}{2\mu Q^2} \hat{J}^2 + V_n(Q) - E_m^n \right] \varphi_m^{(n)}(Q) = 0 \quad (266)$$

Since only $\hat{J}^2$ acts on θ and ϕ, the equation is separable:

$$\varphi_m^{(n)}(Q, \theta, \phi) = F(Q) Y_{JM}(\theta, \phi) = \frac{1}{Q} G(Q) Y_{JM}(\theta, \phi) \quad (267)$$

In equation (267), $Y_{JM}(\theta, \phi)$ are the spherical harmonics that are the eigenfunctions of the angular momentum

operators $\hat{J}^2$ and $\hat{J}_z$:

$$\hat{J}^2 Y_{JM}(\theta,\phi) = \hbar^2 J(J+1) Y_{JM}(\theta,\phi) \tag{268}$$

$$\hat{J}_z Y_{JM}(\theta,\phi) = \hbar M Y_{JM}(\theta,\phi) \tag{269}$$

The reason for writing $F(Q)$ as $\frac{1}{Q}G(Q)$ in equation (267) is to simplify the algebra in later steps of the derivation.

Because

$$\frac{\partial}{\partial Q}\left(\frac{G(Q)}{Q}\right) = -\frac{1}{Q^2}G + \frac{1}{Q}G' \qquad \text{and}$$

$$\frac{\partial^2}{\partial Q^2}\left(\frac{G(Q)}{Q}\right) = \frac{2}{Q^3}G - \frac{2}{Q^2}G' + \frac{1}{Q}G'' \tag{270}$$

Equation (266) can be rewritten as

$$\begin{aligned} &-\frac{\hbar^2}{2\mu}\left[\frac{2}{Q^3}G - \frac{2}{Q^2}G' + \frac{1}{Q}G'' \right.\\ &\left. + \frac{2}{Q}\left(-\frac{1}{Q^2}G + \frac{1}{Q}G'\right)\right] Y_{JM}(\theta,\phi)\\ &+ \frac{1}{2\mu Q^2}\frac{G}{Q}\hbar^2 J(J+1) Y_{JM}(\theta,\phi)\\ &+ \left(V_n(Q) - E_m^n\right)\frac{G(Q)}{Q} Y_{JM}(\theta,\phi) = 0 \end{aligned} \tag{271}$$

Simplifying and multiplying each remaining term of equation (271) by $\frac{Q}{Y_{JM}}$ one obtains

$$\begin{aligned} &-\frac{\hbar^2}{2\mu}\frac{\partial^2}{\partial Q^2}G(Q) + \frac{\hbar^2}{2\mu Q^2}J(J+1)G(Q)\\ &\quad + \left(V_n(Q) - E_m^n\right)G(Q) = 0 \end{aligned} \tag{272}$$

This one-dimensional differential equation can be solved numerically to obtain the vibration–rotation energy levels. To illustrate the meaning of the different terms in equation (272) we make further approximations.

We consider only the region of $V_n(Q)$ close to the minimum $Q_{\min} = R_e$ and write $Q = R_e + \rho$. We then make a Taylor series expansion of $V_n(Q)$ and $\frac{1}{Q^2}$ around R_e.

$$\begin{aligned} V_n(Q) = V_n(R_e) &+ \left(\frac{\partial V_n(Q)}{\partial Q}\right)_{R_e}\cdot\rho\\ &+ \frac{1}{2}\left(\frac{\partial^2 V_n(Q)}{\partial Q^2}\right)_{R_e}\cdot\rho^2 + \cdots \end{aligned} \tag{273}$$

$$\frac{1}{Q^2} = \frac{1}{R_e^2} - \frac{2}{R_e^3}\cdot\rho + \cdots \tag{274}$$

The second term on the right-hand side of equation (273) is zero because $V_n(Q)$ reaches a minimum at R_e. Retaining only the first term of equation (274) and the first two nonzero terms of equation (273) (rigid rotor and harmonic oscillator approximation, respectively) and inserting into equation (272), one obtains the following equation:

$$\begin{aligned} &-\frac{\hbar^2}{2\mu}\frac{\partial^2}{\partial\rho^2}G(\rho) + \underbrace{\frac{\hbar^2}{2\mu R_e^2}J(J+1)}_{hcB_e J(J+1) = E_{\text{rot}}^J} G(\rho)\\ &+ V_n(R_e)G(\rho) + \frac{1}{2}k\rho^2 G(\rho) = E_m^n G(\rho) \end{aligned} \tag{275}$$

with $k = \frac{\partial^2 V(Q)}{\partial Q^2}|_{R_e}$. This equation can be rewritten as

$$\underbrace{\left[-\frac{\hbar^2}{2\mu}\frac{\partial^2}{\partial\rho^2} + \frac{1}{2}k\rho^2\right]}_{\hat{H}\text{ for harmonic oscillator}} G(\rho) = \left[E_m^n - V_n(R_e) - E_{\text{rot}}^J\right]G(\rho) \tag{276}$$

The operator in square brackets on the left-hand side of equation (276) can easily be recognized as the Hamiltonian operator of a harmonic oscillator and we can also write

$$\left[-\frac{\hbar^2}{2\mu}\frac{\partial^2}{\partial\rho^2} + \frac{1}{2}k\rho^2\right]G(\rho) = h\nu_{\text{osc}}\left(v + \frac{1}{2}\right)G(\rho) \tag{277}$$

Comparing the right-hand sides of equations (276) and (277), one can see that the total energy E_m^n is a sum of an electronic energy, a vibrational energy, and a rotational energy:

$$\begin{aligned} E_m^n = &\underbrace{V_n(R_e)}_{\text{electronic energy}} + \underbrace{E_{\text{vib}}^v}_{\text{vibrational energy}} + \underbrace{E_{\text{rot}}^J}_{\text{rotational energy}}\\ &= V_n(R_e) + h\nu_{\text{osc}}\left(v + \frac{1}{2}\right) + hcB_e J(J+1) \end{aligned} \tag{278}$$

Equation (278) describes the energy level structure depicted schematically in Figure 23. One obtains a better approximation of the exact solution of equation (272) by

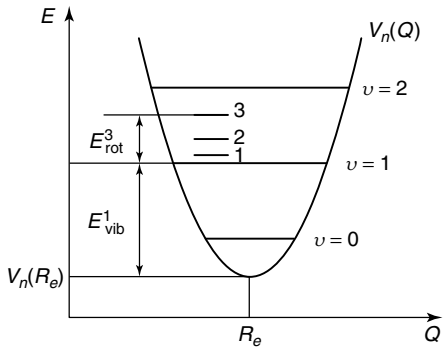

Figure 23 Schematic representation of the rovibronic energy levels of a diatomic molecule.

- keeping the higher terms in equation (273). The potential becomes anharmonic and therefore

$$\frac{E_{\text{vib}}^{v}}{hc} = \omega_{\text{e}}\left(v+\frac{1}{2}\right) - \omega_{\text{e}}x_{\text{e}}\left(v+\frac{1}{2}\right)^2 + \omega_{\text{e}}y_{\text{e}}\left(v+\frac{1}{2}\right)^3 + \cdots \quad (279)$$

  (Note: The constants ω_{e}, $\omega_{\text{e}}x_{\text{e}}$ and $\omega_{\text{e}}y_{\text{e}}$ are wavenumbers usually given in cm^{-1}.)
- keeping higher terms in equation (274). One then can account for the lengthening of the average internuclear distance caused by the anharmonic vibrational motion

$$B_v = B_{\text{e}} - \alpha_{\text{e}}\left(v+\frac{1}{2}\right) + \cdots \quad (280)$$

- taking into account centrifugal distortion (which corresponds to an elongation of the bond as the rotational motion gets faster, i.e., at increasing J values)

$$E_{\text{rot}} = B_v J(J+1) - D_v J^2(J+1)^2 + \cdots \quad (281)$$

The constants ω_{e}, $\omega_{\text{e}}x_{\text{e}}$, $\omega_{\text{e}}y_{\text{e}}$, B_{e}, α_{e}, etc. are tabulated for many electronic states of many diatomic molecules (see Huber and Herzberg (1979), Bernath and McLeod (2001)) and can be used to calculate the rovibronic energies of a diatomic molecule. Nowadays, efficient methods (and good programs) are available to solve equation (272) numerically. For further discussion of spectra and spectroscopic parameters of diatomic molecules as well as the extension to polyatomic molecules, we refer the reader to Albert *et al.* 2011: **Fundamentals of Rotation–Vibration Spectra**, this handbook.

6 INTRODUCTION TO GROUP THEORY AND APPLICATION TO MOLECULAR SPECTROSCOPY

Group theory is an important tool in spectroscopy. It enables one to classify wavefunctions according to their symmetry properties and to determine selection rules in a straightforward manner. Formal introductions to group theory tend to be abstract. Instead of presenting such an introduction, we have selected topics particularly relevant to spectroscopy, which we illustrate by simple examples. Our hope is that such a presentation will help the reader to rapidly get acquainted with the main aspects of group theory as a tool for spectroscopists. This introductory approach should also facilitate the study of almost all the articles in this handbook, but does not replace a comprehensive presentation of group theory. Articles Schnell 2011: **Group Theory for High-resolution Spectroscopy of Nonrigid Molecules**, Oka 2011: **Orders of Magnitude and Symmetry in Molecular Spectroscopy**, Quack 2011: **Fundamental Symmetries and Symmetry Violations from High-resolution Spectroscopy** and Wörner and Merkt 2011: **Fundamentals of Electronic Spectroscopy**, this handbook, provide a more rigorous introduction to and more detailed information on group theory and its applications to molecular physics and spectroscopy. They also contain many references to other articles and textbooks on group theory.

6.1 Symmetry Groups and Symmetry Operations

A group describing the symmetry properties of molecules can be viewed as a set of operations $\hat{S}_i$ that commute with the Hamiltonian $\hat{H}$ describing the molecules, and do not affect the energy spectrum

$$\left[\hat{S}_i, \hat{H}\right] = 0 \quad (282)$$

$\hat{H}$ and $\hat{S}_i$ thus have a common set of eigenfunctions and the eigenvalues of $\hat{S}_i$ can be used as labels for the eigenfunctions. In molecular physics and molecular spectroscopy, two types of groups are particularly important, the point groups and the nuclear-permutation-inversion groups. Point groups are widely used to label the energy levels of rigid or semirigid molecules, whereas nuclear-permutation-inversion groups, in particular the complete nuclear-permutation-inversion (CNPI) and the molecular symmetry groups, are generally employed to label the energy levels of nonrigid molecules, i.e., molecules in which the nuclear framework undergoes large-amplitude motions. The permutation-inversion groups and their use in the treatment of the spectroscopic properties of nonrigid molecules are the object of Schnell 2011: **Group Theory for High-resolution Spectroscopy of Nonrigid Molecules**, this handbook. This section provides an elementary-level introduction to group theory with emphasis on point groups. The general aspects, however, are also valid for permutation-inversion groups.

(a) Point-group operations and point-group symmetry. Point-group symmetry operations include the identity, rotations, reflections, rotation-reflections and the inversion of the molecular framework. The inversion and operations involving reflections are called improper operations. The point-group operations are designated as follows:

  E: Identity (no operation; unit element of the group).

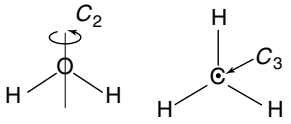

Figure 24 Examples of C_n point-group rotations in H_2O ($n = 2$) and CH_3 ($n = 3$).

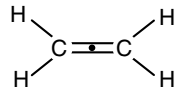

Figure 25 Example of a molecule (here ethylene) with an inversion center indicated by a dot.

C_n: Rotation by $\frac{2\pi}{n}$. The symmetry axis with highest n is chosen as principal z-axis (see examples in Figure 24).

Improper symmetry operations:

σ: Reflection through a plane:

σ_v: vertical planes (contain symmetry z-axis);

σ_h: horizontal plane (is $\perp$ to symmetry z-axis).

i: Inversion. Inversion of all coordinates through the inversion center (see example in Figure 25).

S_n: Rotation–reflection: rotation by $\frac{2\pi}{n}$ around the z-axis followed by a reflection through the plane perpendicular to the rotation axis (see example in Figure 26).

A molecule having an improper operation as symmetry operation cannot be optically active (chiral), if parity is conserved.

(b) Permutation-inversion operations

These operations are at the origin of the complete nuclear permutation-inversion group and the MS group which in general is a subgroup thereof (see Bunker and Jensen (1998), Longuet-Higgins (1963) and also Mills and Quack (2002) for a historical review). They are designated as follows:

E (identity or unit element)

(ij): Permutation of the coordinates of two identical nuclei i and j.

(ijk): Cyclic permutation of the coordinates of three identical nuclei i, j, and k.

$\vdots$

E^*: Inversion of *all* coordinates of *all* particles through the center of the lab-fixed frame (this is different from the point-group inversion i).

$(ij)^*$: Permutation followed by inversion of all coordinates of all particles.

$(ijk)^*$: Cyclic permutation followed by inversion of all coordinates of all particles, and so forth for more particles.

Permutation-inversion operations leave $\hat{H}$ unchanged.

Example 4 **Hamiltonian of CH_2**

(C: 1, H: 2,3)

$$\hat{H} = \frac{-\hbar^2}{2m_1}\Delta_1 - \frac{\hbar^2}{2m_2}\Delta_2 - \frac{\hbar^2}{2m_3}\Delta_3 + \sum_{i=1}^{8}\frac{-\hbar^2}{2m_e}\Delta_i + \frac{e^2}{4\pi\epsilon_0}\left\{\frac{6}{r_{12}} + \frac{6}{r_{13}} + \frac{1}{r_{23}}\right\} - \sum_{k=1}^{3}\sum_{i=1}^{8}\frac{Z_k e^2}{4\pi\epsilon_0 r_{ki}} + \sum_{i=1}^{8}\sum_{j>i}^{8}\frac{e^2}{4\pi\epsilon_0 r_{ij}}. \quad (283)$$

The coordinates only come "squared" in equation (283) and the operation * leaves $\hat{H}$ unchanged. One can also readily verify that the operation (23), which exchanges r_2 with r_3, does not change $\hat{H}$. The labels 1, 2, and 3 used to designate the nuclei are defined in Figure 27.

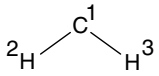

Figure 27 Methylene molecule in which the nuclei have been labeled 1, 2 and 3.

6.2 Definition of a Group and Important Concepts

A group is a set of objects, called *elements*, A, B, C, ... (permutations, transformations, etc.) which are connected by a combination rule (written as a product) $A \cdot B = C$ such that the result of the combination is also an element of the group. Three conditions must be fulfilled:

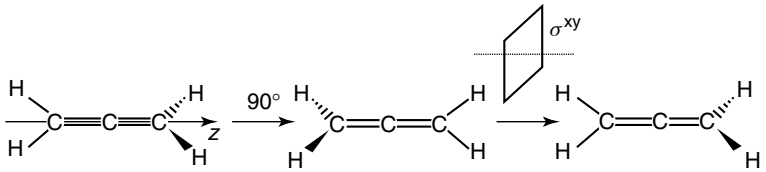

Figure 26 Example of a molecule (here allene) with an S_4-symmetry operation.

1. The combination rule must be associative.
   $A \cdot (B \cdot C) = (A \cdot B) \cdot C$.
2. There must be an element, the identity E, such that $E \cdot R = R \cdot E = R$ for all elements R of the group.
3. Each element R must have an inverse R^{-1} which is also a group element such that
   $R \cdot R^{-1} = R^{-1} \cdot R = E$.

The *order of a group* is equal to the number of elements in the group. While many groups used to describe the symmetry properties of molecules have a finite number of elements, infinite groups, i.e., groups with an infinite number of elements, also exist, examples being the $C_{\infty v}$ and $D_{\infty h}$ point groups of linear molecules and the group K_h used for atoms. The use of infinite groups is illustrated by several examples in Wörner and Merkt 2011: **Fundamentals of Electronic Spectroscopy**, this handbook. In this introductory article, only finite groups are used as illustrations.

The connection between symmetry operation $\hat{S}_i$ discussed above and group theory comes from the fact that if $\hat{S}_i$ and $\hat{S}_j$ leave $\hat{H}$ unchanged when applied individually, they must also leave $\hat{H}$ unchanged when applied in succession. $\hat{S}_i \cdot \hat{S}_j$ must therefore be a symmetry operation if $\hat{S}_i$ and $\hat{S}_j$ are symmetry operations. The notation $\hat{S}_i \cdot \hat{S}_j$ must be understood in the following way: $\hat{S}_j$ acts first, $\hat{S}_i$ second.

Example 5 **The point group of H_2O**

The point group of H_2O is C_{2v} with the symmetry operations (E, C_2^z, σ^{xz}, σ^{yz}).

From Figure 28 one can see that the successive application of any two operations of the C_{2v} point group is equivalent to the application of a third group operation. For instance,

$$\sigma^{xz}\sigma^{yz} = C_2^z,\ \sigma^{xz}\sigma^{xz} = E,\ C_2^z\sigma^{xz} = \sigma^{yz},\ \text{etc.}$$

One can build a combination table (also called *multiplication table*) that summarizes all possible combinations. The multiplication table of the C_{2v} point group with four symmetry operations (E, C_2^z, σ^{xz}, σ^{yz}) is thus a 4×4 table (see Table 2).

Table 2 Multiplication table of the C_{2v} point group.

	First operation (right)			
C_{2v}	E	C_2^z	σ^{xz}	σ^{yz}
Second operation (left)				
E	E	C_2^z	σ^{xz}	σ^{yz}
C_2^z	C_2^z	E	σ^{yz}	σ^{xz}
σ^{xz}	σ^{xz}	σ^{yz}	E	C_2^z
σ^{yz}	σ^{yz}	σ^{xz}	C_2^z	E

$\sigma^{yz} = \sigma^{xz}C_2^z$

In the C_{2v} group, $A \cdot B$ is always equal to $B \cdot A$ (all operations commute), and one says that the group is *abelian*. Not all groups are abelian. An example of a non-abelian group is the point group C_{3v}.

Example 6 **The point group of CH_3Cl**

The point group of CH_3Cl is C_{3v}. The group has the order $h = 6$ with the elements (E, C_3, C_3^2, σ^a, σ^b, σ^c).

With the help of Figure 29, one can derive the multiplication table of the C_{3v} point group presented in Table 3. One sees that the group is not abelian because not all operations

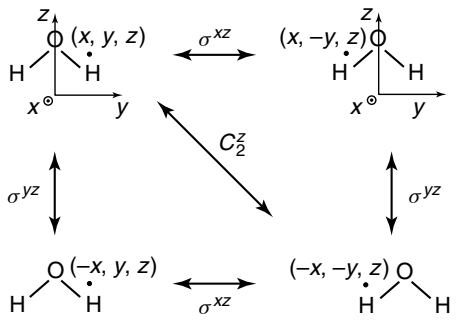

Figure 28 C_{2v} group operations and their effect on a water molecule. The dot indicates schematically the coordinates (x, y, z) of an electron.

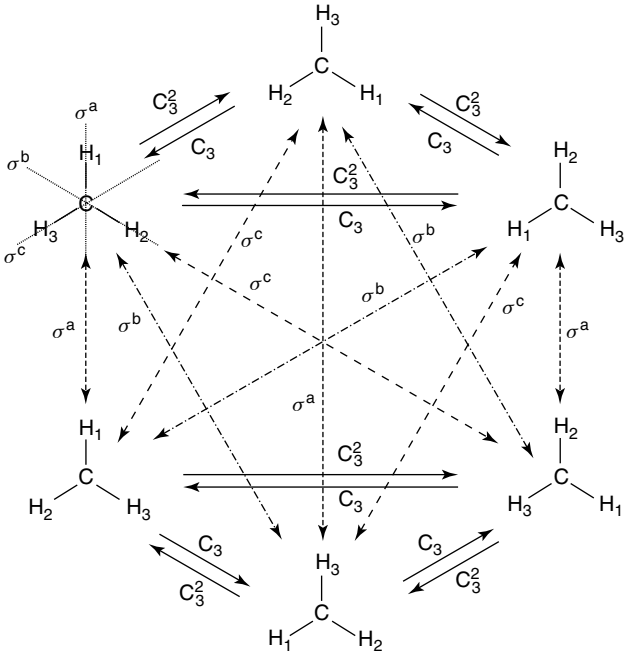

Figure 29 The operations of the C_{3v} point group with the example of the CH_3Cl molecule. The C–Cl bond points out of the plane of the paper and lies parallel to the C_3-axis (z-axis).

Table 3 Multiplication of the C_{3v} point group.

	First operation (right)					
C_{3v}	E	C_3	C_3^2	σ^a	σ^b	σ^c
Second operation (left)	E	E	C_3	C_3^2	σ^a	σ^b	σ^c
	C_3	C_3	C_3^2	E	σ^c	σ^a	σ^b
	C_3^2	C_3^2	E	C_3	σ^b	σ^c	σ^a
	σ^a	σ^a	σ^b	σ^c	E	C_3	C_3^2
	σ^b	σ^b	σ^c	σ^a	C_3^2	E	C_3
	σ^c	σ^c	σ^a	σ^b	C_3	C_3^2	E

commute (e.g., $C_3 \cdot \sigma^a = \sigma^c$ and $\sigma^a \cdot C_3 = \sigma^b$). Moreover, not all elements are their own inverses (e.g., $C_3 \cdot C_3 \neq E$ in Table 3).

Conjugated elements and classes

If A, B, R are all group elements and if they obey the relation

$$RAR^{-1} = B \tag{284}$$

then A and B are called *conjugated elements*. All conjugated elements in a group form a class.

Example 7 **Derivation of the elements of the point group C_{3v} that belong to the same class as C_3**

Inserting $C_3 = A$ in equation (284) and taking for R successively all group operations, one obtains the following results from the C_{3v} multiplication table (Table 3):

$$\begin{aligned}
&R = E: && E^{-1} = E; && EC_3E = C_3.\\
&R = C_3: && C_3^{-1} = C_3^2; && C_3C_3C_3^{-1} = C_3C_3C_3^2 = C_3.\\
&R = C_3^2: && (C_3^2)^{-1} = C_3; && C_3^2C_3C_3 = C_3.\\
&R = \sigma^a: && (\sigma^a)^{-1} = \sigma^a; && \sigma^a \underbrace{C_3\sigma^a}_{\sigma^c} = C_3^2.\\
&R = \sigma^b: && (\sigma^b)^{-1} = \sigma^b; && \sigma^b \underbrace{C_3\sigma^b}_{\sigma^a} = C_3^2.\\
&R = \sigma^c: && (\sigma^c)^{-1} = \sigma^c; && \sigma^c \underbrace{C_3\sigma^c}_{\sigma^b} = C_3^2.
\end{aligned}$$

Consequently, C_3 and C_3^2 are elements of the same class of order 2. Similarly, one can show that σ^a, σ^b, and σ^c form a class of order 3.

Order of an element

The order n of an element A is the smallest integer with $A^n = E$.

C_{3v}: C_3 is of order 3, σ^a of order 2.

All elements of a class have the same order.

6.3 Representations and Character Tables

Group operations can be represented by $n \times n$ matrices $\boldsymbol{B}_i$ that fulfill the combination rule, whereby n represents the dimension of the representation. These matrices represent transformations of vectors or functions of the form of equation (285):

$$\boldsymbol{y} = \boldsymbol{R}_i\boldsymbol{x} \tag{285}$$

The matrices depend on the coordinate system and can be transformed from one coordinate system to another using $\boldsymbol{T}_i = \boldsymbol{S}\boldsymbol{R}_i\boldsymbol{S}^{-1}$ where the new, equivalent representation $\boldsymbol{T}_i$ is obtained from the original representation $\boldsymbol{R}_i$. The trace of a matrix remains unchanged upon a unitary coordinate transformation and the trace of the matrix is called its *character*. For the set of equivalent representations $\boldsymbol{R}_i$ and $\boldsymbol{T}_i$, one thus has

$$\mathrm{Tr}(\boldsymbol{T}_i) = \mathrm{Tr}(\boldsymbol{R}_i) : \text{character of operation} \tag{286}$$

All elements of a class have the same character, as can be seen from equation (284). If the matrices of all elements of a representation of a group can be simultaneously brought into block-diagonal form by a given coordinate transformation, the representation is said to be *reducible*; if not, it is *irreducible*. The *character table* of a group lists *all* irreducible representations and, for each representation, gives the character of each class of elements.

A character table has the structure shown in Table 4. In a character table, $\Gamma^{(n)}$ designates the nth representation, C_i the ith class of elements, and $\chi_j^{(m)}$ the character of the elements of class j in the mth representation. There are as many irreducible representations as classes. Character tables exist for all groups. Many groups have a finite number of representations, but groups with an infinite number of representations also exist such as the $D_{\infty h}$ and $C_{\infty v}$ point groups of diatomic molecules. The character tables of the C_{3v} and C_{2v} point groups are given in Tables 5 and 6, respectively.

In addition to the characters of the elements of the different classes, the character table also indicates, in the last two columns, how the translations T_x, T_y, and T_z (also

Table 4 General structure of a character table.

G	$C_1 = E$	C_2	...	C_n	(x y z)	(R_x R_y R_z)
$\Gamma^{(1)}$	$\chi_1^{(1)}$	$\chi_2^{(1)}$	...	$\chi_n^{(1)}$		
$\Gamma^{(2)}$	$\chi_1^{(2)}$	$\chi_2^{(2)}$				
$\vdots$	$\vdots$	$\vdots$				
$\Gamma^{(n)}$	$\chi_1^{(n)}$	$\chi_2^{(n)}$	...	$\chi_n^{(n)}$		

Table 5 Character table of the C_{3v} point group.

C_{3v}	E	$2C_3$	$3\sigma_v$		
A_1	1	1	1	T_z	
A_2	1	1	−1		R_z
E	2	−1	0	$T_x,\ T_y$	$R_x,\ R_y$

Table 6 Character table of the C_{2v} point group.

C_{2v}	$\hat{E}$	$\hat{C}_2^z$	$\hat{\sigma}^{xz}$	$\hat{\sigma}^{yz}$			
$\Gamma^{(z)} = A_1$	1	1	1	1	z	x^2, y^2, z^2	
$\Gamma^{(xy)} = A_2$	1	1	−1	−1		xy	R_z
$\Gamma^{(x)} = B_1$	1	−1	1	−1	x	xz	R_y
$\Gamma^{(y)} = B_2$	1	−1	−1	1	y	yz	R_x

designated by x, y, and z, respectively) and the rotations R_x, R_y, and R_z transform.

To construct an n-dimensional representation of a group, one takes n linear independent functions or vectors Ψ_i, $i = 1, \ldots, n$ spanning a given n-dimensional space. Applying the group operations on Ψ_i leads to a transformed function that is a linear combination of the original functions:

$$\hat{R}\Psi_i = \sum_{j=1}^{n} D_{ji}(R)\Psi_j \tag{287}$$

Example 8 **One-dimensional representations of the C_{2v} point group**

As possible one-dimensional representations ($n = 1$) of C_{2v}, one can take the functions x, y, or z.

$$\begin{aligned}
\Psi_1 = x: \quad & \hat{E}\cdot x = x & \Psi_2 = y: \quad & \hat{E}\cdot y = y \\
& \hat{C}_2^z \cdot x = -x & & \hat{C}_2^z \cdot y = -y \\
& \hat{\sigma}^{xz}\cdot x = x & & \hat{\sigma}^{xz}\cdot y = -y \\
& \hat{\sigma}^{yz}\cdot x = -x & & \hat{\sigma}^{yz}\cdot y = y
\end{aligned}$$

$$\begin{aligned}
\Psi_3 = z: \quad & \hat{E}\cdot z = z \\
& \hat{C}_2^z \cdot z = z \\
& \hat{\sigma}^{xz}\cdot z = z \\
& \hat{\sigma}^{yz}\cdot z = z
\end{aligned}$$

Therefore x, y, and z correspond to the irreducible representations B_1, B_2, and A_1 of C_{2v}, respectively, in accord with the third column of the character table of the C_{2v} point group (Table 6).

Instead of using x, y, or z, more complicated functions can be used to generate a one-dimensional representation, such as x^2, xy, or $\sin x$.

$$\begin{aligned}
\Psi_4 = x^2: \quad & (\hat{E}x^2) = (\hat{E}x)(\hat{E}x) = x^2 \\
& (\hat{C}_2^z x^2) = (\hat{C}_2^z x)(\hat{C}_2^z x) = x^2 \\
& (\hat{\sigma}^{xz} x^2) = (\hat{\sigma}^{xz} x)(\hat{\sigma}^{xz} x) = x^2 \\
& (\hat{\sigma}^{yz} x^2) = (\hat{\sigma}^{yz} x)(\hat{\sigma}^{yz} x) = x^2 \\
\Psi_5 = xy: \quad & (\hat{E}(xy)) = (\hat{E}x)(\hat{E}y) = xy \\
& (\hat{C}_2^z (xy)) = (\hat{C}_2^z x)(\hat{C}_2^z y) = xy \\
& (\hat{\sigma}^{xz} (xy)) = (\hat{\sigma}^{xz} x)(\hat{\sigma}^{xz} y) = -xy \\
& (\hat{\sigma}^{yz} (xy)) = (\hat{\sigma}^{yz} x)(\hat{\sigma}^{yz} y) = -xy \\
\Psi_6 = \sin x: \quad & (\hat{E}\sin x) = \sin x \\
& (\hat{C}_2^z \sin x) = \sin(-x) = -\sin x \\
& (\hat{\sigma}^{xz} \sin x) = \sin x \\
& (\hat{\sigma}^{yz} \sin x) = \sin(-x) = -\sin x
\end{aligned}$$

One sees that x^2, xy, and $\sin x$ transform as A_1, A_2, and B_1, respectively. It is easy to verify that $\chi^{xy} = \chi^x \cdot \chi^y$, a result that can be written as a direct product $\Gamma^x \otimes \Gamma^y = B_1 \otimes B_2 = (1\ -1\ 1\ -1) \otimes (1\ -1\ -1\ 1) = (1\ 1\ -1\ -1) = A_2$.

To evaluate a direct product, such as $A_2 \otimes B_2 = B_1$ in C_{2v}, one multiplies the characters of each class of elements pairwise and obtains as direct product a representation of the group that can be either irreducible or reducible. In the latter case, the reducible representation is usually reduced following the method described below in Section 6.4.

One can also look at the transformation properties of rotations, which, in the case of the R_z operation of the C_{2v} group, is illustrated in Figure 30. The following results are obtained:

$$\begin{aligned}
& E(R_z) = R_z \\
& C_2^z(R_z) = R_z \\
& \sigma^{xz}(R_z) = -R_z \quad \text{Direction of rotation reversed.} \\
& \sigma^{yz}(R_z) = -R_z \quad \text{Direction of rotation reversed.}
\end{aligned}$$

One can verify that R_x and R_y transform as B_2 and B_1, respectively.

Representations of higher dimensions can be obtained by looking at the transformation properties of two or more functions, as explained in the next two examples.

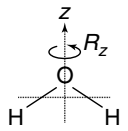

Figure 30 Schematic representation of a rotation R_z around the z axis of the molecule-fixed coordinate system of H_2O.

Example 9 **Two-dimensional representation $\binom{x}{y}$ of the C_{2v} point group**

C_{2v}: Two-dimensional representation $\binom{x}{y}$

$$E \cdot \begin{pmatrix} x \\ y \end{pmatrix} = \begin{pmatrix} x \\ y \end{pmatrix} = \begin{pmatrix} 1 & 0 \\ 0 & 1 \end{pmatrix} \begin{pmatrix} x \\ y \end{pmatrix},$$

$$\text{with } \chi_E^{\binom{x}{y}} = Tr \begin{pmatrix} 1 & 0 \\ 0 & 1 \end{pmatrix} = 2$$

$$C_2^z \cdot \begin{pmatrix} x \\ y \end{pmatrix} = \begin{pmatrix} -x \\ -y \end{pmatrix} = \begin{pmatrix} -1 & 0 \\ 0 & -1 \end{pmatrix} \begin{pmatrix} x \\ y \end{pmatrix},$$

$$\text{with } \chi_{C_2^z}^{\binom{x}{y}} = -2$$

$$\sigma^{xz} \cdot \begin{pmatrix} x \\ y \end{pmatrix} = \begin{pmatrix} x \\ -y \end{pmatrix} = \begin{pmatrix} 1 & 0 \\ 0 & -1 \end{pmatrix} \begin{pmatrix} x \\ y \end{pmatrix},$$

$$\text{with } \chi_{\sigma^{xz}}^{\binom{x}{y}} = 0$$

$$\sigma^{yz} \cdot \begin{pmatrix} x \\ y \end{pmatrix} = \begin{pmatrix} -x \\ y \end{pmatrix} = \begin{pmatrix} -1 & 0 \\ 0 & 1 \end{pmatrix} \begin{pmatrix} x \\ y \end{pmatrix},$$

$$\text{with } \chi_{\sigma^{yz}}^{\binom{x}{y}} = 0$$

The two-dimensional representation of $\binom{x}{y}$ is given in Table 7. This representation is not an irreducible representation of C_{2v}. It is reducible, i.e., it corresponds to a linear combination of irreducible representations $\Gamma^{\binom{x}{y}} = B_1 \oplus B_2$ (see Table 8).

Table 7 Two-dimensional representation $\binom{x}{y}$ of the C_{2v} point group.

C_{2v}	E	C_2^z	σ^{xz}	σ^{yz}
2×2 Matrix	$\begin{pmatrix} 1 & 0 \\ 0 & 1 \end{pmatrix}$	$\begin{pmatrix} -1 & 0 \\ 0 & -1 \end{pmatrix}$	$\begin{pmatrix} 1 & 0 \\ 0 & -1 \end{pmatrix}$	$\begin{pmatrix} -1 & 0 \\ 0 & 1 \end{pmatrix}$
$\Gamma^{\binom{x}{y}}$	2	−2	0	0

Table 8 Reduction of the two-dimensional representation $\binom{x}{y}$ of C_{2v}.

B_1	1	−1	1	−1
B_2	1	−1	−1	1
$B_1 \oplus B_2$	2	−2	0	0

Example 10 **Two-dimensional representation of C_{2v} spanned by 1s atomic orbitals $\binom{\phi_{1s(H_1)}}{\phi_{1s(H_2)}}$ centered on the H atoms of a water molecule H_2O**

The two H 1s atom orbitals of H_2O are depicted in Figure 31 and form a two-dimensional representation of C_{2v}. Proceeding as in the previous example, we obtain

$$E \begin{pmatrix} \phi_{1s(H_1)} \\ \phi_{1s(H_2)} \end{pmatrix} = \begin{pmatrix} \phi_{1s(H_1)} \\ \phi_{1s(H_2)} \end{pmatrix} = \begin{pmatrix} 1 & 0 \\ 0 & 1 \end{pmatrix} \begin{pmatrix} \phi_{1s(H_1)} \\ \phi_{1s(H_2)} \end{pmatrix};$$

$$\chi_E = 2$$

$$C_2^z \begin{pmatrix} \phi_{1s(H_1)} \\ \phi_{1s(H_2)} \end{pmatrix} = \begin{pmatrix} \phi_{1s(H_2)} \\ \phi_{1s(H_1)} \end{pmatrix} = \begin{pmatrix} 0 & 1 \\ 1 & 0 \end{pmatrix} \begin{pmatrix} \phi_{1s(H_1)} \\ \phi_{1s(H_2)} \end{pmatrix};$$

$$\chi_{C_2^z} = 0$$

$$\sigma^{xz} \begin{pmatrix} \phi_{1s(H_1)} \\ \phi_{1s(H_2)} \end{pmatrix} = \begin{pmatrix} \phi_{1s(H_2)} \\ \phi_{1s(H_1)} \end{pmatrix} = \begin{pmatrix} 0 & 1 \\ 1 & 0 \end{pmatrix} \begin{pmatrix} \phi_{1s(H_1)} \\ \phi_{1s(H_2)} \end{pmatrix};$$

$$\chi_{\sigma^{xz}} = 0$$

$$\sigma^{yz} \begin{pmatrix} \phi_{1s(H_1)} \\ \phi_{1s(H_2)} \end{pmatrix} = \begin{pmatrix} \phi_{1s(H_1)} \\ \phi_{1s(H_2)} \end{pmatrix} = \begin{pmatrix} 1 & 0 \\ 0 & 1 \end{pmatrix} \begin{pmatrix} \phi_{1s(H_1)} \\ \phi_{1s(H_2)} \end{pmatrix};$$

$$\chi_{\sigma^{yz}} = 2$$

$\phi_{1s}(H_1)$: 1s atom orbital on H_1 $\phi_{1s}(H_2)$: 1s atom orbital on H_2

Figure 31 1s atomic orbitals on the H atoms of H_2O.

The representation is two-dimensional and corresponds to $A_1 \oplus B_2$ as can be verified by inspection of the C_{2v} character table (see Tables 6 and 9).

Table 9 Two-dimensional representation of the C_{2v} point group spanned by the two H(1s) atomic orbitals of H_2O and its reduction.

C_{2v}	E	C_2^z	σ^{xz}	σ^{yz}
2×2 Matrix	$\begin{pmatrix} 1 & 0 \\ 0 & 1 \end{pmatrix}$	$\begin{pmatrix} 0 & 1 \\ 1 & 0 \end{pmatrix}$	$\begin{pmatrix} 0 & 1 \\ 1 & 0 \end{pmatrix}$	$\begin{pmatrix} 1 & 0 \\ 0 & 1 \end{pmatrix}$
$A_1 \oplus B_2$	2	0	0	2

6.4 Reducing Reducible Representations

All representations in a character table form a set of orthogonal vectors that span the complete space

$$\sum_R \chi^i(R)^* \chi^j(R) = h\delta_{ij} \tag{288}$$

where h represents the order of the group and R runs over all the elements of the group (Note that some classes of non-abelian groups contain more than one element). Any reducible representation can thus be expressed as a linear combination of irreducible representations

$$\Gamma^{\text{red}} = \sum_k c_k^{\text{red}} \Gamma^k \tag{289}$$

where Γ^k represents an irreducible representation. The expansion coefficients c_k^{red} can be determined using the reduction formula (equation (290)):

$$c_k^{\text{red}} = \frac{1}{h} \sum_R \chi^{\text{red}}(R)^* \chi^k(R) \quad \text{Reduction formula} \tag{290}$$

Example 10 (*continuation*):**Reduction of** $\Gamma^{(2)} = (2\,0\,0\,2)$:

$$\begin{aligned}
c^2_{A_1} &= \tfrac{1}{4}(2 \cdot 1 + 0 \cdot 1 + 0 \cdot 1 + 2 \cdot 1) = 1 \\
c^2_{A_2} &= \tfrac{1}{4}(2 \cdot 1 + 0 \cdot 1 + 0 \cdot 1 + 2 \cdot (-1)) = 0 \\
c^2_{B_1} &= \tfrac{1}{4}(2 \cdot 1 + 0 \cdot (-1) + 0 \cdot 1 + 2 \cdot (-1)) = 0 \\
c^2_{B_2} &= \tfrac{1}{4}(2 \cdot 1 + 0 \cdot (-1) + 0 \cdot (-1) + 2 \cdot 1) = 1 \\
\Rightarrow\ & \Gamma^2 = A_1 \oplus B_2.
\end{aligned}$$

One can therefore construct one linear combination of the two $\phi_{1s(H)}$ orbitals of H_2O with A_1 symmetry (totally symmetric) and one with B_2 symmetry.

6.5 Determining Symmetrized Linear Combinations

To find the symmetrized linear combination of the functions (or objects) used to derive a given representation (such as symmetrized linear combinations of atomic orbitals (LCAO)), one uses so-called *projectors* P^Γ and applies them onto either of the two $\phi_{1s(H)}$ orbitals. The projectors are defined as

$$P^\Gamma = \frac{1}{h} \sum_R \chi^\Gamma(R)^* \cdot \hat{R} \quad \text{Projection formula} \tag{291}$$

Example 10 (*continuation*)

The symmetrized LCAOs of the two 1s orbitals on the H atoms of H_2O and the ground state electronic configuration of H_2O can be derived from Equation (291) as follows:

$$\begin{aligned}
P^{A_1}(\phi_{1s(H_1)}) &= \frac{1}{4}(1 \cdot E\phi_{1s(H_1)} + 1C_2^z \phi_{1s(H_1)} + 1\sigma^{xz}\phi_{1s(H_1)} \\
&\quad + 1\sigma^{yz}\phi_{1s(H_1)}) \\
&= \frac{1}{4}(\phi_{1s(H_1)} + \phi_{1s(H_2)} + \phi_{1s(H_2)} + \phi_{1s(H_1)}) \\
&= \frac{1}{2}(\phi_{1s(H_1)} + \phi_{1s(H_2)}) \\
P^{A_2}(\phi_{1s(H_1)}) &= \frac{1}{4}(1 \cdot E\phi_{1s(H_1)} + 1C_2^z \phi_{1s(H_1)} - 1\sigma^{xz}\phi_{1s(H_1)} \\
&\quad - 1\sigma^{yz}\phi_{1s(H_1)}) \\
&= \frac{1}{4}(\phi_{1s(H_1)} + \phi_{1s(H_2)} - \phi_{1s(H_2)} - \phi_{1s(H_1)}) = 0
\end{aligned}$$

As expected, no A_2 linear combination can be formed from the $\phi_{1s(H)}$ functions. Similarly one finds $P^{B_1}(\phi_{1s(H_1)}) = 0$, and

$$P^{B_2}(\phi_{1s(H_1)}) = \frac{1}{2}(\phi_{1s(H_1)} - \phi_{1s(H_2)}).$$

These two orbital combinations of A_1 and B_2 symmetry can be represented schematically as in Figure 32.

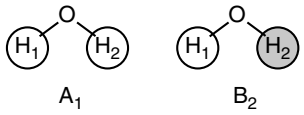

Figure 32 Schematic representations of the two linear combinations of the 1s orbitals of the two H atoms of a water molecule, which transform as the A_1 and B_2 irreducible representations of the C_{2v} point group.

The symmetrized LCAO can be used to determine the chemical bonds that can be formed with the p orbitals on the O atom. To this end, one must first determine the transformation properties of the p orbitals on the O atom depicted schematically in Figure 33.

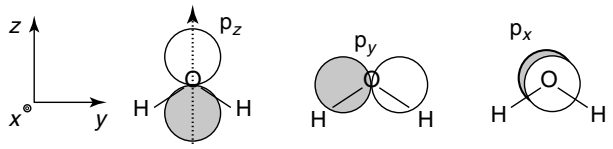

Figure 33 Schematic representation of the three 2p orbitals of the O atom of a water molecule from which their symmetry properties in the C_{2v} point group can be derived.

$$\begin{aligned}
&E\mathrm{p}_z = \mathrm{p}_z;\ C_2^z \mathrm{p}_z = \mathrm{p}_z;\ \sigma^{xz}\mathrm{p}_z = \mathrm{p}_z;\ \sigma^{yz}\mathrm{p}_z = \mathrm{p}_z \\
&\Gamma^{\mathrm{p}_z} = A_1 \\
&E\mathrm{p}_y = \mathrm{p}_y;\ C_2^z \mathrm{p}_y = -\mathrm{p}_y;\ \sigma^{xz}\mathrm{p}_y = -\mathrm{p}_y;\ \sigma^{yz}\mathrm{p}_y = \mathrm{p}_y \\
&\Gamma^{\mathrm{p}_y} = B_2 \\
&E\mathrm{p}_x = \mathrm{p}_x;\ C_2^z \mathrm{p}_x = -\mathrm{p}_x;\ \sigma^{xz}\mathrm{p}_x = \mathrm{p}_x;\ \sigma^{yz}\mathrm{p}_x = -\mathrm{p}_x \\
&\Gamma^{\mathrm{p}_x} = B_1
\end{aligned}$$

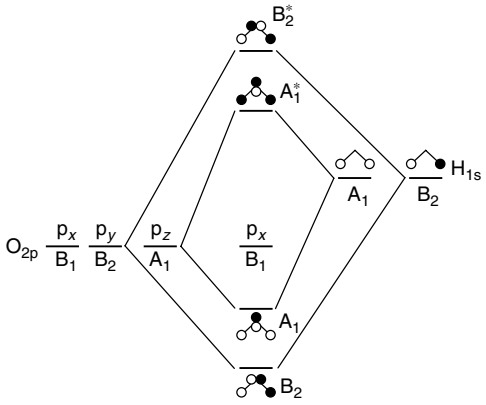

Figure 34 Schematic representation of the valence molecular orbitals of H_2O built from symmetrized H(1s) "ligand" orbitals and the 2p atomic orbitals of O. Antibonding orbitals are designated by an asterisk(*).

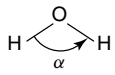

Figure 35 Bond angle α.

Only orbitals of the same symmetry can be combined to form bonding or antibonding molecular orbitals. The five symmetrized orbitals of H_2O derived above can be used to form five molecular orbitals according to Figure 34, which neglects the 1s and 2s orbitals on the oxygen atom by assuming that they are not involved in the formation of chemical bonds. Considering only the two 1s electrons of H and the four 2p electrons of O, and placing the six valence electrons in these molecular orbitals depicted in Figure 34 following Pauli's Aufbau principle gives the ground state configuration: . . . $(b_2)^2(a_1)^2(b_1)^2$ with an overall symmetry A_1. Because four of the six electrons are in bonding orbitals and two in a nonbonding p_x orbital, one expects two chemical bonds in H_2O. The energetical ordering of the two bonding molecular orbitals of B_2 and A_1 symmetry depends on the bond angle α defined in Figure 35. Whereas the a_1 orbital becomes nonbonding at $\alpha = 180^\circ$, the b_2 orbital remains bonding at $\alpha = 180^\circ$ but becomes antibonding at small angles. The angle dependence of the energies of the molecular orbitals in triatomic molecules can be exploited to predict whether the molecules are linear or bend in specific electronic states by means of correlation diagrams called *Walsh* diagrams, as discussed in Wörner and Merkt 2011: **Fundamentals of Electronic Spectroscopy**, this handbook.

6.6 Determining the Symmetry of Normal Modes

We consider the $3N_k$-dimensional reducible representation spanned by the set of $3N_k$ Cartesian displacement coordinates of the nuclei in a molecule and reduce it into irreducible representations of the corresponding group. For H_2O, $3N_k = 9$ and the representation is nine-dimensional. The $3N_k = 9$ Cartesian coordinates are depicted in Figure 36. All irreducible representations of C_{2v} are one-dimensional, but only three vibrational modes $(3N_k - 6)$ exist in H_2O. The symmetry of these modes will be obtained by eliminating the six irreducible representations corresponding to the three translational and the three rotational degrees of freedom of the molecule. The procedure followed here can be extended to molecules consisting of more atoms in a straightforward way. A more complete treatment of the vibrational motion of polyatomic molecules and of symmetry-adapted normal modes can be found in Wilson *et al*. (1955) (*see also* Albert *et al*. 2011: **Fundamentals of Rotation–Vibration Spectra**, this handbook).

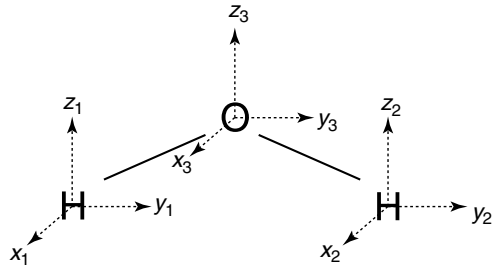

Figure 36 $3N_k$ displacement coordinates used to derive a nine-dimensional representation of the C_{2v} group suitable to derive the symmetry of the normal modes of H_2O.

The C_{2v} symmetry operations are represented by 9×9 matrices:

$\boldsymbol{E}$:

$$E\begin{pmatrix} x_1 \\ y_1 \\ z_1 \\ x_2 \\ y_2 \\ z_2 \\ x_3 \\ y_3 \\ z_3 \end{pmatrix} = \begin{pmatrix} x_1 \\ y_1 \\ z_1 \\ x_2 \\ y_2 \\ z_2 \\ x_3 \\ y_3 \\ z_3 \end{pmatrix}$$

$$= \begin{pmatrix} 1 & 0 & 0 & 0 & 0 & 0 & 0 & 0 & 0 \\ 0 & 1 & 0 & 0 & 0 & 0 & 0 & 0 & 0 \\ 0 & 0 & 1 & 0 & 0 & 0 & 0 & 0 & 0 \\ 0 & 0 & 0 & 1 & 0 & 0 & 0 & 0 & 0 \\ 0 & 0 & 0 & 0 & 1 & 0 & 0 & 0 & 0 \\ 0 & 0 & 0 & 0 & 0 & 1 & 0 & 0 & 0 \\ 0 & 0 & 0 & 0 & 0 & 0 & 1 & 0 & 0 \\ 0 & 0 & 0 & 0 & 0 & 0 & 0 & 1 & 0 \\ 0 & 0 & 0 & 0 & 0 & 0 & 0 & 0 & 1 \end{pmatrix} \begin{pmatrix} x_1 \\ y_1 \\ z_1 \\ x_2 \\ y_2 \\ z_2 \\ x_3 \\ y_3 \\ z_3 \end{pmatrix} \quad (292)$$

$\boldsymbol{C}_2^z$:

$$C_2^z \begin{pmatrix} x_1 \\ y_1 \\ z_1 \\ x_2 \\ y_2 \\ z_2 \\ x_3 \\ y_3 \\ z_3 \end{pmatrix} = \begin{pmatrix} -x_2 \\ -y_2 \\ z_2 \\ -x_1 \\ -y_1 \\ z_1 \\ -x_3 \\ -y_3 \\ z_3 \end{pmatrix}$$

$$= \begin{pmatrix} 0 & 0 & 0 & -1 & 0 & 0 & 0 & 0 & 0 \\ 0 & 0 & 0 & 0 & -1 & 0 & 0 & 0 & 0 \\ 0 & 0 & 0 & 0 & 0 & 1 & 0 & 0 & 0 \\ -1 & 0 & 0 & 0 & 0 & 0 & 0 & 0 & 0 \\ 0 & -1 & 0 & 0 & 0 & 0 & 0 & 0 & 0 \\ 0 & 0 & 1 & 0 & 0 & 0 & 0 & 0 & 0 \\ 0 & 0 & 0 & 0 & 0 & 0 & -1 & 0 & 0 \\ 0 & 0 & 0 & 0 & 0 & 0 & 0 & -1 & 0 \\ 0 & 0 & 0 & 0 & 0 & 0 & 0 & 0 & 1 \end{pmatrix} \begin{pmatrix} x_1 \\ y_1 \\ z_1 \\ x_2 \\ y_2 \\ z_2 \\ x_3 \\ y_3 \\ z_3 \end{pmatrix} \tag{293}$$

$\chi^E = 9;\ \chi^{C_2^z} = -1.$

The character of the unity operation is always equal to the dimension of the representation. Because the characters of the reducible representation only have contribution from atoms that are not exchanged by the symmetry operations, only these atoms must be considered to determine χ^R.

In H_2O, σ^{xz} exchanges the two H atoms and only the O atom needs to be considered:

$$\sigma^{xz}x_3 = x_3;\ \ \sigma^{xz}y_3 = -y_3;\ \ \sigma^{xz}z_3 = z_3 \ \ \Rightarrow \ \ \chi^{\sigma^{xz}} = 1 \tag{294}$$

σ^{yz} does not exchange any atom. For each atom, the x coordinate is inverted, and the y and z coordinates are preserved:

$$-1+1+1-1+1+1-1+1+1=3$$
$$\Rightarrow \quad \chi^{\sigma^{yz}} = 3.$$

The reducible nine-dimensional representation is, therefore, as in Table 10.

Table 10 Nine-dimensional representation of the C_{2v} point group corresponding to the nine Cartesian nuclear displacement coordinates of H_2O.

C_{2v}	E	C_2^z	σ^{xz}	σ^{yz}
Γ^{9D}	9	−1	1	3

This representation can be reduced using the reduction formula (equation 290):

$$c_{A_1} = \frac{1}{4}(9-1+1+3) = 3 \tag{295}$$

$$c_{A_2} = \frac{1}{4}(9-1-1-3) = 1 \tag{296}$$

$$c_{B_1} = \frac{1}{4}(9+1+1-3) = 2 \tag{297}$$

$$c_{B_2} = \frac{1}{4}(9+1-1+3) = 3 \tag{298}$$

$$\Gamma^{9D} = 3A_1 \oplus A_2 \oplus 2B_1 \oplus 3B_2 \tag{299}$$

Of these nine irreducible representations, three correspond to translations ($\Gamma^x = B_1,\ \Gamma^y = B_2,\ \Gamma^z = A_1$) and three correspond to rotations ($\Gamma^{R_x} = B_2$, $\Gamma^{R_y} = B_1$, $\Gamma^{R_z} = A_2$). The remaining three, namely, $2A_1 \oplus B_2$, correspond to the three vibrational modes of H_2O ($3N_k - 6 = 3$, as H_2O is a nonlinear molecule). To determine these modes, one can use the projection formula (equation 291).

Example 11 **Nuclear motion corresponding to the B_2 vibrational mode of H_2O**

Normal mode of H_2O of B_2 symmetry. In practice, it is convenient to first treat the x, y, and z displacements separately, and then to combine the x, y, and z motions.

x-dimension:

$$P^{B_2}x_1 = \frac{1}{4}\left(1Ex_1 - 1C_2^z x_1 - 1\sigma^{xz}x_1 + 1\sigma^{yz}x_1\right)$$
$$= \frac{1}{4}(x_1 + x_2 - x_2 - x_1) = 0. \tag{300}$$

The B_2 mode does therefore not involve x-coordinates.

y- and z-dimensions:

$$P^{B_2}y_1 = \frac{1}{4}\left(1Ey_1 - 1C_2^z y_1 - 1\sigma^{xz}y_1 + 1\sigma^{yz}y_1\right)$$
$$= \frac{1}{4}(y_1 + y_2 + y_2 + y_1) = \frac{1}{2}(y_1 + y_2) \tag{301}$$
$$P^{B_2}z_1 = \frac{1}{4}\left(1Ez_1 - 1C_2^z z_1 - 1\sigma^{xz}z_1 + 1\sigma^{yz}z_1\right)$$
$$= \frac{1}{4}(z_1 - z_2 - z_2 + z_1) = \frac{1}{2}(z_1 - z_2) \tag{302}$$

The B_2 mode involves both y and z coordinates. Drawing the displacement vectors, one obtains a vectorial representation of the motion of the H atoms in the B_2 mode. The motion of the O atom can be reconstructed by ensuring that the center of mass of the molecule remains stationary (Figure 37).

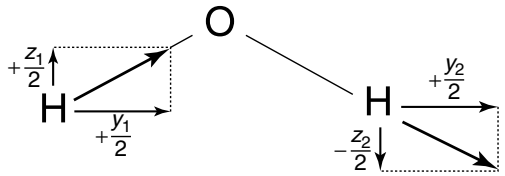

Figure 37 Determination of the nuclear motion corresponding to the B_2 vibrational mode of water.

The mode is easily seen to be the asymmetric stretching mode.

We draw attention to the fact that the definition of the symmetry labels depends upon the axis definitions used for the molecule. Depending on this, B_1 and B_2 can exchange their role in C_{2v}.

6.7 Determining the Symmetry of Vibrational Levels

The nomenclature to label the vibrational states of a polyatomic molecule is

$$\nu_1^{v_1},\ \nu_2^{v_2}, \cdots, \nu_{3N-6}^{v_{3N-6}} \tag{303}$$

where ν_i designate the mode and v_i the corresponding vibrational quantum number. Usually only those modes ν_i are indicated for which $v_i \neq 0$. Alternatively, the notation

$$(v_1,\ v_2, \cdots, v_{3N-6}) \tag{304}$$

can be used; yet another convention writes $v_1\nu_1 + v_2\nu_2 + v_3\nu_3 \cdots$, retaining only $v_i \neq 0$. For the ordering of the modes, the totally symmetric modes come first in order of descending frequency, then the modes corresponding to the second irreducible representation in the character table in order of descending frequency, etc.

Example 12 **The different nomenclature systems illustrated with the $v_1 = 2$, $v_2 = 1$, $v_3 = 3$ level of H_2O**

Notation 1 $1^2\ 2^1\ 3^3$ (sometimes lower indices are also used for the electronic ground state $1_2\ 2_1\ 3_3$). One often uses the upper indices to label vibrational levels in excited electronic states, *see* Stohner and Quack (2011): **Conventions, Symbols, Quantities, Units and Constants for High-resolution Molecular Spectroscopy**, this handbook.
Notation 2 (2 1 3).
Notation 3 $2\nu_1 + \nu_2 + 3\nu_3$.

To find the overall symmetry of the vibrational wavefunction, one must build the direct product

$$\Gamma_{\text{vib}} = (\Gamma_1)^{v_1} \otimes (\Gamma_2)^{v_2} \otimes \cdots \otimes (\Gamma_{3N-6})^{v_{3N-6}} \tag{305}$$

Example 13 **Symmetry of the $(1^2\ 2^1\ 3^3)$ vibrational level of H_2O**

$$\Gamma_v(\mathrm{H_2O},\ 1^2\ 2^1\ 3^3) = \underbrace{\mathrm{A_1} \otimes \mathrm{A_1}}_{v_1} \otimes \underbrace{\mathrm{A_1}}_{v_2} \otimes \underbrace{\mathrm{B_2} \otimes \mathrm{B_2} \otimes \mathrm{B_2}}_{v_3} = \mathrm{B_2} \tag{306}$$

Extensive tables of practical use for determining the symmetry of vibrational levels can be found in Wilson *et al.* (1955).

6.8 Determining the Symmetry Label of Electronic States/Configurations

Only partially filled subshells must be considered and the electronic symmetry labels of the configurations are obtained from a direct product of the symmetry of occupied orbitals. Moreover, one denotes the symmetry of molecular orbitals by small letters and that of electronic states by capital letters.

Example 14 **The ground electronic states of H_2O and H_2O^+**

$$\mathrm{H_2O}\text{:}\ \underbrace{\ldots}_{\mathrm{A_1}}(\mathrm{b_2})^2(\mathrm{a_1})^2(\mathrm{b_1})^2 :\ \tilde{\mathrm{X}}\,{}^1\mathrm{A_1}$$

$$\Gamma_{\text{el}} = \mathrm{b_2} \otimes \mathrm{b_2} \otimes \mathrm{a_1} \otimes \mathrm{a_1} \otimes \mathrm{b_1} \otimes \mathrm{b_1} = \mathrm{A_1} \tag{307}$$

$$\mathrm{H_2O^+}\text{:}\ \underbrace{\ldots}_{\mathrm{A_1}}(\mathrm{b_2})^2(\mathrm{a_1})^2(\mathrm{b_1})^1 :\ \tilde{\mathrm{X}}^+\,{}^2\mathrm{B_1}$$

$$\Gamma_{\text{el}} = \mathrm{b_2} \otimes \mathrm{b_2} \otimes \mathrm{a_1} \otimes \mathrm{a_1} \otimes \mathrm{b_1} = \mathrm{B_1} \tag{308}$$

The letter $\tilde{\mathrm{X}}/\tilde{\mathrm{X}}^+$ designates the ground electronic state. The first excited states of the same spin multiplicity as the ground state are labeled $\tilde{\mathrm{A}}/\tilde{\mathrm{A}}^+$, $\tilde{\mathrm{B}}/\tilde{\mathrm{B}}^+$ . . .. Electronically excited states of other spin multiplicity are labeled $\tilde{\mathrm{a}}$, $\tilde{\mathrm{b}}$, $\tilde{\mathrm{c}}$, . . . In diatomic molecules, one does not write the "tilde" but only X, A, B, C,. . ., a, b, c, ... There are, however, many exceptions to this nomenclature, as discussed in Wörner and Merkt 2011: **Fundamentals of Electronic Spectroscopy**, this handbook.

Example 15 **Electronic ground state configuration of the methyl radical CH_3**

The methyl radical (CH_3) belongs to the D_{3h} point group (see Table 11 and Figure 38).

We follow the same procedure as for H_2O in Section 6.5, retaining the 2s and 2p orbitals on C and the 1s orbitals

Table 11 Character table of the D_{3h} point group.

D_{3h}	E	$2C_3$	$3C_2$	σ_h	$2S_3$	$3\sigma_v$		
A_1'	1	1	1	1	1	1		
A_2'	1	1	−1	1	1	−1		R_z
E'	2	−1	0	2	−1	0	x, y	
A_1''	1	1	1	−1	−1	−1		
A_2''	1	1	−1	−1	−1	1	z	
E''	2	−1	0	−2	1	0		R_x, R_y

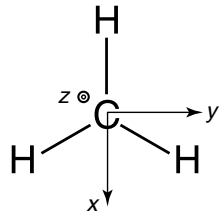

Figure 38 CH_3 molecule with its coordinate system.

on H. First, symmetrized "ligand" orbitals are constructed from the H 1s orbitals; then these are combined with the C-atom 2s and 2p orbitals to form bonding and antibonding orbitals.

For the ligand orbitals, a 3D representation Γ^{3D} is spanned by the three 1s atomic orbitals on the H atom (Table 12).

Table 12 Three-dimensional representation of the D_{3h} point group spanned by the three H(1s) atomic orbitals of CH_3.

D_{3h}	E	$2C_3$	$3C_2$	σ_h	$2S_3$	$3\sigma_v$
Γ^{3D}	3	0	1	3	0	1

This representation can be reduced using the reduction formula (equation (290)):

$$c_{A_1'} = \frac{1}{12}[3\cdot 1\cdot 1 + 0\cdot 2\cdot 1 + 1\cdot 3\cdot 1 + 3\cdot 1\cdot 1 + 0\cdot 1\cdot 1 + 1\cdot 3\cdot 1] = \frac{12}{12} = 1 \tag{309}$$

$$c_{A_2'} = \frac{1}{12}[3\cdot 1\cdot 1 + 0 + 1\cdot 3\cdot(-1) + 3\cdot 1\cdot 1 + 0 + 1\cdot 3\cdot(-1)] = 0 \tag{310}$$

$$c_{E'} = \frac{1}{12}[3\cdot 1\cdot 2 + 0 + 1\cdot 3\cdot 0 + 3\cdot 1\cdot 2 + 0 + 1\cdot 3\cdot 0] = 1 \tag{311}$$

$$\Gamma^{3D} = A_1' \oplus E' \tag{312}$$

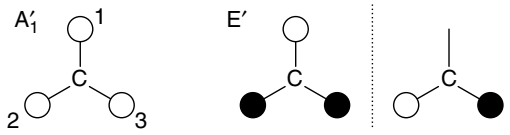

Figure 39 Schematic representation of the ligand orbitals of CH_3, which can be constructed with the three H 1s atom orbitals.

Figure 39 shows the ligand orbital of A_1' symmetry found by intuition. The ligand orbitals of E′ symmetry can be determined by using the projection formula (equation (291)); Note that the factor $\frac{1}{h}$ in the projection formula is not really useful, because the orbital would need to be normalized anyway.

$$\begin{aligned} P^{E'} &= \frac{1}{12}\left[2\cdot E\ 1s(1) - 1\cdot C_3\ 1s(1) - 1\cdot C_3^2\ 1s(1) + 2\cdot\sigma_h\ 1s(1) - 1\cdot S_3\ 1s(1) - 1\cdot S_3^2\ 1s(1)\right] \\ &= \frac{1}{12}[2\cdot 1s(1) - 1\cdot 1s(2) - 1\cdot 1s(3) + 2\cdot 1s(1) - 1\cdot 1s(2) - 1\cdot 1s(3)] \\ &= \frac{1}{3}\left[1s(1) - \frac{1}{2}[1s(2) + 1s(3)]\right] \end{aligned} \tag{313}$$

To find the second orbital of E′ symmetry, one can repeat the procedure using the 1s(2) and 1s(3) orbitals to find two further molecular orbitals $\frac{1}{3}[1s(2) - \frac{1}{2}[1s(1) + 1s(3)]]$ and $\frac{1}{3}[1s(3) - \frac{1}{2}[1s(1) + 1s(2)]]$. These three orbitals are linearly dependent. One can use linear algebra to eliminate one of these three orbitals and to find an orthogonal set of two orbitals of E′ symmetry (see Figure 39) using the Gram–Schmidt orthogonalization procedure. The molecular orbitals are finally found by determining the symmetry of the 2s and 2p orbitals of the central C atom and combining the orbitals of the same symmetry into bonding and antibonding orbitals (see Figure 40). One

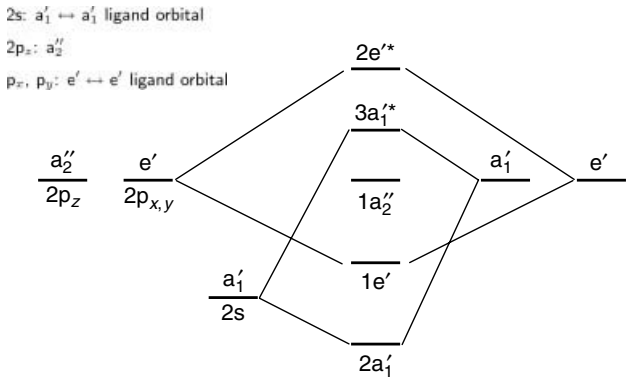

Figure 40 Energy-level diagram of valence molecular orbitals of CH_3.

sees that the $2p_z$ orbital of a_2'' symmetry must remain nonbonding because there are no ligand orbitals of a_2'' symmetry.

The electronic configuration of CH_3 (in total nine electrons) is, therefore,

$$\underbrace{(1a_1')^2(2a_1')^2(1e')^4}_{A_1'}(1a_2'')^1 \tag{314}$$

where the $1a_1'$ orbital is the 1s orbital on C. Therefore, the ground state is $\tilde{X}\,^2A_2''$. The radical has three bonds and an unpaired electron in the p_z orbital of $1a_2''$ symmetry.

6.9 Determining Selection Rules with Group Theory

Certain general aspects concerning selection rules for radiative and nonradiative transitions are discussed in Quack 2011: **Fundamental Symmetries and Symmetry Violations from High-resolution Spectroscopy**, this handbook. Here we provide a first discussion in terms of molecular point groups.

In the dipole approximation, the interaction between molecules and electromagnetic radiation is assumed to only come from the interaction

$$\hat{V} = -\hat{\boldsymbol{M}} \cdot \boldsymbol{E} \tag{315}$$

$\boldsymbol{M}$ is used here to distinguish the dipole moment of the molecule in the laboratory-fixed frame from $\boldsymbol{\mu}$, which is the dipole moment in the molecule-fixed frame. The polarization vector $\boldsymbol{E}$ of the radiation is defined in the laboratory-fixed frame (X, Y, Z), whereas the components of $\boldsymbol{\mu}$ are defined in the molecule-fixed frame (x, y, z). For linearly polarized light, $\boldsymbol{E} = (0, 0, E)$

$$\hat{V} = -\hat{M}_z E \tag{316}$$

The selection rule may be written as follows:

$$\langle \mathrm{f}|\hat{M}_z|\mathrm{i}\rangle \tag{317}$$

The space-fixed components M_x, M_y, and M_z of $\boldsymbol{M}$ vary as the molecule rotates. The molecule-fixed components μ_x, μ_y, and μ_z remain the same when the molecule rotates and the selection rules are expressed in terms of μ_x, μ_y, and μ_z.

$$\mu_\xi = \sum_{i=1}^{N} e_i \xi_i \tag{318}$$

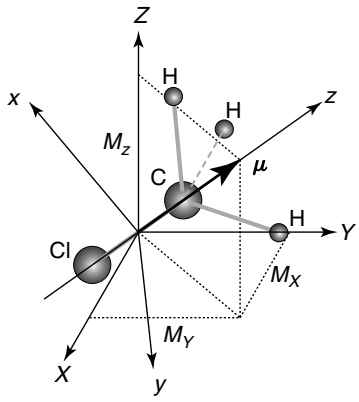

Figure 41 Relationship between the laboratory- and molecule-fixed frames using the example of the CH_3Cl molecule. The permanent dipole moment of CH_3Cl lies along the C–Cl bond, i.e., along the z axis in the molecule-fixed frame.

where $\xi = x, y, z$ and e_i is the charge of particle i. The relationship between M and μ is illustrated in Figure 41.

The relative orientation of the space-fixed and molecule-fixed coordinate system is given by the three Euler angles (ϕ, θ, χ) defined by three successive rotations depicted in Figure 42 and defined as follows (*see also* Bauder 2011: **Fundamentals of Rotational Spectroscopy**, this handbook):

1. Rotation around Z by ϕ $(\rightarrow x', y', z')$
2. Rotation around y' by θ $(\rightarrow x'', y'', z'')$
3. Rotation around z'' by χ $(\rightarrow x, y, z)$.

These operations can be described by the following matrix multiplications

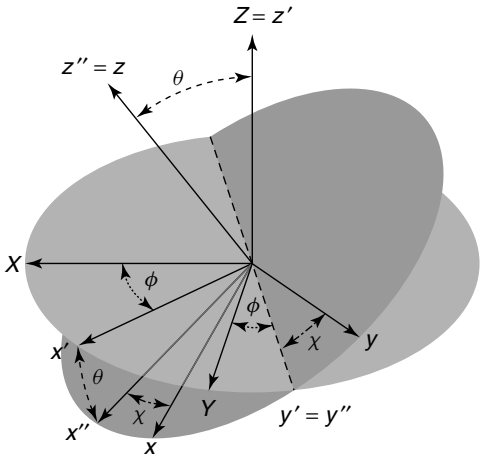

Figure 42 Euler angles ϕ, θ, χ used to relate the molecule-fixed and the space-fixed reference frames. [Adapted from Zare (1988).]

$$\begin{bmatrix} x' \\ y' \\ z' \end{bmatrix} = R_Z(\phi) \begin{bmatrix} X \\ Y \\ Z \end{bmatrix}$$

$$= \begin{bmatrix} \cos\phi & \sin\phi & 0 \\ -\sin\phi & \cos\ \phi & 0 \\ 0 & 0 & 1 \end{bmatrix} \begin{bmatrix} X \\ Y \\ Z \end{bmatrix}$$

$$\begin{bmatrix} x'' \\ y'' \\ z'' \end{bmatrix} = R_{y'}(\theta) \begin{bmatrix} x' \\ y' \\ z' \end{bmatrix}$$

$$= \begin{bmatrix} \cos\theta & 0 & -\sin\theta \\ 0 & 1 & 0 \\ \sin\theta & 0 & \cos\theta \end{bmatrix} \begin{bmatrix} x' \\ y' \\ z' \end{bmatrix} \quad (319)$$

$$\begin{bmatrix} x \\ y \\ z \end{bmatrix} = R_z(\chi) \begin{bmatrix} x'' \\ y'' \\ z'' \end{bmatrix}$$

$$= \begin{bmatrix} \cos\chi & \sin\chi & 0 \\ -\sin\chi & \cos\chi & 0 \\ 0 & 0 & 1 \end{bmatrix} \begin{bmatrix} x'' \\ y'' \\ z'' \end{bmatrix}$$

Using equation (319), the laboratory- and molecule-fixed frames can be linked by the following transformation:

$$\begin{bmatrix} x \\ y \\ z \end{bmatrix} = R_z(\chi) R_{y'}(\theta) R_Z(\phi) \begin{bmatrix} X \\ Y \\ Z \end{bmatrix}$$

$$= \begin{bmatrix} \cos\phi\ \cos\theta\ \cos\chi - \sin\phi\ \sin\chi & \sin\phi\ \cos\theta\ \cos\chi + \cos\phi\ \sin\chi & -\sin\theta\ \cos\chi \\ -\cos\phi\ \cos\theta\ \sin\chi - \sin\phi\ \cos\chi & -\sin\phi\ \cos\theta\ \sin\chi + \cos\phi\ \cos\chi & \sin\theta\ \sin\chi \\ \cos\phi\ \sin\theta & \sin\phi\ \sin\theta & \cos\theta \end{bmatrix} \begin{bmatrix} X \\ Y \\ Z \end{bmatrix} \quad (320)$$

or its inverse

$$\begin{bmatrix} X \\ Y \\ Z \end{bmatrix} = \begin{bmatrix} \cos\phi\ \cos\theta\ \cos\chi - \sin\phi\ \sin\chi & -\cos\phi\ \cos\theta\ \sin\chi - \sin\phi\ \cos\chi & \cos\phi\ \sin\theta \\ \sin\phi\ \cos\theta\ \cos\chi + \cos\phi\ \sin\chi & -\sin\phi\ \cos\theta\ \sin\chi + \cos\phi\ \cos\chi & \sin\phi\ \sin\theta \\ -\sin\theta\ \cos\chi & \sin\theta\ \sin\chi & \cos\theta \end{bmatrix} \begin{bmatrix} x \\ y \\ z \end{bmatrix}$$

$$= \boldsymbol{\lambda} \begin{bmatrix} x \\ y \\ z \end{bmatrix} \quad (321)$$

In Equation (321), $\boldsymbol{\lambda}$ is the direction cosine matrix and can be used to express the components of a vector in the laboratory-fixed frame as a function of the components of the same vector in the molecule-fixed frame. A rotation of the molecule in space leads to a change of the Euler angles, and the rotational wavefunctions $\phi_{\text{rot}}(\phi, \theta, \chi)$ are expressed in the space-fixed frame as a function of these angles. Expressing M_Z as a function of μ_x, μ_y, and μ_z,

$$M_Z = \lambda_{Zx}\mu_x + \lambda_{Zy}\mu_y + \lambda_{Zz}\mu_z \quad (322)$$

and using the product forms

$$\psi_{\text{f}} = \phi'_{\text{el}}\ \phi'_{\text{espin}}\ \phi'_{\text{vib}}\ \phi'_{\text{rot}}\ \phi'_{\text{nspin}} \quad (323)$$

$$\psi_{\text{i}} = \phi''_{\text{el}}\ \phi''_{\text{espin}}\ \phi''_{\text{vib}}\ \phi''_{\text{rot}}\ \phi''_{\text{nspin}} \quad (324)$$

for the molecular wavefunctions, the transition moment $\langle\psi_{\text{f}}|M_Z|\psi_{\text{i}}\rangle$ can be written as

$$\langle\phi'_{\text{el}}\ \phi'_{\text{espin}}\ \phi'_{\text{vib}}\ \phi'_{\text{rot}}\ \phi'_{\text{nspin}}| \sum_\alpha \lambda_{Z\alpha}\ \mu_\alpha |\phi''_{\text{el}}\ \phi''_{\text{espin}}\ \phi''_{\text{vib}}\ \phi''_{\text{rot}}\ \phi''_{\text{nspin}}\rangle \quad (325)$$

Equation (325) can be simplified if one makes several assumptions:

1. Only ϕ_{nspin} depends on the nuclear spin variables, and only ϕ_{espin} depends on the electron spin variables. The integration can thus be separated

$$\langle\phi'_{\text{espin}}|\phi''_{\text{espin}}\rangle\langle\phi'_{\text{nspin}}|\phi''_{\text{nspin}}\rangle\langle\phi'_{\text{el}}\ \phi'_{\text{vib}}\ \phi'_{\text{rot}}| \sum_\alpha \lambda_{Z\alpha}\ \mu_\alpha |\phi''_{\text{el}}\ \phi''_{\text{vib}}\ \phi''_{\text{rot}}\rangle \quad (326)$$

Because electron- and nuclear-spin functions are orthogonal, equation (326) vanishes (transition forbidden) unless $\phi'_{\text{espin}} = \phi''_{\text{espin}}$ and $\phi'_{\text{nspin}} = \phi''_{\text{nspin}}$, from which the selection rules

$$\Delta S = 0 \quad \text{intercombination } \textit{Verbot} \tag{327}$$

$$\Delta I = 0 \quad \text{nuclear-spin conservation rule} \tag{328}$$

follow.

2. The remaining rovibronic (rotational–vibrational–electronic) transition moment $\langle \phi'_{\text{el}}\ \phi'_{\text{vib}}\ \phi'_{\text{rot}}| \sum_\alpha \lambda_{Z\alpha}\ \mu_\alpha |\phi''_{\text{el}}\ \phi''_{\text{vib}}\ \phi''_{\text{rot}}\rangle$ can be further simplified. The functions ϕ_{el}, ϕ_{vib}, and μ_α do not depend on the Euler angles: $\phi_{\text{el}}(q_i, Q)$, $\phi_{\text{vib}}(Q)$, $\mu_\alpha(q_i, Q)$. However, the direction cosine elements $\lambda_{Z\alpha}$ and ϕ_{rot} only depend on ϕ, θ, χ and the rovibronic transition moment can be further separated in an integral over angular variables and an integral over electronic coordinates and normal modes:

$$\sum_\alpha \langle \phi'_{\text{rot}}|\lambda_{Z\alpha}|\phi''_{\text{rot}}\rangle \langle \phi'_{\text{el}}\phi'_{\text{vib}}|\mu_\alpha|\phi''_{\text{el}}\phi''_{\text{vib}}\rangle \tag{329}$$

The integral $\langle \phi'_{\text{rot}}|\lambda_{Z\alpha}|\phi''_{\text{rot}}\rangle$ leads to angular momentum selection rules:

- $\Delta J = 0, \pm 1;\ 0 \not\leftrightarrow 0$: angular momentum conservation (330)
- $\alpha = z$: $\Delta K = 0$: symmetric top (331)

  $\Delta \Lambda = 0$: diatomic molecule (332)
- $\alpha = x, y$: $\Delta K = \pm 1$: symmetric top (333)

  $\Delta \Lambda = \pm 1$: diatomic molecule (334)
- M_Z : $\Delta M = 0$ (335)

  M_X, M_Y : $\Delta M = \pm 1$ (336)

The integral

$$\langle \phi'_{\text{el}}\ \phi'_{\text{vib}}|\mu_\alpha|\phi''_{\text{el}}\ \phi''_{\text{vib}}\rangle \tag{337}$$

represents a selection rule for transitions between electronic and vibrational levels and its evaluation can be simplified if one considers specific cases.

Case 1: $\phi'_{\text{el}} = \phi''_{\text{el}}$, $\phi'_{\text{vib}} = \phi''_{\text{vib}}$; rotational spectroscopy. Equation (337) represents the expectation value of μ_α. Transitions are only allowed for molecules with a *permanent* dipole moment. The angular momentum selection rules are as above.

Case 2: $\phi'_{\text{el}} = \phi''_{\text{el}}$, $\phi'_{\text{vib}} \neq \phi''_{\text{vib}}$; vibrational spectroscopy. Since, in the BO approximation, only ϕ_{el} and μ_α depend on the electron coordinates q_i, the integration over q_i can be performed first:

$$\langle \phi'_{\text{vib}}(Q)|\underbrace{\langle \phi'_{\text{el}}(Q,q_i)|\mu_\alpha(Q,q_i)|\phi''_{\text{el}}(Q,q_i)\rangle_{q_i}}_{\mu_{\text{el},\alpha}(Q)}|\phi''_{\text{vib}}(Q)\rangle_Q$$

$$= \langle \phi'_{\text{vib}}(Q)|\mu_{\text{el},\alpha}(Q)|\phi''_{\text{vib}}(Q)\rangle \tag{338}$$

Whether equation (338) vanishes or not can be determined by group theory. Indeed, an integral over a set of coordinates (here normal modes Q) is only nonvanishing if the integrand contains the totally symmetric representation. Integration over nontotally symmetric functions vanishes because for each positive value $f(Q_i)$ of a function f, there exists a negative value $f(-Q_i) = -f(Q_i)$. Therefore, if

$$\Gamma'_{\text{vib}} \otimes \Gamma_\alpha \otimes \Gamma''_{\text{vib}} \ni \text{A}_1 \tag{339}$$

the transition is allowed and if

$$\Gamma'_{\text{vib}} \otimes \Gamma_\alpha \otimes \Gamma''_{\text{vib}} \not\ni \text{A}_1 \tag{340}$$

it is forbidden. Γ_α ($\alpha = x, y, z$) transforms as the components of a vector and thus as α. In Equations (339) and (340), we use A_1 to designate the totally symmetric representation although, in some groups, the totally symmetric representation is labeled A'_1, A, Σ^+_{g}, Σ^+, ...

Example 16 **Vibrational transition of H_2O**

$\phi''_{\text{vib}} = (0,0,0)$, $\Gamma''_{\text{vib}} = \text{A}_1$
$\Gamma_{\mu_x} = \text{B}_1$, $\Gamma_{\mu_y} = \text{B}_2$, $\Gamma_{\mu_z} = \text{A}_1$

(a) $\phi'_{\text{vib}} = (1,0,0)$, $\Gamma'_{\text{vib}} = \text{A}_1$

$$\Gamma' \otimes \Gamma_\alpha \otimes \Gamma'' = \text{A}_1 \otimes \begin{Bmatrix} \text{B}_1 \\ \text{B}_2 \\ \text{A}_1 \end{Bmatrix} \otimes \text{A}_1 = \begin{Bmatrix} \text{B}_1 \\ \text{B}_2 \\ \text{A}_1 \end{Bmatrix}$$

The allowed transition originates from the z-component of the transition dipole moment.

(b) $\phi'_{\text{vib}} = (0,0,1)$, $\Gamma'_{\text{vib}} = \text{B}_2$

$$\text{B}_2 \otimes \begin{Bmatrix} \text{B}_1 \\ \text{B}_2 \\ \text{A}_1 \end{Bmatrix} \otimes \text{A}_1 = \begin{Bmatrix} \text{A}_2 \\ \text{A}_1 \\ \text{B}_2 \end{Bmatrix}$$

The allowed transition originates from the y-component of the transition dipole moment. The component of the

permanent dipole moment along the y-axis is zero in H_2O. Nevertheless, a transition can be observed. The condition for a vibrational transition to be observable is that a *change* of the dipole moment must occur when exciting the vibration. This is obviously the case when the antisymmetric stretching mode is excited in H_2O.

In H_2O, transitions to all vibrational levels are allowed by symmetry. However, overtones are often weaker than fundamental excitations, although this is not necessarily always the case as explained in Albert *et al*. 2011: **Fundamentals of Rotation–Vibration Spectra**, this handbook.

Case 3: $\phi'_{el} \neq \phi''_{el}$; electronic spectroscopy. The left-hand side of equation (338) can be written as

$$\langle \phi'_{vib}(Q) | \underbrace{\langle \phi'_{el}(Q, q_i) | \mu_\alpha(Q, q_i) | \phi''_{el}(Q, q_i) \rangle_{q_i}}_{} | \phi''_{vib}(Q) \rangle_Q \tag{341}$$

where the inner integral represents an electronic transition moment $\mu^{fi}_{el,\alpha}$ obtained by integration over the electronic coordinates. An *electronically allowed transition* is one for which $\mu^{fi}_{el,\alpha} \neq 0$, which is fulfilled if $\Gamma'_{el} \otimes \Gamma_\alpha \otimes \Gamma''_{el} \ni A_1$.

Example 17 **Electronically allowed and forbidden transitions in H_2O**

$\tilde{X}\ ^1A_1$, . . .$(1b_2)^2(3a_1)^2(1b_1)^2$ (orbital symmetry designations are in small letters)

$$\Gamma'_{el} \otimes \Gamma_\alpha \otimes \Gamma''_{el} = \begin{Bmatrix} B_1 \\ B_2 \\ A_1 \end{Bmatrix} \otimes \begin{Bmatrix} B_1 \\ B_2 \\ A_1 \end{Bmatrix} \otimes A_1 = \begin{Bmatrix} A_1 \\ A_1 \\ A_1 \end{Bmatrix}$$

Electric dipole transitions to electronic states of B_1, B_2, and A_1 symmetry are electronically allowed and transitions to electronic states of A_2 symmetry are electronically forbidden in H_2O.

If one assumes that the transition moment function $\mu^{fi}_{el,\alpha}(Q)$ varies slowly with Q, then $\mu^{fi}_{el,\alpha}(Q)$ can be described by a Taylor series and one can in good approximation neglect higher terms:

$$\mu^{fi}_{el,\alpha}(Q) = \mu^{fi}_{el,\alpha}\big|_{eq} + \sum_j^{3N-6} \left.\frac{\partial \mu^{fi}_{el,\alpha}}{\partial Q_j}\right|_{eq} Q_j + \ldots \tag{342}$$

In electronically allowed transitions, the first term in equation (342) is often the dominant one and the transition moment (equation 341) becomes

$$\langle \phi'_{vib}(Q) | \phi''_{vib}(Q) \rangle \ \mu_{el,\alpha}\big|_{eq} \tag{343}$$

The intensity of a transition is proportional to the square of the transition moment and thus,

$$I \propto \left| \langle \phi'_{vib}(Q) | \phi''_{vib}(Q) \rangle \right|^2 \tag{344}$$

$\left| \langle \phi'_{vib}(Q) | \phi''_{vib}(Q) \rangle \right|^2$ is called a *Franck–Condon factor* and represents the square of the overlap of the vibrational wavefunctions. Equation (344) implies the vibrational selection rule for electronically allowed transitions

$$\Gamma'_{vib} \otimes \Gamma''_{vib} \ni A_1 \tag{345}$$

Example 18 $\mathbf{H_2O\ \tilde{X}\ ^1A_1(0,0,0) \rightarrow H_2O\ \tilde{C}\ ^1B_1}$**:**

$\Gamma''_{vib} = A_1 \Rightarrow \Gamma'_{vib} \stackrel{!}{=} A_1$

Only the symmetric stretch (ν_1) and the bending (ν_2) modes can be excited. The asymmetric stretch ν_3 of B_2 symmetry can only be excited if v_3 is even.

Electronically forbidden transitions can become weakly allowed if the electronic and vibrational degrees of freedom cannot be separated as in equation (341). The condition for them to be weakly observable is that

$$\underbrace{\Gamma'_{vib} \otimes \Gamma'_{el}}_{\Gamma'_{ev}} \otimes \Gamma_\alpha \otimes \underbrace{\Gamma''_{vib} \otimes \Gamma''_{el}}_{\Gamma''_{ev}} \ni A_1 \tag{346}$$

Example 19 **Vibronically allowed Transition in H_2O**

Transitions from H_2O $\tilde{X}\ ^1A_1$ (0,0,0) to electronically excited states of A_2 symmetry (electronically forbidden) may become weakly allowed (vibronically allowed) if a nontotally symmetric mode is excited.

$\tilde{X}\ ^1A_1$ (0,0,0): $\Gamma''_{el} = A_1$, $\Gamma''_{vib} = A_1$,

$\Gamma''_{ev} = A_1 \otimes A_1 = A_1$

A_2 (0,0,1): $\Gamma'_{el} = A_2$, $\Gamma'_{vib} = B_2$, $\Gamma'_{ev} = A_2 \otimes B_2 = B_1$

$$\Gamma'_{ev} \otimes \Gamma_\alpha \otimes \Gamma''_{ev} = B_1 \otimes \begin{Bmatrix} B_1 \\ B_2 \\ A_1 \end{Bmatrix} \otimes A_1 = \begin{Bmatrix} A_1 \\ A_2 \\ B_1 \end{Bmatrix}$$

The vibronically allowed transition originates from μ_x.

Further examples of electronically allowed and electronically forbidden transitions are presented in Wörner and Merkt 2011: **Fundamentals of Electronic Spectroscopy**, this handbook. Many examples can also be found in Herzberg (1945, 1966).

7 RADIATIONLESS TRANSITIONS AND SPECTRAL LINESHAPES

7.1 General Aspects

Radiative and radiationless transitions limit the lifetime Δt of excited states and from this one can conclude by means of the fourth Heisenberg uncertainty relation $\Delta E\,\Delta t \geq h/(4\pi)$ that the energy distribution in excited states cannot be a δ-function, although it should be obvious that the inequality does not allow one to derive an *equation* to calculate an energy width ΔE from a known Δt.

Lifetimes of excited states determined only by their spontaneous emission lead to the so-called "natural linewidth" of the spectral line. Sometimes, the concept is extended to reactive decays of excited states, for instance, by dissociation (then called *predissociation* in this context (see Herzberg (1950)) or ionization (then called *preionization*, *autoionization*, or *Auger effect*). These phenomena were all observed in the early days of spectroscopy and quantum mechanics. Spectral line broadening by the Auger effect was discussed and photodissociation observed for NH_3 by Bonhoeffer and Farkas (1928) following an earlier observation of Henri (1923) and Henri and Teves (1924) in spectra of S_2, which become diffuse below about 260 nm. The quantum theory of radiationless transitions was presented at about the same time by Wentzel (1927, 1928). The early history is well narrated in Herzberg (1950).

In the present section, we discuss the basic concepts for exponential decay as related to line broadening with a Lorentzian lineshape. We also give a brief summary of other origins of spectral line broadening in high-resolution spectra: Doppler broadening with Gaussian lineshape, Voigt lineshapes, collisional broadening mechanisms, intensity or power broadening already discussed in Section 3, and residence or interaction time broadening.

7.2 Lorentzian Probability Distribution of Energies and Exponential Decay

If in a general expansion of the time-dependent wavefunctions in $\Psi(r, t)$ in a densely spaced or continuous spectrum the probability distribution $p(E)$ is Lorentzian with full width at half maximum (FWHM) equal to Γ,

$$p(E) = \frac{1}{\pi}\frac{(\Gamma/2)}{(E - E_m)^2 + (\Gamma/2)^2} \tag{347}$$

then one can show that the survival probability of the initial state,

$$p_{(A)}(t) = |\langle\Psi(r, t)\rangle|\langle\Psi(r, 0)\rangle|^2 = |\langle\Psi(r, 0)\rangle|\langle\Psi(r, t)\rangle|^2 \tag{348}$$

with $p_{(A)}(0) = 1$, obviously follows an exponential decay law

$$p_{(A)}(t) = \exp(-kt) \tag{349}$$

with k being given by

$$k = \frac{2\pi\Gamma}{h} \tag{350}$$

This follows directly from the time-dependent Schrödinger equation by inserting the wavefunction in the eigenstate basis with the appropriate initial condition and noting the mathematical Fourier transformation relationship between the exponential function and the Lorentzian (Cauchy) function. While this is well known, it is probably less widely appreciated that this provides no insight into the dynamical origin of the Lorentzian distribution. A priori one could choose a Lorentzian energy distribution as initial state of an arbitrary quantum system and obtain the exponential decay of the survival probability $p_A(t)$. For instance, Marquardt and Quack (1994, 1996) have shown that a simple harmonic oscillator will show such an exponential decay if one chooses a Lorentzian energy distribution instead of the common Poisson distribution of the coherent state. In this case, one can derive the wave packet associated with a decay, corresponding simply to a movement of the wave packet away from the initial position. Strictly speaking, the distribution for the harmonic oscillator is discrete

$$p(E) = \sum_{n=0}^{\infty} p_n(E_n)\delta(E - E_n) \tag{351}$$

with the Dirac delta function and the energy-level spacing $E_n - E_{n-1} = \Delta E = h\nu$. However, if one has $\Gamma \gg \Delta E$ one finds the expected exponential decay initially, and oscillations with period

$$\tau = \frac{h}{\Delta E} \tag{352}$$

are only observed at very long times. The "recurrence" time $\tau = t_r \gg \tau_{\text{decay}} = 1/k$ is much longer than the decay time and, formally, one could consider the limit $\Delta E \to 0$ with $\tau \to \infty$.

Another aspect that is not widely appreciated concerns the uncertainty relation $\Delta E\,\Delta t$ being satisfied by the pair Lorentzian/exponential quite perfectly (one has $\Delta E \Delta t =$

$\infty \geq h/4\pi$), but obviously, the uncertainty relation cannot then be used to derive equation (350) leading to a misunderstanding, which is, indeed, one of the most common flaws in textbooks.

The key to understanding the physics of spectral line broadening and exponential decay are thus *mechanisms* providing either a Lorentzian energy distribution in the eigenstate spectrum or an exponential decay of some meaningful physical initial state.

7.3 Perturbation Theory and the Bixon–Jortner Model for Exponential Decay

Figure 43 shows a scheme that is commonly used in the treatment of exponential decay. The Hamiltonian is decomposed into a zero-order Hamiltonian $\hat{H}_0$ and a coupling. For instance, $\hat{H}_0$ could be the BO Hamiltonian describing an excited electronic state, which, by means of non-BO coupling $\hat{V}$, can make a transition to dissociative continuum states of the electronic ground state. This would be the prototypical situation for predissociation. An early quantum mechanical theory of predissociation was presented by Wentzel (1927, 1928) who derived a rate constant expression from perturbation theory

$$k = \frac{4\pi^2 |V|^2}{h} \rho \tag{353}$$

where ρ is the density of quantum states in the continuum (or quasi-continuum). Various derivations of this expression can be found in the textbook literature (e.g. Messiah

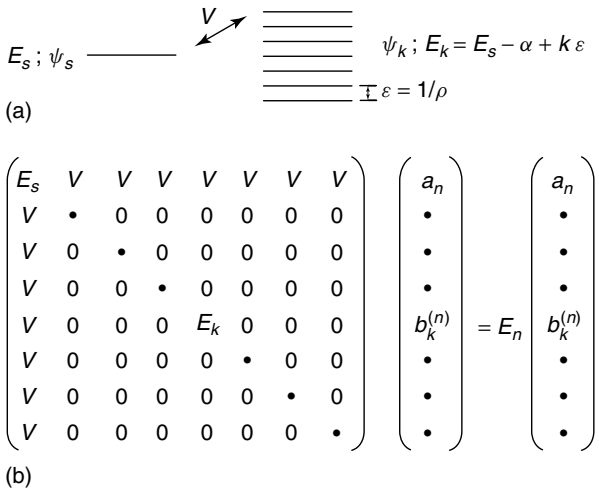

Figure 43 (a) The model of Bixon and Jortner (1968) describing the coupling between the state ψ_s and an equidistant manifold of states ψ_k (spacing ϵ) with constant coupling strength $V_{ks} = V$. (b) Coupling scheme in the model of Bixon and Jortner expressed in the matrix representation of the Schrödinger equation.

1961, Cohen-Tannoudji *et al*. 1973) and we shall not reproduce these here. We note, however, that the derivation of the expression by perturbation theory has a number of weak points, but provides a correct result. The expression (353) is also frequently called *Fermi's Golden Rule* for no good historical reason.

In a very insightful paper, Bixon and Jortner (1968) showed that a scheme with the quantitative properties shown in Figure 43 (constant level spacing $\varepsilon = 1/\rho$ in the continuum and constant (real) coupling matrix elements V between ψ_s and ψ_k) can be solved exactly by diagonalization of the Hamiltonian giving eigenfunctions

$$\varphi_n = a_n \psi_s + \sum_k b_k^{(n)} \psi_k \tag{354}$$

with

$$|a_n|^2 = \frac{V^2}{(E_n - E_s)^2 + V^2 + (\pi V^2/\varepsilon)^2} \tag{355}$$

In the limit that $\pi^2 V^2/\varepsilon^2 \gg 1$ or $|V| \gg \varepsilon$, this approaches a Lorentzian distribution with Γ(FWHM) being given by

$$\Gamma = 2\pi V^2 \rho \tag{356}$$

which provides an exact derivation of the Golden Rule expression for this particular model.

The physical motivation for this picture is shown in Figure 44. The special "zero-order" state ψ_s might have the property of carrying a large transition moment from the ground state (a "bright state" or "chromophore state"), whereas the zero-order background states would carry no oscillator strengths. It would thus be natural that light absorption generates initially ψ_s, which then decays by the coupling V. An important contribution of Bixon and Jortner (1968) is to show that this result can be obtained exactly, not requiring the usual approximations of perturbation theory. Another important result was to show that essentially exponential decay for electronic relaxation by internal conversion (IC) or intersystem crossing (ISC) can be obtained not only for continua but also in discrete spectra (spacing ε). The initial decay can be exponential, while the recurrence time $\tau = h/\varepsilon$ can be exceedingly long for high densities of states applicable for polyatomic molecules (*see* Albert *et al*. 2011: **Fundamentals of Rotation–Vibration Spectra** and Quack 2011: **Fundamental Symmetries and Symmetry Violations from High-resolution Spectroscopy**, this handbook).

In the eigenstate picture of ultrahigh resolution one could, however, see individual spectral lines (Figure 44b), where the envelope of the intensities of the lines follows a Lorentzian, which provides the overall spectral

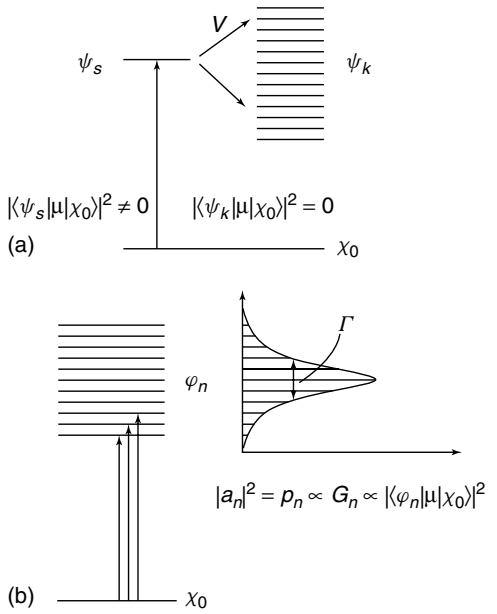

Figure 44 Description of the initial state after optical excitation. (a) In the model of Bixon and Jortner (1968), the operator $\hat{H}_0$ is chosen so that only state ψ_s (chromophore) is optically accessible from the ground state with a large dipole transition moment $\langle\psi_s|\hat{\mu}_{\mathrm{el}}|\psi_0\rangle$. The coupling to the equidistant manifold of states ψ_k leads to a Lorentzian distribution of line strengths G_n in the eigenstate picture. (b) In the eigenstate picture, the optical excitation from the ground state leads to an occupation distribution p_n of the eigenstates ϕ_n with eigenvalues E_n, which corresponds to a Lorentzian distribution with width Γ.

lineshape. In this picture, a short pulse excitation with broadband light would generate a probability distribution with Lorentzian shape because of the transition line strengths, and a subsequent exponential decay of this time-dependent initial state because of the very general relations (348)–(350).

We might conclude here that particularly when the first-order contribution to decay vanishes (for symmetry reasons, for instance) one can include higher-order perturbations. The corresponding golden rule expression to second order (see Figure 45 for the coupling scheme) will then be

$$k = \frac{4\pi^2}{h}\left\langle\left|V_{jn} + \sum_m \frac{V_{jm}V_{mn}}{E_n - E_m}\right|^2\right\rangle\langle\rho(E)\rangle \qquad (357)$$

where $\langle|X|^2\rangle$ indicates the average absolute square of the expression, which is the proper quantity to be introduced in general, provided that the distribution of matrix elements satisfies some mild conditions. $\langle\rho(E)\rangle$ is the average density of states. For further discussion of electronic radiationless transitions we refer to Jortner *et al.* (1969).

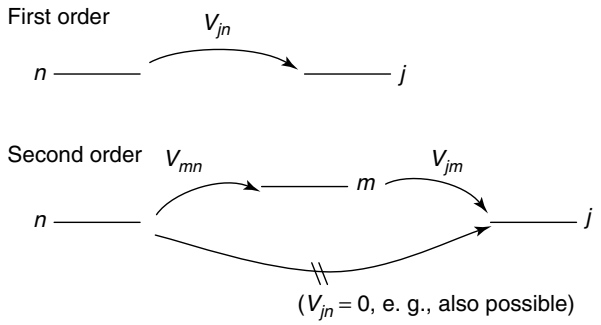

Figure 45 Schematic representation of first-order ($n \rightarrow j$) and second-order ($n \rightarrow m \rightarrow j$) transitions in a perturbation-theory treatment of the level coupling.

7.4 More General Coupling Models, Nonexponential Decays, and Non-Lorentzian Lineshapes

Mies and Krauss (1966) have discussed a more general coupling model as described in Figure 46. This model has been more extensively investigated by Mies (1968, 1969a,b) and discussed in relation to a statistical theory of unimolecular reactions by Quack and Troe (1974, 1981).

In the model by Mies and Krauss, a set of *reactant states* with density ρ (or equal spacing $\delta = \rho^{-1}$) is coupled with a constant coupling V to product states ρ_p, where one introduces a coupling parameter $\Gamma = 2\pi\,|V|^2\,\rho_p$ as abbreviation into the model. It is easily seen that this model includes situations, different from the Bixon–Jortner model, where one has a dense set of initial states, which might all decay. Physically, such a situation might apply for the dissociation of larger polyatomic molecules, where one has a high density of vibrational (–rotational) states (*see also* Quack 2011: **Fundamental Symmetries and Symmetry Violations from High-resolution Spectroscopy**, this handbook). This model leads to an expression for the initial decay rate constant (in general, with a nonexponential

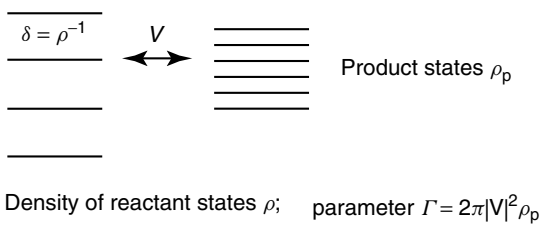

Figure 46 Model of Mies and Krauss (1966) describing the coupling between manifolds of reactant and product states as described in detail in the text.

decay).

$$k = \frac{2\pi\Gamma\rho}{\left(1+\frac{\pi}{2}\Gamma\rho\right)^2}\cdot\frac{1}{h\rho} = \gamma\cdot\frac{1}{h\rho} \tag{358}$$

One recognizes the limiting case with $\Gamma \ll \rho^{-1}$, $\Gamma\rho \ll 1$, $\gamma \ll 1$. This results in the Golden Rule expression (350), the reactant states lead to isolated, well-separated Lorentzian lines and individual exponential decays of the corresponding states similar to the Bixon–Jortner model. One also sees that the factor

$$0 \le \gamma \le \frac{2\pi\Gamma\rho}{\left(1+\frac{\pi}{2}\Gamma\rho\right)^2} \tag{359}$$

plays the role of a transmission coefficient for a quasi-periodic motion with period $\tau = h\rho$ in the reactant spectrum. The maximum value $\gamma = 1$ is obtained when $\pi\Gamma\rho/2 = 1$, leading to a maximum (uncertainty limited) decay rate. As discussed by Quack and Troe (1974, 1975), inclusion of a total number of accessible continua (open adiabatic channels) $W(E, J, \ldots)$, taking also angular momentum conservation and other symmetries into account, one obtains a statistical expression for unimolecular decay

$$k(E, J, \ldots) = \langle\gamma\rangle\,\frac{W(E, J, \ldots)}{h\rho(E, J, \ldots)} \tag{360}$$

where $0 \le \langle\gamma\rangle \le 1$ is an average transmission coefficient and the rate constant has to be interpreted as a statistical average over a sufficiently large sample. This provides an independent route to statistical rate constant expressions that are more commonly derived by microcanonical transition state theory (see Quack and Troe (1998) for further discussion). In the limit where $\Gamma\rho \ll 1$ one obtains the perturbation theory result of Eq. (353) (with ρ_p).

7.5 Other Sources of Line Broadening

In interpreting spectral lineshapes in terms of intramolecular processes, some caution is needed, as there are many other sources of line broadening. We have already mentioned intensity (power) broadening in Section 3. Instrumental line broadening is a trivial source of broadening. The most common source of line broadening in high-resolution gas phase spectra is the inhomogeneous Doppler broadening with a width (FWHM) $\Delta\nu_D$ and a Gaussian lineshape resulting from the Doppler effect in combination with the thermal Maxwell–Boltzmann distribution of translational speeds. One finds thus for the absorption cross section of the ideal Doppler shape,

$$\sigma_G(\nu) = \sigma_0 \exp\left[-c^2(\nu-\nu_0)^2/(\upsilon_W^2\nu_0^2)\right] \tag{361}$$

where υ_W is the most probable speed of molecules of mass m at temperature T

$$\upsilon_W = \left(\frac{2kT}{m}\right)^{1/2} \tag{362}$$

The Doppler lineshape can thus be used to evaluate the temperature of a sample by spectroscopy. When one has a true intramolecular process leading to a homogeneous Lorentzian lineshape combined with an inhomogeneous Doppler line shape one finds a shape from convolution of the two functions, a Voigt lineshape (*see* Albert *et al.* 2011: **High-resolution Fourier Transform Infrared Spectroscopy**, this handbook). Sometimes, with very good data, the individual homogeneous and inhomogeneous contributions can be separately evaluated (see, for instance, Hippler *et al.* (2007) for an example).

However, it is not always possible to simply convolute lineshapes. If the Lorentzian lineshape results from a bimolecular (pseudo-first-order) process by collisions with a heat bath (*see* Albert *et al.* 2011: **High-resolution Fourier Transform Infrared Spectroscopy**, this handbook), then the collisional broadening lineshape cannot be simply convoluted with the Doppler shape, but one can have many complex effects such as Dicke narrowing, line mixing and shifting, etc. Such situations have to be dealt with by appropriate techniques (*see* Albert *et al.* 2011: **High-resolution Fourier Transform Infrared Spectroscopy**, this handbook, and Hartmann *et al.* (2008)). It is nevertheless true that at higher pressures, when pressure broadening exceeds Doppler broadening, one may estimate the Lorentzian "pressure-broadening width" from its behavior, which is proportional to gas pressure (or collision rate or gas density). We refer to Hartmann *et al.* (2008) for a more detailed discussion.

Another broadening that has to be mentioned is residence-time and interaction-time broadening. At very high resolution, this becomes important, as the limited interaction time in the spectroscopic experiment can lead to a limitation on resolution owing to the uncertainty principle. On the other hand, the effect of Doppler broadening can be removed by the methods of Doppler-free spectroscopy (Demtröder 2011: **Doppler-free Laser Spectroscopy**, this handbook).

7.6 Summary of Intramolecular Processes as Related to Molecular Spectroscopy

The processes discussed here and in other parts of the handbook can be summarized briefly as follows.

1. spontaneous radiative decay (natural lineshape; usually, Lorentzian).
   Fluorescence—conserves electron spin.
   Phosphorescence—changes electron spin.
2. predissociation (frequently exponential, with Lorentzian lineshape);
3. internal conversion (IC) by change of electronic state with conservation of electronic spin (often exponential);
4. intersystem crossing (ISC) by change of electronic state with change of spin (often exponential);
5. intramolecular vibrational redistribution (IVR, frequently nonexponential, *see* Albert *et al.* 2011: **Fundamentals of Rotation–Vibration Spectra**, this handbook);
6. autoionization.

In the photochemistry and photophysics of polyatomic molecules, these processes are often summarized by the Jablonski diagram such as shown in Figure 47. The original diagram by Jablonski contained fewer processes (Jablonski, 1931, 1933), and, in particular, IVR has been added only during the last few decades (*see* Albert *et al.* 2011: **Fundamentals of Rotation–Vibration Spectra**, this handbook). The relative importance of the various processes occurring in competition is frequently characterized by the quantum yield Φ_i for a given process (see also Jortner *et al.* 1969)

$$\Phi_i = \frac{k_i}{\sum_j k_j} \tag{363}$$

where the k_j are the rate constants for the individual processes, which we have assumed to be exponential.

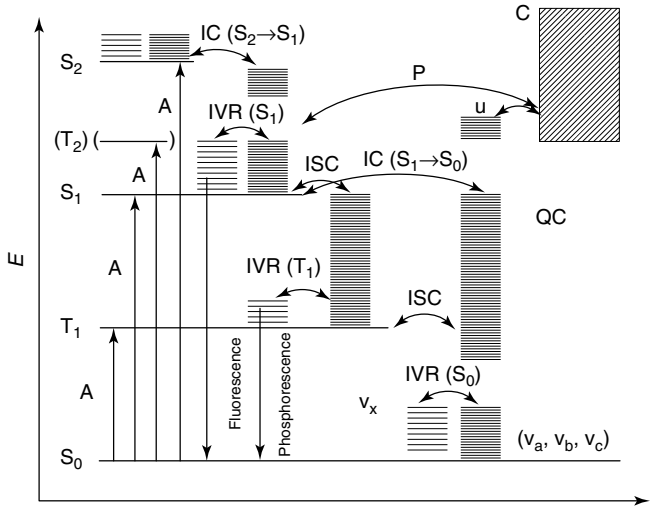

Figure 47 Generalized Jablonski scheme with various radiative and radiationless processes as discussed in the text. A and C are used for "Absorption" and "Continuum", respectively.

8 CONCLUDING REMARKS

In this introductory article to the Handbook of High-Resolution Spectroscopy, we have summarized the basic concepts of molecular spectroscopy with a largely didactic goal. Much further reaching and detailed information will be found in the individual chapters of the handbook, some of which we refer to explicitly in the list of references and also under the heading "Related Articles." The selection is somewhat arbitrary, in as much as to some extent, all articles of the present handbook might have been cited here, and we explicitly draw attention also to those articles not mentioned. We apologize for any specific omission that might have occurred and hope that the reader will find the relevant information in the remaining articles of the handbook.

ACKNOWLEDGMENT

Our work is supported by ETH Zürich and by Schweizerischer Nationalfonds.

ABBREVIATIONS AND ACRONYMS

BO	Born–Oppenheimer
CARS	coherent anti-Stokes Raman scattering
CNPI	complete nuclear-permutation-inversion
DFWM	degenerate four-wave mixing
EPR	electron paramagnetic resonance
FWHM	full width at half maximum
IC	internal conversion
ISC	intersystem crossing
IVR	intramolecular vibrational redistribution
LCAO	linear combination of atomic orbitals
LIF	laser-induced fluorescence
MS	molecular symmetry
NMR	nuclear magnetic resonance
UV	ultraviolet
WF-QRA	weak-field quasi-resonant approximation

REFERENCES

Albert, S., Albert, K.K., Hollenstein, H., Manca Tanner, C., and Quack, M. (2011) Fundamentals of rotation–vibration spectra, in *Handbook of High-resolution Spectroscopy*, Quack, M. and Merkt, F. (eds), John Wiley & Sons, Ltd., Chichester, UK.

Albert, S., Albert, K.K., and Quack, M. (2011) High-resolution Fourier transform infrared spectroscopy, in *Handbook of High-resolution Spectroscopy*, Quack, M. and Merkt, F. (eds), John Wiley & Sons, Ltd., Chichester, UK.

Balmer, J.J. (1885a) Notiz über die Spectrallinien des Wasserstoffs. *Verhandlungen der Naturforschenden Gesellschaft Basel*, **7**, 548–560.

Balmer, J.J. (1885b) Zweite Notiz über die Spectrallinien des Wasserstoffs. *Verhandlungen der Naturforschenden Gesellschaft Basel*, **7**, 750–752.

Bauder, A. (2011) Fundamentals of rotational spectroscopy, in *Handbook of High-resolution Spectroscopy*, Quack, M. and Merkt, F. (eds), John Wiley & Sons, Ltd., Chichester, UK.

Bernath, P.F. and McLeod, S. (2001) DiRef, a database of references associated with the spectra of diatomic molecules. *Journal of Molecular Spectroscopy*, **207**, 287.

Bixon, M. and Jortner, J. (1968) Intramolecular radiationless transitions. *Journal of Chemical Physics*, **48**(2), 715–726.

Bohr, N. (1913a) On the constitution of atoms and molecules, Part I. *Philosophical Magazine*, **26**, 1–25.

Bohr, N. (1913b) On the constitution of atoms and molecules, Part II. Systems containing only a single nucleus. *Philosophical Magazine*, **26**, 476–502.

Bohr, N. (1913c) On the constitution of atoms and molecules, Part III. Systems containing several nuclei. *Philosophical Magazine*, **26**, 857–875.

Bohr, N. (1913d) The spectra of helium and hydrogen. *Nature*, **92**, 231–232.

Bonhoeffer, K.F. and Farkas, L. (1928) The analysis of diffuse molecular spectrums. Experiments on photochemical ammonia corrosion. *Zeitschrift für Physikalische Chemie—Stöchiometrie und Verwandtschaftslehre*, **134**(5/6), 337–344.

Brabec, T. and Krausz, F. (2000) Intense few-cycle laser fields: frontiers of nonlinear optics. *Reviews of Modern Physics*, **72**(2), 545–591.

Breidung, J. and Thiel, W. (2011) Predictions of vibrational spectra from ab initio theory, in *Handbook of High-resolution Spectroscopy*, Quack, M. and Merkt, F. (eds), John Wiley & Sons, Ltd., Chichester, UK.

Bunker, P.R. and Jensen, P. (1998) *Molecular Symmetry and Spectroscopy*, 2nd edition, NRC Research Press, Ottawa.

Carrington, A., Leach, C.A., Marr, A.J., Moss, R.E., Pyne, C.H., and Steimle, T.C. (1993) Microwave spectra of the D_2^+ and HD^+ ions near their dissociation limits. *Journal of Chemical Physics*, **98**(7), 5290–5301.

Cohen-Tannoudji, C., Dupont-Roc, J., and Grynberg, G. (1992) *Atom-Photon Interaction*, John Wiley & Sons, Ltd., New York.

Cohen-Tannoudji, C., Laloë, F., and Diu, B. (1973) *Mécanique Quantique*, Hermann, Paris.

Demtröder, W. (2011) Doppler-free laser spectroscopy, in *Handbook of High-resolution Spectroscopy*, Quack, M. and Merkt, F. (eds), John Wiley & Sons, Ltd., Chichester, UK.

Dirac, P.A.M. (1927) On quantum algebra. *Proceedings of the Cambridge Philosophical Society*, **23**, 412–418.

Dirac, P.A.M. (1929) Quantum mechanics of many-electron systems. *Proceedings of the Royal Society of London Series A*, **123**(792), 714–733.

Dirac, P.A.M. (1958) *The Principles of Quantum Mechanics*, 4th edition, Clarendon Press, Oxford.

Einstein, A. (1905) Über einen die Erzeugung und Verwandlung des Lichtes betreffenden heuristischen Gesichtspunkt. *Annalen der Physik*, **17**(6), 132–148.

Einstein, A. (1916a) Strahlungs-emission und -absorption nach der Quantentheorie. *Verhandlungen der Deutschen Physikalischen Gesellschaft*, **13/14**, 318–324.

Einstein, A. (1916b) Zur Quantentheorie der Strahlung. *Mitteilungen der Physikalischen Gesellschaft Zürich*, **18**, 47–62.

Einstein, A. (1917) Zur Quantentheorie der Strahlung. *Physikalische Zeitschrift*, **18**, 121–128.

Ernst, R., Bodenhausen, G., and Wokaun, A. (1987) *Principles of Nuclear Magnetic Resonance in One and Two Dimensions*, Clarendon Press, Oxford.

Field, R.W., Baraban, J.H., Lipoff, S.H., and Beck, A.R. (2011) Effective hamiltonians for electronic fine structure and polyatomic vibrations, in *Handbook of High-resolution Spectroscopy*, Quack, M. and Merkt, F. (eds), John Wiley & Sons, Ltd., Chichester, UK.

Gallmann, L. and Keller, U. (2011) Femtosecond and attosecond light sources and techniques for spectroscopy, in *Handbook of High-resolution Spectroscopy*, Quack, M. and Merkt, F. (eds), John Wiley & Sons, Ltd., Chichester, UK.

Glauber, R.J. (1963a) Coherent and incoherent states of radiation field. *Physical Review*, **131**(6), 2766–2788.

Glauber, R.J. (1963b) Quantum theory of optical coherence. *Physical Review*, **130**(6), 2529–2539.

Goldstein, H. (1980) *Classical Mechanics*, 2nd edition, Addison Wesley, Menlo Park.

Grabow, J.-U. (2011) Fourier transform microwave spectroscopy measurement and instrumentation, in *Handbook of High-resolution Spectroscopy*, Quack, M. and Merkt, F. (eds), John Wiley & Sons, Ltd., Chichester, UK.

Hartmann, J.-M., Boulet, C., and Robert, D. (2008) *Collisional Effects on Molecular Spectra*, Elsevier, Amsterdam.

Heisenberg, W. (1925) Über quantentheoretische Umdeutung kinematischer und mechanischer Beziehungen. *Zeitschrift für Physik*, **33**, 879–893.

Heisenberg, W. (1930) *Die physikalischen Prinzipien der Quantentheorie*, Hirzel, Leipzig.

Henri, V. (1923) Structure des molécules et spectres d'absorption des corps à l'état de vapeur. *Comptes Rendus Hebdomadaires Des Séances De L'Academie Des Sciences*, **177**, 1037–1040.

Henri, V. and Teves, M.C. (1924) Absorption spectrum and constitution of sulphur vapour—predissociation of molecules. *Nature*, **114**, 894–895.

Herzberg, G. (1945) *Molecular Spectra and Molecular Structure*, Vol. II, *Infrared and Raman Spectra of Polyatomic molecules*, van Nostrand, New York.

Herzberg, G. (1950) *Molecular Spectra and Molecular Structure*, Vol. I, *Spectra of Diatomic Molecules*, van Nostrand Reinhold, New York.

Herzberg, G. (1966) *Molecular Spectra and Molecular Structure*, Vol. III, *Electronic Spectra and Electronic Schedule of Polyatomic Molecules*, van Nostrand, New York.

Hippler, M., Oeltjen, L., and Quack, M. (2007) High-resolution continuous-wave-diode laser cavity ring-down spectroscopy of

the hydrogen fluoride dimer in a pulsed slit jet expansion: two components of the N = 2 triad near 1.3 micrometer. *Journal of Physical Chemistry A*, **111**(49), 12659–12668.

Hippler, M., Miloglyadov, E., Quack, M., and Seyfang, G. (2011) Mass and isotope-selective infrared spectroscopy, in *Handbook of High-resolution Spectroscopy*, Quack, M. and Merkt, F. (eds), John Wiley & Sons, Ltd., Chichester, UK.

Huber, K.P. and Herzberg, G. (1979) *Molecular Spectra and Molecular Structure, Volume IV, Constants of Diatomic Molecules*, Van Nostrand Reinhold Company, New York.

Iro, H. (2002) *Classical Mechanics*, World Scientific, Singapore.

Jablonski, A. (1931) Über das Entstehen der breiten Absorptions- und Fluoreszenzbanden in Farbstofflösungen. *Zeitschrift für Physik*, **73**, 460.

Jablonski, A. (1933) Efficiency of anti-Stokes fluorescence in dyes. *Nature*, **131**, 839–840.

Jäger, W. and Xu, Y. (2011) Fourier transform microwave spectroscopy of doped helium clusters, in *Handbook of High-resolution Spectroscopy*, Quack, M. and Merkt, F. (eds), John Wiley & Sons, Ltd., Chichester, UK.

Jortner, J., Rice, S.A., and Hochstrasser, R. (1969) Radiationless transitions and photochemistry, in *Advances in photochemistry*, Pitts, B.O. and Hammond, G. (eds), John Wiley & Sons, Ltd., New York.

Korobov, V.I. (2006) Leading-order relativistic and radiative corrections to the rovibrational spectrum of H_2^+ and HD^+ molecular ions. *Physical Reviews A*, **74**(5), 052506.

Korobov, V.I. (2008) Relativistic corrections of $m\alpha^6$ order to the rovibrational spectrum of H_2^+ and HD^+ molecular ions. *Physical Reviews A*, **77**(2), 022509.

Landau, L.D. and Lifshitz, E.M. (1966) *Mécanique*, Editions Mir, Moscow.

Landau, L.D. and Lifshitz, E.M. (1985) *Quantum Mechanics: Non-relativistic Theory*, 3rd edition, *Course of Theoretical Physics*, Pergamon Press, Oxford, Vol. 3.

Leach, C.A. and Moss, R.E. (1995) Spectroscopy and quantum mechanics of the hydrogen molecular cation: a test of molecular quantum mechanics. *Annual Reviews of Physical Chemistry*, **46**, 55–82.

Liu, J., Sprecher, D., Jungen, Ch, Ubachs, W., and Merkt, F. (2010) Determination of the ionization and dissociation energies of the deuterium molecule (D_2). *The Journal of Chemical Physics*, **132**(15), 154301.

Longuet-Higgins, H.C. (1963) The symmetry groups of non-rigid molecules. *Molecular Physics*, **6**(5), 445–460.

Marquardt, R. and Quack, M. (1989) Infrared-multiphoton excitation and wave packet motion of the harmonic and anharmonic-oscillators - exact-solutions and quasiresonant approximation. *Journal of Chemical Physics*, **90**(11), 6320–6327.

Marquardt, R. and Quack, M. (1994) Statistical aspects of the radiative excitation of the harmonic-oscillator. *Journal of Physical Chemistry*, **98**(13), 3486–3491.

Marquardt, R. and Quack, M. (1996) Radiative excitation of the harmonic oscillator with applications to stereomutation in chiral molecules. *Zeitschrift für Physik D*, **36**(3–4), 229–237.

Marquardt, R. and Quack, M. (2011) Global analytical potential energy surfaces for high-resolution molecular spectroscopy and reaction dynamics, in *Handbook of High-resolution Spectroscopy*, Quack, M. and Merkt, F. (eds), John Wiley & Sons, Ltd., Chichester, UK.

Mastalerz, R. and Reiher, M. (2011) Relativistic electronic structure theory for molecular spectroscopy, in *Handbook of High-resolution Spectroscopy*, Quack, M. and Merkt, F. (eds), John Wiley & Sons, Ltd., Chichester, UK.

Messiah, A. (1961) *Quantum Mechanics*, North-Holland, Amsterdam.

Mies, F.H. (1968) Configuration interaction theory. Effects of overlapping resonances. *Physical Review*, **175**(1), 164–175.

Mies, F.H. (1969a) Resonant scattering theory of association reactions and unimolecular decomposition. 2. Comparison of collision theory and absolute rate theory. *Journal of Chemical Physics*, **51**(2), 798–807.

Mies, F.H. (1969b) Resonant scattering theory of association reactions and unimolecular decomposition. I. A united theory of radiative and collisional recombination. *Journal of Chemical Physics*, **51**(2), 787–797.

Mies, F.H. and Krauss, M. (1966) Time-dependent behavior of activated molecules. High-pressure unimolecular rate constant and mass spectra. *Journal of Chemical Physics*, **45**(12), 4455–4468, 86967.

Miller, W.H. (1974) Classical limit quantum mechanics and the theory of molecular collisions. *Advances in Chemical Physics*, **25**, 69–190.

Miller, W.H. (1975) The classical s-matrix in molecular collisions. *Advances in Chemical Physics*, **30**, 77–148.

Mills, I. and Quack, M. (2002) The symmetry groups of non-rigid molecules—comment. *Molecular Physics*, **100**, 9–10.

Miron, C. and Morin, P. (2011) High-resolution inner-shell photoionization, photoelectron and coincidence spectroscopy, in *Handbook of High-resolution Spectroscopy*, Quack, M. and Merkt, F. (eds), John Wiley & Sons, Ltd., Chichester, UK.

Moss, R.E. (1993a) Calculations for vibration-rotation levels of HD^+, in particular for high N. *Molecular Physics*, **78**(2), 371–405.

Moss, R.E. (1993b) Electronic g/u symmetry breaking in H_2^+. *Chemical Physics Letters*, **206**(1–4), 83–90.

Moss, R.E. (1996) On the adiabatic and non-adiabatic corrections in the ground electronic state of the hydrogen molecular cation. *Molecular Physics*, **89**(1), 195–210.

Oka, T. (2011) Orders of magnitude and symmetry in molecular spectroscopy, in *Handbook of High-resolution Spectroscopy*, Quack, M. and Merkt, F. (eds), John Wiley & Sons, Ltd., Chichester, UK.

Pais, A. (1991) *Niels Bohr's Times in Physics, Philosophy and Polity*, Clarendon Press, Oxford.

Perelomov, A. (1986) *Generalized Coherent States and their Applications*, Springer, Berlin.

Planck, M. (1900a) Über das Gesetz der Energieverteilung im Normalspectrum. *Verhandlungen der Deutschen Physikalischen Gesellschaft*, **2**, 202–236.

Planck, M. (1900b) Zur Theorie des Gesetzes der Energieverteilung im Normalspektrum. *Verhandlungen der Deutschen Physikalischen Gesellschaft*, **2**, 237–245.

Quack, M. (1978) Theory of unimolecular reactions induced by monochromatic infrared radiation. *Journal of Chemical Physics*, **69**(3), 1282–1307.

Quack, M. (1982) Reaction dynamics and statistical mechanics of the preparation of highly excited states by intense infrared radiation, in *Advances in Chemical Physics*, Lawley, K., Prigogine, I., and Rice, S.A. (eds), John Wiley & Sons, Ltd., New York, pp. 395–473, Vol. 50.

Quack, M. (1998) Multiphoton excitation, in *Encyclopedia of Computational Chemistry*, von Ragué Schleyer, P., Allinger, N., Clark, T., Gasteiger, J., Kollman, P.A., Schaefer, H., Schreiner, P.R. (eds), John Wiley & Sons, pp. 1775–1791, Vol. 3.

Quack, M. (2011) Fundamental symmetries and symmetry violations from high resolution spectroscopy, in *Handbook of High-resolution Spectroscopy*, Quack, M. and Merkt, F. (eds), John Wiley & Sons, Ltd., Chichester, UK.

Quack, M. and Stockburger, M. (1972) Resonance fluorescence of aniline vapor. *Journal of Molecular Spectroscopy*, **43**(1), 87–116.

Quack, M. and Troe, J. (1974) Specific rate constants of unimolecular processes. *Berichte der Bunsen-Gesellschaft für Physikalische Chemie*, **78**, 240–252.

Quack, M. and Troe, J. (1975) Product state distributions after dissociation. *Berichte der Bunsen-Gesellschaft für Physikalische Chemie*, **79**, 469–475.

Quack, M. and Troe, J. (1981) Statistical methods in scattering, in *Theoretical Chemistry: Advances and Perspectives (Theory of Scattering, Papers in Honor of Henry Eyring)*, Henderson, D. (eds), Academic Press, New York, pp. 199–276, Vol. 6B.

Quack, M. and Troe, J. (1998) Statistical adiabatic channel model, in *Encyclopedia of Computational Chemistry*, vonRague Schleyer, P., Allinger, N., Clark, T., Gasteiger, J., Kollman, P. A., Schaefer, H., and Schreiner, P.R. (eds), John Wiley & Sons, pp. 2708–2726., Vol. 4.

Rabi, I.I. (1937) Space quantization in a gyrating magnetic field. *Physical Review*, **51**(8), 652–654.

Rabi, I.I., Zacharias, J.R., Millman, S., and Kusch, P. (1938) A new method of measuring nuclear magnetic moment. *Physical Review*, **53**(4), 318–318.

Ritz, W. (1908) Über ein neues Gesetz der Serienspektren. *Physikalische Zeitschrift*, **9**, 521–529.

Sakurai, J.J. (1985) *Modern Quantum Mechanics*, Benjamin/ Cummings Publishing, Menlo Park—California.

Schinke, R. (2011) Photodissociation dynamics of polyatomic molecules: diffuse structures and nonadiabatic coupling, in *Handbook of High-resolution Spectroscopy*, Quack, M. and Merkt, F. (eds), John Wiley & Sons, Ltd., Chichester, UK.

Schnell, M. (2011) Group theory for high-resolution spectroscopy of nonrigid molecules, in *Handbook of High-resolution Spectroscopy*, Quack, M. and Merkt, F. (eds), John Wiley & Sons, Ltd., Chichester, UK.

Schrödinger, E. (1926a) Quantisierung als Eigenwertproblem I. *Annalen der Physik*, **79**(4), 361–376.

Schrödinger, E. (1926b) Quantisierung als Eigenwertproblem II. *Annalen der Physik*, **79**(6), 489–527.

Schrödinger, E. (1926c) Quantisierung als Eigenwertproblem III. *Annalen der Physik*, **80**(13), 437–490.

Schrödinger, E. (1926d) Quantisierung als Eigenwertproblem IV. *Annalen der Physik*, **81**(18), 109–139.

Schrödinger, E. (1926e) Über das Verhältnis der Heisenberg-Born-Jordanschen Quantenmechanik zu der meinen. *Annalen der Physik*, **79**(8), 734–756.

Schweiger, A. and Jeschke, G. (2001) *Principles of Pulse Electron Paramagnetic Resonance*, Oxford University Press, Oxford.

Sinha, M.P., Schultz, A., and Zare, R.N. (1973) Internal state distribution of alkali dimers in supersonic nozzle beams. *Journal of Chemical Physics*, **58**(2), 549–556.

Snels, M., Horká-Zelenková, V., Hollenstein, H., and Quack, M. (2011) High-resolution FTIR and diode laser spectroscopy of supersonic jets, in *Handbook of High-resolution Spectroscopy*, Quack, M. and Merkt, F. (eds), John Wiley & Sons, Ltd., Chichester, UK.

Sommerfeld, A. (1919) *Atombau und Spektrallinien*, Vieweg, Braunschweig.

Stockburger, M. (1973) Fluorescence of aromatic molecular vapours, in *Organic Molecular Photophysics*, Birks, J. B. (ed), John Wiley & Sons, Ltd., New York, pp. 57–102, Vol. 1.

Stohner, J. and Quack, M. (2011) Conventions, symbols, quantities, units and constants for high-resolution molecular spectroscopy, in *Handbook of High-resolution Spectroscopy*, Quack, M. and Merkt, F. (eds), John Wiley & Sons, Ltd., Chichester, UK.

Tew, D.P., Klopper, W., Bachorz, R.A., and Hättig, C. (2011) Ab initio theory for accurate spectroscopic constants and molecular properties, in *Handbook of High-resolution Spectroscopy*, Quack, M. and Merkt, F. (eds), John Wiley & Sons, Ltd., Chichester, UK.

Weber, A. (2011) High-resolution Raman spectroscopy of gases, in *Handbook of High-resolution Spectroscopy*, Quack, M. and Merkt, F. (eds), John Wiley & Sons, Ltd., Chichester, UK.

Wentzel, G. (1927) Über strahlungslose Quantensprünge. *Zeitschrift für Physik*, **29**, 524–530.

Wentzel, G. (1928) Die unperiodischen Vorgänge in der Wellenmechanik. *Physikalische Zeitschrift*, **29**, 321–337.

Wester, R. (2011) Spectroscopy and reaction dynamics of anions, in *Handbook of High-resolution Spectroscopy*, Quack, M. and Merkt, F. (eds), John Wiley & Sons, Ltd., Chichester, UK.

Wilson, E.B., Decius, J.C., and Cross, P.C. (1955) *Molecular Vibrations: The Theory of Infrared and Raman Vibrational Spectra*, McGraw-Hill, New York.

Wörner, H.J. and Corkum, P.B. (2011) Attosecond spectroscopy, in *Handbook of High-resolution Spectroscopy*, Quack, M. and Merkt, F. (eds), John Wiley & Sons, Ltd., Chichester, UK.

Wörner, H. and Merkt, F. (2011) Fundamentals of electronic spectroscopy, in *Handbook of High-resolution Spectroscopy*, Quack, M. and Merkt, F. (eds), John Wiley & Sons, Ltd., Chichester, UK.

Yamaguchi, Y. and Schaefer, H.F. (2011) Analytical derivative methods in molecular electronic structure theory: a new dimension to quantum chemistry and its applications to spectroscopy, in *Handbook of High-resolution Spectroscopy*, Quack, M. and Merkt, F. (eds), John Wiley & Sons, Ltd., Chichester, UK.

Zare, R.N. (1988) *Angular Momentum*, John Wiley & Sons, New York.

RELATED ARTICLES

Albert *et al*. 2011: **Fundamentals of Rotation–Vibration Spectra**
Albert *et al*. 2011: **High-resolution Fourier Transform Infrared Spectroscopy**
Bauder 2011: **Fundamentals of Rotational Spectroscopy**
Demtröder 2011: **Doppler-free Laser Spectroscopy**
Field *et al*. 2011: **Effective Hamiltonians for Electronic Fine Structure and Polyatomic Vibrations**
Gallmann and Keller 2011: **Femtosecond and Attosecond Light Sources and Techniques for Spectroscopy**
Grabow 2011: **Fourier Transform Microwave Spectroscopy Measurement and Instrumentation**
Hippler *et al*. 2011: **Mass and Isotope-selective Infrared Spectroscopy**
Jäger and Xu 2011: **Fourier Transform Microwave Spectroscopy of Doped Helium Clusters**
Marquardt and Quack 2011: **Global Analytical Potential Energy Surfaces for High-resolution Molecular Spectroscopy and Reaction Dynamics**
Mastalerz and Reiher 2011: **Relativistic Electronic Structure Theory for Molecular Spectroscopy**
Miron and Morin 2011: **High-resolution Inner-shell Photoionization, Photoelectron and Coincidence Spectroscopy**
Oka 2011: **Orders of Magnitude and Symmetry in Molecular Spectroscopy**
Quack 2011: **Fundamental Symmetries and Symmetry Violations from High-resolution Spectroscopy**
Schinke 2011: **Photodissociation Dynamics of Polyatomic Molecules: Diffuse Structures and Nonadiabatic Coupling**
Schnell 2011: **Group Theory for High-resolution Spectroscopy of Nonrigid Molecules**
Snels *et al*. 2011: **High-resolution FTIR and Diode Laser Spectroscopy of Supersonic Jets**
Stohner and Quack 2011: **Conventions, Symbols, Quantities, Units and Constants for High-resolution Molecular Spectroscopy**
Tew *et al*. 2011: **Ab Initio Theory for Accurate Spectroscopic Constants and Molecular Properties**
Weber 2011: **High-resolution Raman Spectroscopy of Gases**
Wester 2011: **Spectroscopy and Reaction Dynamics of Anions**
Wörner and Corkum 2011: **Attosecond Spectroscopy**
Wörner and Merkt 2011: **Fundamentals of Electronic Spectroscopy**